EUROPEAN COMMISSION

Community Research

SEVENTH FRAMEWORK PROGRAMME

ARCHER

Collaborative Project (CP)

Co-funded by the European Commission under the Euratom Research and Training Programme on Nuclear Energy within the Seventh Framework Programme

Grant Agreement Number : 269892

Start date : 01/02/2011 Duration : 48 Months

www.archer-project.eu

Archer

Advanced Reactor for Cogeneration of Heat & Electricity-R&D

Application of Spectra water/steam ingress models to an HTGR design

Author : STEMPNIEWICZ Marek (NRG)

ARCHER - Contract Number: 269892
Advanced High-Temperature Reactors for Cogeneration of Heat and Electricity R&D
EC Scientific Officer: Dr. Panagiotis Manolatos

Document title	Application of Spectra water/steam ingress models to an HTGR design
Author(s)	STEMPNIEWICZ Marek
Number of pages	95
Document type	Deliverable
Work Package	WP 22
Document number	D22.22
Issued by	NRG
Date of completion	25/01/2015
Dissemination level	Confidential, only for members of the consortium (including the Commission Services).

Summary

This document presents results of water ingress analysis for a reference HTR plant. A double-ended guillotine break of one heating tube of the steam generator has been studied. Through the analysis of the transient behavior of the reactor during water-ingress accidents, the design functions of the relevant systems are investigated. The results serve as a check of the inherent safety of the reference HTR plant. The obtained results lead to the following conclusions: If the break is located at the bottom of SG, the total mass entering the primary system is larger but it consists mostly of liquid which remains in the SG head and does not enter the core. If the break is located at the top of SG, the total mass entering the primary system is smaller but it consists of mainly steam which enters the core and causes corrosion of pebbles. If the blower flaps fail to close, a reverse natural circulation flow will be established after the blower is stopped. This will gradually bring a large amount of steam into the core and cause relatively large oxidation. Therefore the largest oxidation depth is observed when blower flaps fail to close. Even in the worst case, the largest oxidation depth was less than 0.5 mm. This is less than 10% of the thickness of the fuel-free zone, equal to 5 mm. The largest increase of power due to positive reactivity feedback was only 4%. Current results are in agreement with the results obtained by INET with RETRAN-02. With the present, integrated (primary + secondary) model, it was possible to eliminate some conservatism taken in the earlier analyses and show that the maximum water ingress in a design base cases is less than 230 kg, compared to the earlier conservative estimation of 600 kg. Current results were obtained without taking into account the helium purification system. With the helium purification system working, steam ingress can be removed from the vessel within several hours. From the calculated results it is conc

Approval

Date	By
26/01/2015	Michael FUTTERER
27/01/2015	Norbert KOHTZ
27/01/2015	Steven KNOL

Distribution list

Name	Organisation	Comments
P. Manolatos	EC DG RTD	Through the EC participant portal
All beneficiaries	ARCHER	Through the private online workspace

Table of contents

1 Introduction

The work described in this report, has been performed within the ARCHER project, Work Package WP22 - Water Ingress.

Direct steam generation coupled to the primary HTR system circuit, necessitates water/steam ingress accident evaluation as a part of safety and licensing analysis. Experience in this field dates back to 1980's, before intermediate heat exchanger and direct primary system turbine cycles were introduced. Currently there is strong evidence that the short to medium term market requires in majority steam supply which re-opens the potential application of direct steam generation.

The work package objective is to assess the potential issues that arise in this type of accidents, and establish a basis for safety evaluation and licensing according to current day standards. This requires the capability of assessing water/steam ingress experimentally, and offers the opportunity with current day advanced computer tools to assess this type of accidents more accurately, and following currently accepted safety standards. Specific attention must be given to temperature dependency of chemical reactions in the reactor core and the potential for formation of flammable or explosive gas mixtures in blow down devices or the reactor building. The experience from the past is available, and will be studied and summarized, as basis and guidance for the efforts in this work package.

One of the tasks to be performed within the ARCHER WP22, is an analysis of consequences of a 2F break (guillotine break with total break area equal two times the tube area) of a single steam generator tube with a two-phase system code SPECTRA. The advantage of using a two-phase system code here is the possibility of modeling the entire system (reactor vessel, steam generator, sub-systems) to calculate the transport of water and steam throughout the reactor system.

Previous work performed within this project [6] includes a review of available correlations for graphite oxidation by steam. Accuracy of the available correlations were investigated by performing comparisons with available data. A new correlation was proposed. The new correlation is an extension of the existing correlation of Kubaschewski-Heinrich, obtained by introducing a pressure dependent and burn-off dependent multiplier for best estimate as well as conservative calculations. The best estimate correlation shows significant improvement of accuracy when compared with the same data. The correlation has been implemented into a system code SPECTRA.

The present report describes results of water ingress analysis for the reference HTR plant. A double-ended guillotine break of one heating tube of the steam generator (DBA) has been studied. Through the analysis of the transient behavior of the reactor during water-ingress accidents, the design functions of the relevant systems are investigated. The results serve as a check of the inherent safety of the reference HTR plant.

Section 2 gives a brief description of the SPECTRA code. Section 3 describes the reference HTR plant and the SPECTRA model used for analysis. Section 4 presents results of calculations. The results are summarized in section 5. Finally, section 7 presents the conclusions.

2 SPECTRA Code

2.1 General Description of the SPECTRA Code

The SPECTRA code [1] is a computer code developed at NRG, the Netherlands. SPECTRA (Sophisticated Plant Evaluation Code for Thermal-hydraulic Response Assessment) is a fully integrated system code designed for thermal-hydraulic analyses of nuclear or conventional power plants. It is applicable to Light Water Reactors, High Temperature Gas Cooled Reactors, and Liquid Metal Reactors.

The program structure is shown in Figure 2-1. The modeling approach is based on the Control Volume (CV) concept. A model of a certain physical system consists of Control Volumes connected by junctions (JN). Within a Control Volume, four fluid components may exist: two continuous components (atmosphere and pool), and two dispersed components (droplets and bubbles). The gas components (atmosphere and bubbles) are assumed to be mixtures of non-condensable gases and steam. Non-equilibrium is assumed between each of the four fluid components, with the inter-component heat and mass transfer modeled in a mechanistic way.

Fluid property tables consist of the properties of water, steam, and several non-condensable gases, which are treated as real gases. The water properties are available for temperature range from 273.16 K to critical temperature (647 K). The steam properties were obtained using the NRC/NBC steam tables program interpolated using pre-computed tables, covering the range from 270 K to 3070 K, and from virtually 0.0 Pa to 2.1×10^{7} Pa. Alternatively the user can define fluid properties in input. This way the liquid metal reactor coolants, such as sodium or lead, can be used.

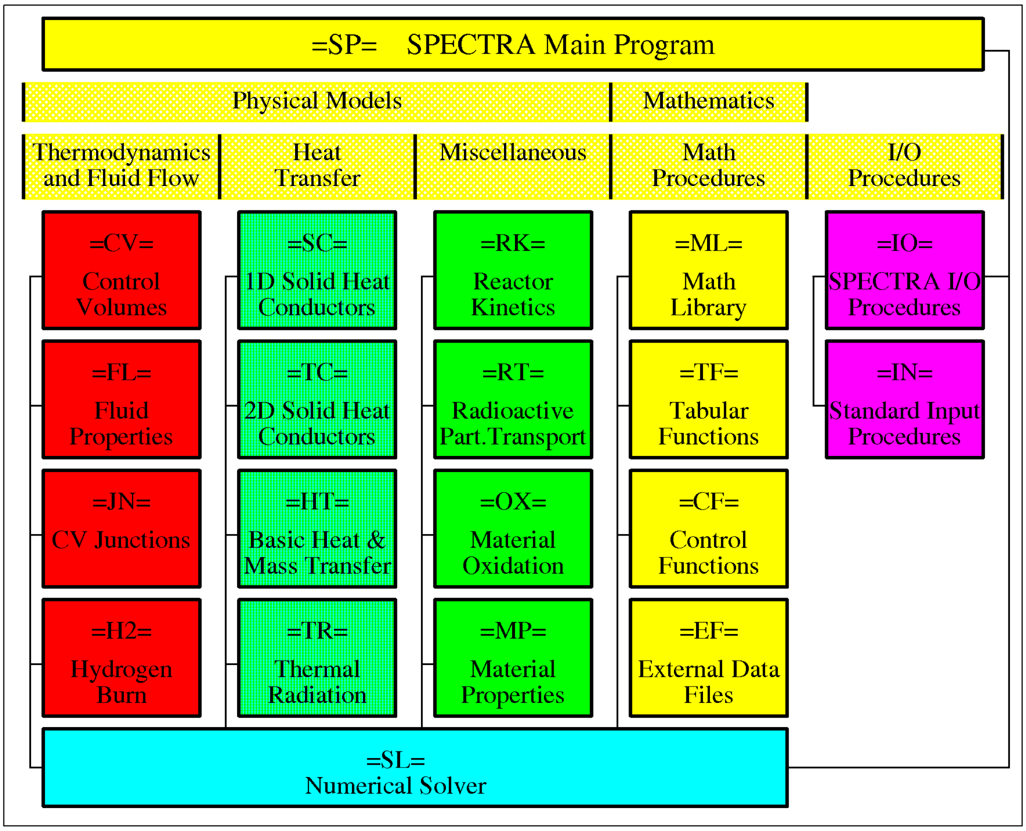

Figure 2-1 : SPECTRA code structure

Heat conduction is calculated by the 1-D and 2-D Solid Heat Conductor Packages, using a general transient heat conduction equation, The heat transfer at the boundaries of the Solid Heat Conductors is obtained from the Heat and Mass Transfer Package, which provides models for natural and forced convection, condensation with and without non-condensable gases, nucleate boiling, critical heat flux, transition boiling, Leidenfrost transition, film boiling, heat transfer in two-phase flow, as well as non-equilibrium boiling and condensation (“flashing” and “fogging”). The heat and mass transfer models include correlations valid for wall-fluid, pool-atmosphere, atmosphere-droplets, and pool-bubbles interfaces. Models for the bubble collapse as well as the heat and mass transfer to bubbles in swarms are included (see reference [1] for details).

A detailed thermal radiation model is provided, including grey enclosure models, with and without participating gas. The gas radiation model is based on the Hottel gas approach, [2].

The point reactor kinetics model is available, with reactivity feedback from control rods, fuel temperature, moderator temperature, void fraction, as well as changes in isotope concentrations. The Isotope Transformation model is available as a part of the Reactor Kinetics Package. It allows computing core composition changes (due to fuel burn-up, production of poisons, such as Xe-135, fuel reload, etc.), and their effect on reactivity as well as decay heat production. The model is based mainly on data from references [3], [4].

The Radioactive Particle Transport Package deals with release of fission products, aerosol transport, deposition, and resuspension. Radioactive chains of fission products are tracked. The models for the transport and deposition of aerosols include Brownian diffusion, thermophoresis, and gravitational settling. For turbulent flow conditions, turbulent deposition models for the diffusional deposition, turbulent eddy impaction, and inertia impaction regime are included. Moreover, gravitational, Brownian, and turbulent coagulation are modeled. Two state-of-the-art dynamic resuspension models are available. Alternatively, resuspension can be modeled using a parametric model with user-defined coefficients directly obtained from resuspension experiments (see reference [1] for details).

A hydrogen burn model is available, which includes slow deflagrations, fast turbulent deflagrations, and detonations. The model is based mainly on data from reference [5].

An oxidation model is available that contains models for zircaloy, steel oxidation by steam and oxygen, carbon oxidation by oxygen, as well as a general oxidation equation with user-defined coefficients. Via this equation any oxidation reaction may be modeled. Multiple reactions (for example simultaneous oxidation of zircaloy by steam and oxygen) are possible (see reference [1] for details). Oxidation model applied in the present analyses is defined via the general oxidation model and is described in section 2.2.

On top of the models mentioned above, general-purpose utilities, called Tabular Functions, Control Functions, are available. With these functions the user can define certain quantities in the physics packages. They can be applied for example:

- to provide boundary conditions to the analyzed problem,
- to model control systems of a reactor,
- to model safety system activations; etc.

The Numerical Solver Package is responsible for solving all Packages simultaneously, using a stable implicit solution scheme. Control Functions are included in the implicit solution, which allows solving stiff differential equations. The solution scheme allows performing calculations without making practically any mass or energy error. The SPECTRA program performs a global mass and energy check at the end of each time step. In absence of the thermal radiation model, the mass and energy errors are caused only by round-off errors of double precision arithmetics, which give relative errors of order of 10^{-15}.

The SPECTRA code provides extensive diagnostics of input data. All input entries are checked for consistency. Errors and warning messages are given in a separate file. These messages allow an easy correction of input errors and inconsistencies.

2.2 Oxidation Model

The oxidation model used in the present analysis is described in detail in [6] and shortly described below for the primary heterogeneous reaction (section 2.2.1), secondary heterogeneous reaction (section 2.2.2), and secondary homogeneous reaction (section 2.2.3).

2.2.1 Primary Heterogeneous Reaction

Correlations recommended in [6] for best estimate and conservative analyses are used. The correlation for the reaction kinetics of the primary heterogeneous reaction:

$$C + H_2O \rightarrow H_2 + CO$$

is as follows:

$$\frac{dm}{dt} = K(T, p_i) \cdot M(B, P)$$

The main part is the correlation of Kubaschewski-Heinrich [19] converted to SI units (see reference [6]):

$$K(T, p_i) = \frac{1.12 \cdot 10^4 \cdot \exp\left[-\frac{30788}{T}\right] \cdot (p_{H2O})^{0.44}}{1 + 2.37 \cdot 10^{-7} \cdot \exp\left[\frac{14552}{T}\right] \cdot (p_{H2})^{0.9} (p_{H2O})^{-0.4}}$$

- Best Estimate

  For best estimate calculations, a multiplier depending on burn-off and total pressure is defined following [20]:

$$M_{BE}(B, P) = f_B(B) \cdot [f_{P,\infty}(P) - f_{P,0}(P)] + f_{P,0}(P)$$

  Pressure-dependent factors:

$$f_{P,0}(P) = 0.35 \cdot \exp(-7.0 \times 10^{-8} P)$$
$$f_{P,\infty}(P) = 1.70 \cdot \exp(-1.8 \times 10^{-7} P)$$

  The correlations for pressure-dependent factor are applicable for P<55×10^5 Pa. The burn-off dependent factor is defined as:

$$f_B(B) = \begin{cases} 1 - \left(\frac{B}{B_\infty}\right)^2 & if\ B < B_\infty \\ 1 & if\ B > B_\infty \end{cases}$$

  The burn-off B is the average depth of the oxidized material [m]. The value of B_∞ is 0.3×10^{-3} m.

  The values of best estimate multiplier, $M_{BE}(B,P)$, are between 0.24 and 1.67, depending on burn-off and pressure [6]. The maximum deviation of the correlation results and experimental data is –27% and +15%. The range of application of the correlation is:

  - temperatures: T 1000 K ÷1300 K
  - pressures: p 10^5 Pa ÷ 55×10^5 Pa
  - steam pressures p_{H2O} 14 Pa ÷ 10^5 Pa

- <u>Conservative</u>

  For conservative calculations, a constant multiplier is used following [20]:

$$M_C = 1.8$$

Both best estimate and conservative correlations were defined in the input model of the HTR-PM. They were used for the best estimate and the conservative analyses, described in section 4.

2.2.2 Secondary Heterogeneous Reaction

The secondary heterogeneous reaction (or the Boudouard reaction) is:

$$C + CO_2 \rightarrow 2CO$$

For this reaction, the correlation of Moorman [16] can used. Converted to SI units (see reference [6]), the reaction is:

$$\frac{dm}{dt} = \frac{0.145 \cdot \exp\left(-25{,}000/T\right) \cdot p_{CO2}}{1 + 3.4 \times 10^{-5} \cdot \exp\left(7000/T\right) \cdot (p_{CO2})^{0.5}}$$

The correlation was defined in the input model of the HTR-PM but was not activated for the present calculations.

2.2.3 Secondary Homogenous Reaction

The secondary homogeneous reaction (or the water-shift reaction) is:

$$CO + H_2O \rightarrow CO_2 + H_2$$

For this reaction, the correlation of Graven and Long [17] can be used. Converted to SI units (see reference [6]), the reaction is:

$$\frac{dm}{dt} = \frac{1.04 \cdot 10^{8} \cdot \exp\left(-\frac{33{,}000}{T}\right) \cdot c_{H2O} \cdot \sqrt{c_{CO}}}{\sqrt{1 + 1.2 \cdot 10^{4} \cdot c_{H2}}}$$

The water-shift reaction can effectively reduce graphite corrosion [10]. For the current analyses the reaction was not modeled. Consequently it is expected that the obtained amounts of graphite corrosion are conservative.

3 HTR Reference Plant

Several different designs of high-temperature gas-cooled reactors exist:

- PBMR, 400 MWth pebble bed reactor with direct cycle [14].
- NGNP, 500 MWth pebble bed reactor with indirect cycle[12].
- HTR-Modul, 200 MWth pebble bed reactor indirect cycle [13].
- HTR-PM, 250 MWth pebble bed reactor indirect cycle [10].

The reference HTR plant chosen for the current analysis of water ingress is HTR-PM. This decision was made because currently this is the only design that will be built in the near future. A short description of the reference plant is provided in section 3.1. Section 3.2 provides a short description of the model used for the water ingress analyses.

3.1 Description of HTR Reference Plant

The description of the HTR plant provided in the following sections, is based on reference [10]. The description below includes the following parts:

- First, a short general description of the main components of the plant is given in section 3.1.1.

- Next, the main components of the plant are described, including:
  - reactor core, section 3.1.2,
  - steam generator and primary circulator (blower), section 3.1.3,
  - residual heat removal system, section 3.1.4.

- Finally, sub-systems important for water ingress scenario are discussed, including:
  - primary pressure release system, section 3.1.5.1,
  - secondary circuit isolation system, section 3.1.5.2,
  - steam generator emergency draining system, section 3.1.5.3,
  - helium purification facility, section 3.1.5.4,
  - confinement sub-pressure ventilation system, section 3.1.5.5.

3.1.1 General Description of the HTR Plant

The HTR-PM nuclear power plant consists of two pebble-bed module reactors with a total power of 500 MWth, which connect to one steam-turbine generator with a generating efficiency of about 42% [10]. A reactor module is shown in Figure 3-1. Each reactor module consists of reactor pressure vessel (RPV), the steam generator pressure vessel (SGPV), and the connecting horizontal coaxial hot-gas duct pressure vessel (HDPV) as well as their internal components, while the RPV and SGPV are installed in their own concrete shielding cavities respectively. The main helium blower is mounted on the upper part of the SGPV. The hot helium with an average temperature of 750°C heated in the reactor core transfers heat to the secondary loop water in the steam generator to produce high-pressure superheated steam, which drives the steam turbine to generate electricity of about 210 MWe.

The HTR-PM has the following design technical features:

- The side by side arrangement of the RPV and the SGPV ensures that the steam generator is placed below the reactor core to avoid any direct water flow into the core by gravity.

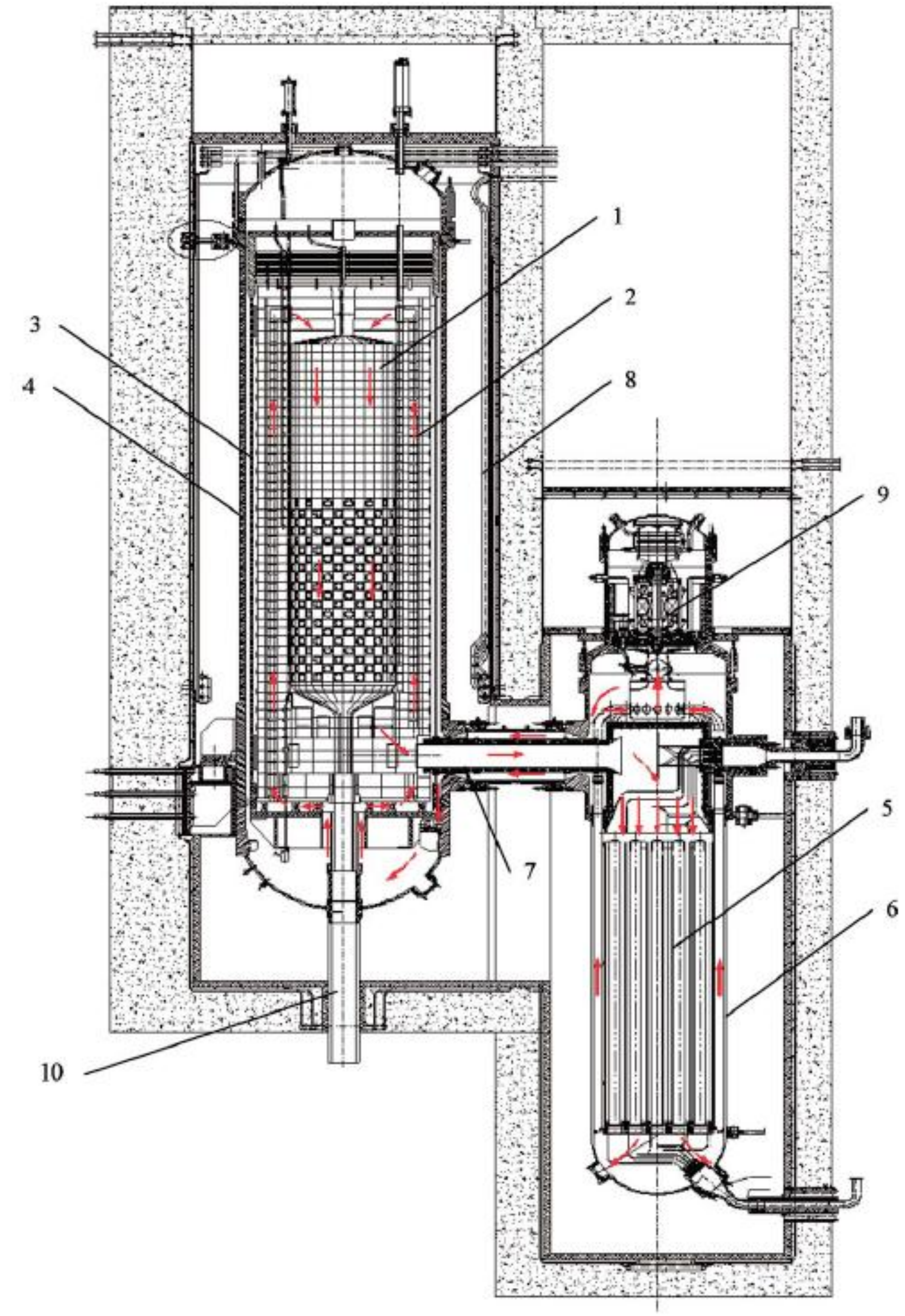

Fig. 1 Cross-section of the HTR-PM reactor: (1) reactor core, (2) side reflector and carbon thermal shield, (3) core barrel, (4) reactor pressure vessel, (5) steam generator, (6) steam generator vessel, (7) coaxial gas duct, (8) water-cooling panel, (9) blower, (10) fuel discharging tube, (11) control rod driving system, and (12) small absorber sphere unit

Figure 3-1 : Cross section of the HTR plant [10]

- The spherical fuel elements containing coated TRISO particles can effectively retain all relevant radioactive fission products up to the temperature of 1620°C. The reactor core is designed to ensure that the fuel element temperature never exceeds that safety limit under any operational and accidental conditions.

- The decay heat can be removed by means of passive heat transfer mechanisms to the cavity cooler outside the RPV due to its large height-diameter ratio of the “thin-core layout”. Therefore, active core cooling is not necessary for decay heat removal during accidents.

- A continuous fuel loading and discharging operation mode is adopted. The fuel elements drop into the reactor core from the central fuel loading tube and are discharged through a tube at the core bottom with an average circulation of 15 times to pass through the core. The fuel elements that have not reached the designated burn-up will be re-circulated into the reactor core in order to efficiently utilize the nuclear fuel.

- Two independent shutdown systems, the control rod system and the small absorber sphere system, are installed and placed in the side graphite reflectors, which can drop freely into borehole of the reflectors by gravity to shut down the reactor.

- The active core zone is merely enclosed by graphite and carbon bricks without metal components so that the core internals structure can endure higher temperature. • Due to the high activity retention of the fuel elements, a pressure- tight reactor building is not necessary. The reactor building is accessible for repair work at any time after an accident because of the low activity release.

3.1.2 Reactor Core

The reactor core with a mean power density of 3.22 MW/m^3, located inside the RPV, is a loose packed bed with an average height of 11 m and a diameter of 3 m, which consists of about 420,000 spherical fuel elements in the equilibrium state [10]. For each fuel element, approx. 12,000 “TRISO” coated fuel particles of 0.92 mm diameter are scattered in the inner graphite matrix with a diameter of 5.0 cm to form the fuel zone, and the outer shell with a thickness of 0.5 cm is a fuel-free zone. The heavy-metal loading of each fuel element is set to be 7 g. The average core outlet temperature is 750°C, while the mean inlet cold helium temperature is 250°C. After 15 passes through the reactor core, the fuel elements will reach the final maximum burn-up of about 100 GWd/tU and will be discharged and transported into the spent fuel storage tank.

The ceramic internals consist of graphite reflectors and carbon bricks, which enclose the reactor pebble bed. In the side reflector near the reactor core, 8 control rods are installed for the reactivity adjustment and serve as the first shutdown system which can make the reactor reach a safety shutdown state, while 22 small absorber sphere shutdown units are designed as the second shutdown system to achieve cold shutdown state. Additionally, there are 30 cold gas channels located in the outer side reflector for the helium flow. The fuel loading tube with a diameter of 6.5 cm is located at the top of the reactor core, while the fuel discharging tube is set at the bottom of the reactor core. The metallic internals consist of core barrel, bottom supporting structure and top thermal shield, which support the whole weight of the core ceramic structure. During normal operation, the annular area between the RPV and the core barrel is filled with cold helium of 250°C, which guarantees that the RPV temperature will not exceed the designed limitations.

The cold helium is pumped into the RPV by the primary circuit blower, and then flows downwards along the space between the core vessel and the RPV to the bottom of the reactor. A small part of helium flows into the fuel discharging tube and then merges into the main helium flow after cooling the fuel elements in the discharging tube. After passing through the steel support components at the reactor bottom, most of the helium flows upwards through the 30 coolant boreholes in the side reflector and is collected in the cold helium plenum located in the upper part of the top reflector. Then, a small part of helium flows into the control rod channels serving as coolant of the control rods. From top of the core, the mainstream of helium goes downwards, passing through the reactor core and the channels in the bottom reflector successively, and finally flows into the hot helium plenum in the bottom reflector, where it merges other branch streams. The helium flows with different temperatures are sufficiently mixed in the hot helium plenum and the mixture with an average temperature of 750°C flows out of the RPV.

3.1.3 Steam Generator and Blower

The steam generator is designed as a once-through assembly type of helical tube steam generator [10]. The hot helium is fed into the steam generator above the heating tube bundle, then flows around the heating tubes and transfers its heat to the secondary loop feed-water of 205°C in the tubes to produce superheated steam of 571°C, whereby it cools down from approx. 750 to 250°C. In order to keep the flow stability and reduce the water-ingress rate, flow restrictors are individually incorporated into each tube at the feed-water entrance plate. The feed-water flows through the helical tubes form the bottom to the top in the steam generator. Then all the superheated live-steam is collected at the top main plate and passes through the live-steam line to the machine hall. A conventional super high-pressure steam-turbine generator is adopted for the HTR-PM, which can reach a high electrical efficiency of about 42%.

The primary circuit blower, located in the SG vessel, adopts a single-stage vertical compressor with a speed-controlled electric submerged motor. The blower is driven by a frequency converter outside the SGPV [10]. In order to minimize the steam ingress into the core, two kinds of blower flaps with different driving mechanisms are located respectively on the suction side and the exhaust side of the blower to actively separate the core from the steam generator region within 15 s if a leak of the steam generator tube has been detected.

3.1.4 Residual Heat Removal System

In normal operations as well as in accident conditions, the Residual Heat Removal System (RHRS), designed as a passive system, can carry out the decay heat from the core to the final heat sink – the atmosphere, and thereby ensure the thermal integrity of the fuel element, the ceramic internals, the RPV and the cavity concrete. Besides, inside the reinforced concrete wall of the reactor cavity and the steam generator cavity, a water-cooling system is installed to keep the concrete temperature below 100°C under any condition, so that the strength of the concrete cavity can be ensured. The design capability of the RHRS for each reactor module is 1.2 MW. It consists of three independent trains, while each train has 50% design capability and includes a water-cooling panel, inlet and outlet manifolds, air coolers, coupling pipes, a water tank, etc. After the reactor shutdown, the decay heat of the core will be transferred firstly to the RPV, and then to the water-cooling panel by radiation and natural convection. The heated water in the tubes flows upwards to the air cooler in the air-cooling tower and finally transfers the heat to the atmosphere.

3.1.5 Sub-Systems

3.1.5.1 Primary Pressure Release System

In order to effectively protect the pressure vessel units from overpressure, the primary pressure release system is designed as two-fold redundancy [10]. The set-points of the two safety valves are 7.9 and 8.25 MPa respectively. For any overpressure, the first train with lower set-point value and smaller diameter is actuated firstly and discharges the primary helium with a flow rate of about 0.18 kg/s. In case the first valve fails to open and the primary pressure continuously rises, the second train will be actuated, discharging the primary helium with a flow rate of approximately 12 kg/s. Both the safety valves will close again once the primary pressure has reached its design value of 6.9 MPa.

3.1.5.2 Secondary Circuit Isolation System

The action of isolating the secondary circuit includes closing the isolation valves both on the feed-water line and the live-steam line [10]. During the steam generator heating tube break accident, the timely secondary circuit isolation can limit the amount of water and steam ingress into the primary circuit. To ensure credible isolation, two different feed-water isolation valves, as well as two live-steam isolation valves, are designed elaborately, while the former can rapidly close within 5 s and the latter can close within 10 s.

3.1.5.3 Steam Generator Emergency Draining System

Water-ingress amount will be limited by draining the steam generator as soon as high humidity in the primary circuit has been detected [10]. An airtight drainage tank, installed inside the reactor building below the steam generator, is connected to the feed-water line via two parallel and independent relief lines. Each relief line has two relief valves. The total content of the steam and water between the two isolation valves on the feed-water line and the live-steam line is approx. 4 t, which can be discharged within 30 s.

3.1.5.4 Helium Purification Facility

The helium purification facility is designed to purify the primary coolant to specified values by removing chemical impurities (H_2O, O_2, CO, CO_2, N_2, H_2, CH_4, etc.), as well as to regulate the helium inventory and thereby to control the primary pressure. In water-ingress accidents, after the reactor scram, a stand-by accident purification line, which is specially designed with water separators and serves for both modules, can start up to remove the superfluous water, as well as cool down the hot core, so as to effectively mitigate the accident. The throughput of the stand-by line is about 100% of the primary circuit inventory per hour.

3.1.5.5 Confinement Sub-Pressure Ventilation System

In normal operations, the desired sub-pressure is maintained in the confinement and the vent air is released to the environment after being filtered by the normal sub-pressure ventilation system [10]. If, as a result of small leakages in primary pressure boundary, the confinement pressure increases, the accident sub-pressure ventilation system (comprises efficient filter and de-iodination device) is switched on. While the pressure increases sharply due to a large leakage, a bursting disc blows up, and the unfiltered gas is directly discharged to the atmosphere via the pressure release pipelines and the vent stack. When the pressure of confinement decreases and approaches the atmospheric pressure, a valve in the upstream of the pipeline before the bursting disc will be closed so that the accident sub-pressure ventilation system can again be switched on to filter and release the vent air and the primary gas, maintaining the confinement in a desired sub-pressure.

3.2 SPECTRA Model of HTR Reference Plant

3.2.1 General Description of the Plant Model

A model of the HTR plant has been developed, including primary system, steam generator, residual heat removal system, confinement building, as well as the main sub-systems. Figure 3-2 shows nodalization of the confinement building with an overview of reactor vessel and steam generator. Details on the reactor vessel and steam generator are shown in sections 3.2.2 and 3.2.3.

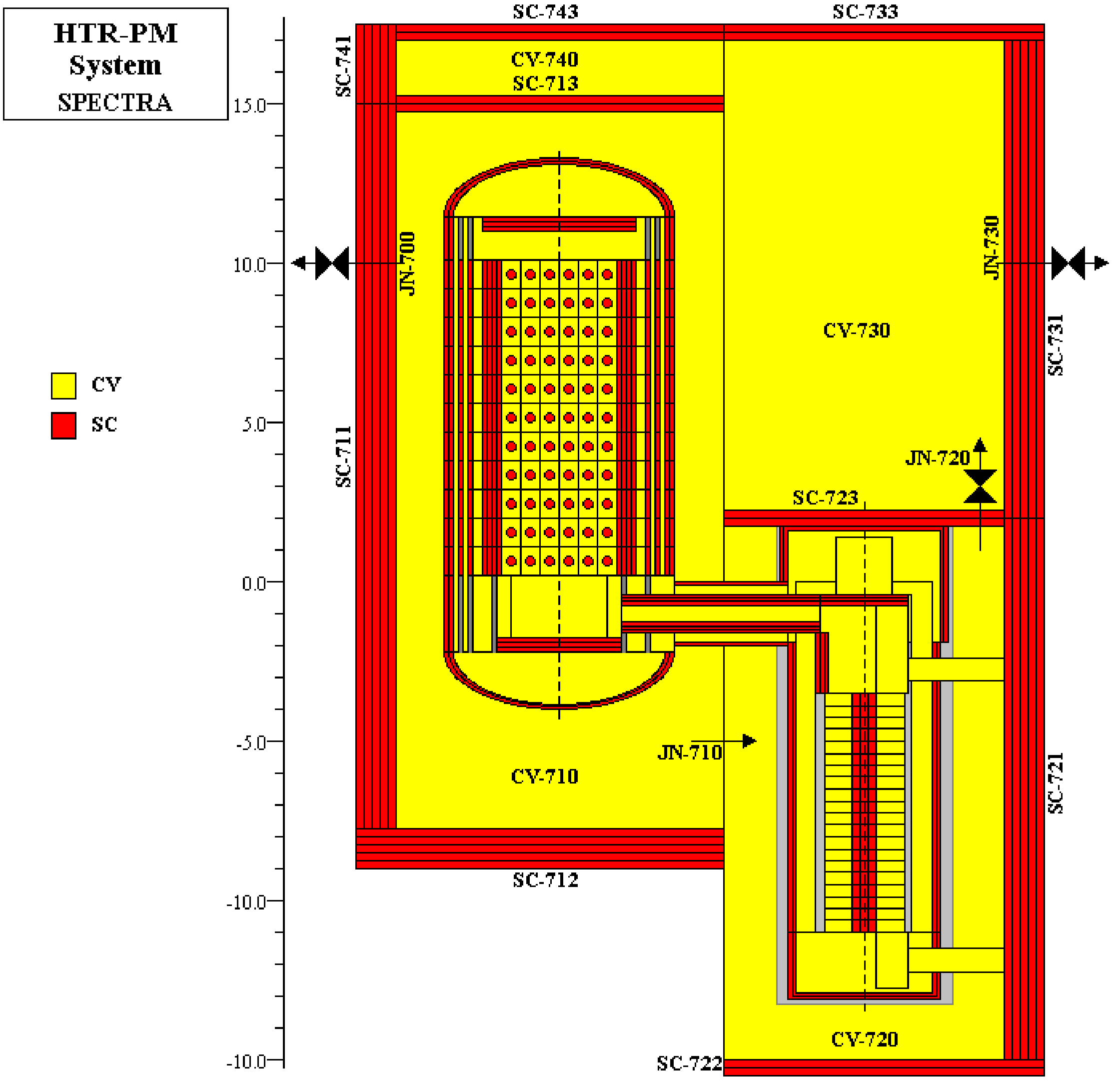

Figure 3-2 : Nodalization of confinement building

3.2.2 Reactor Core

The Reactor Vessel is shown in Figure 3-3. A horizontal cross section showing the reflector, thermal shield, inlet channels, and the CR channels, is shown in Figure 3-4. The pebble bed is shown in Figure 3-5. The pebble bed is modeled using 11 axial levels and 3 radial rings.

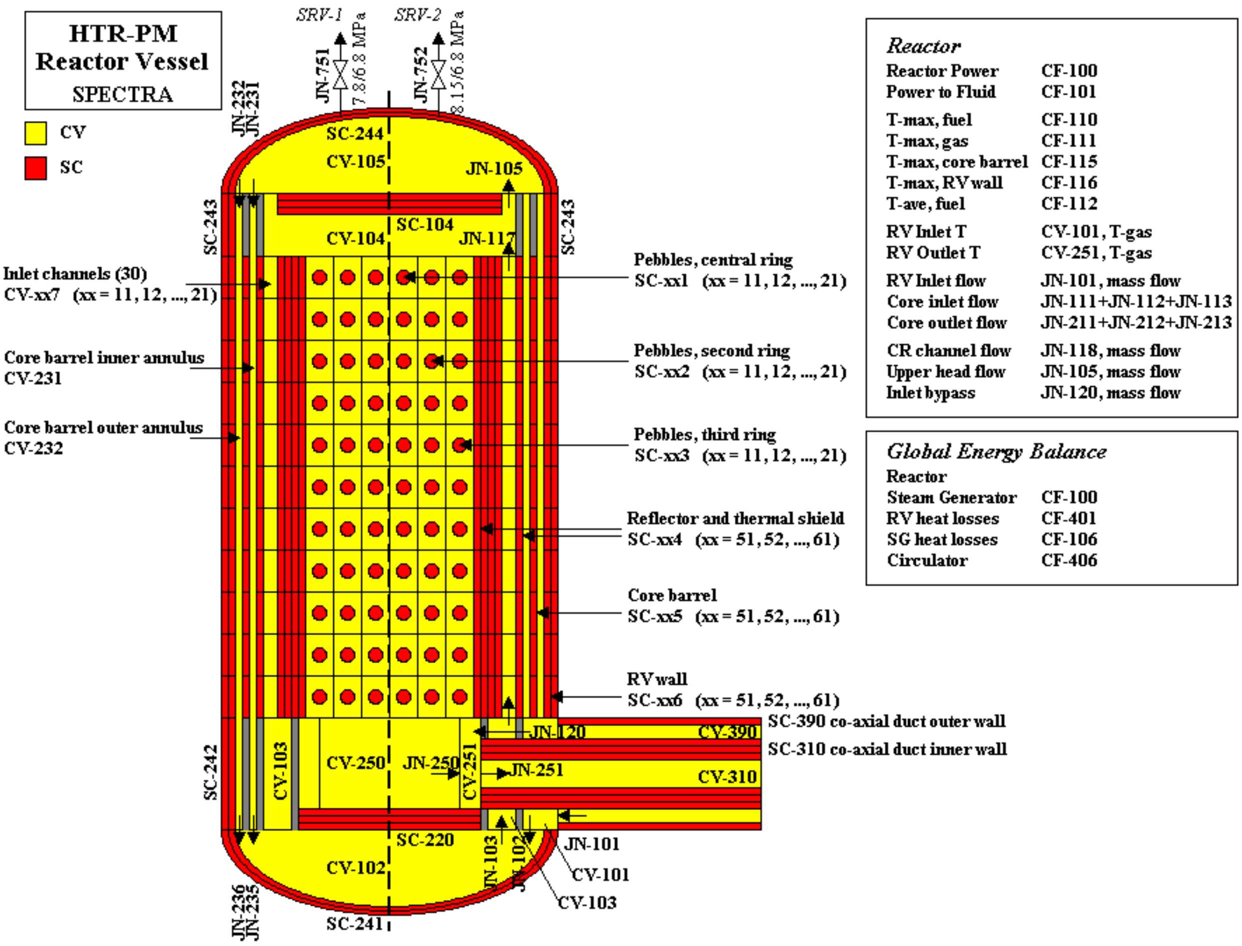

Figure 3-3 : Nodalization of reactor vessel

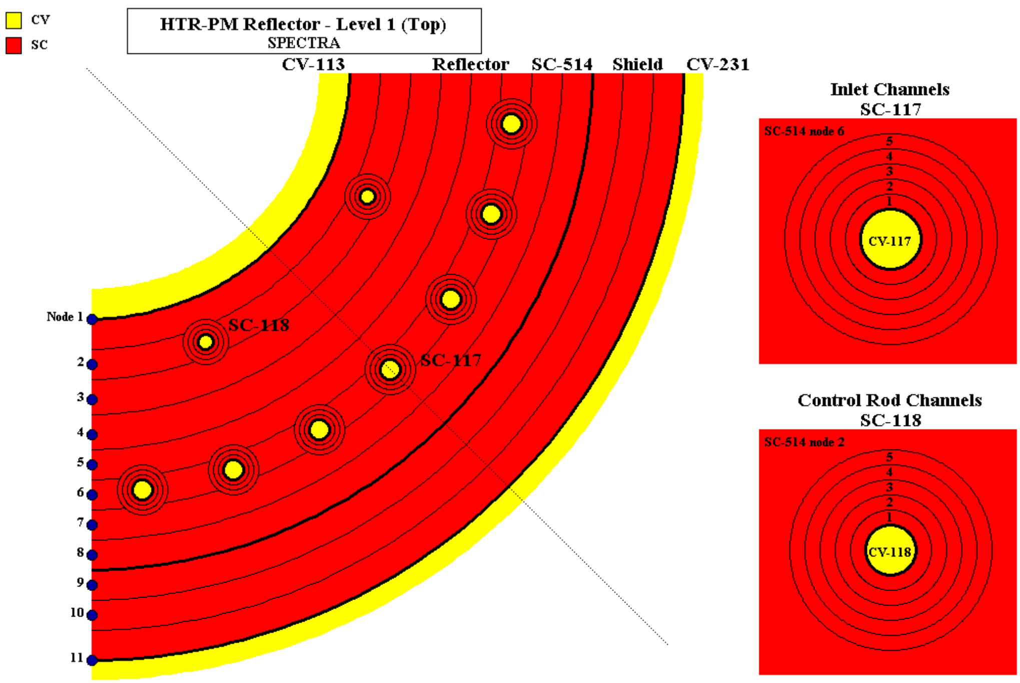

Figure 3-4 :

Nodalization of reflector, thermal shield, inlet channels, CR channels

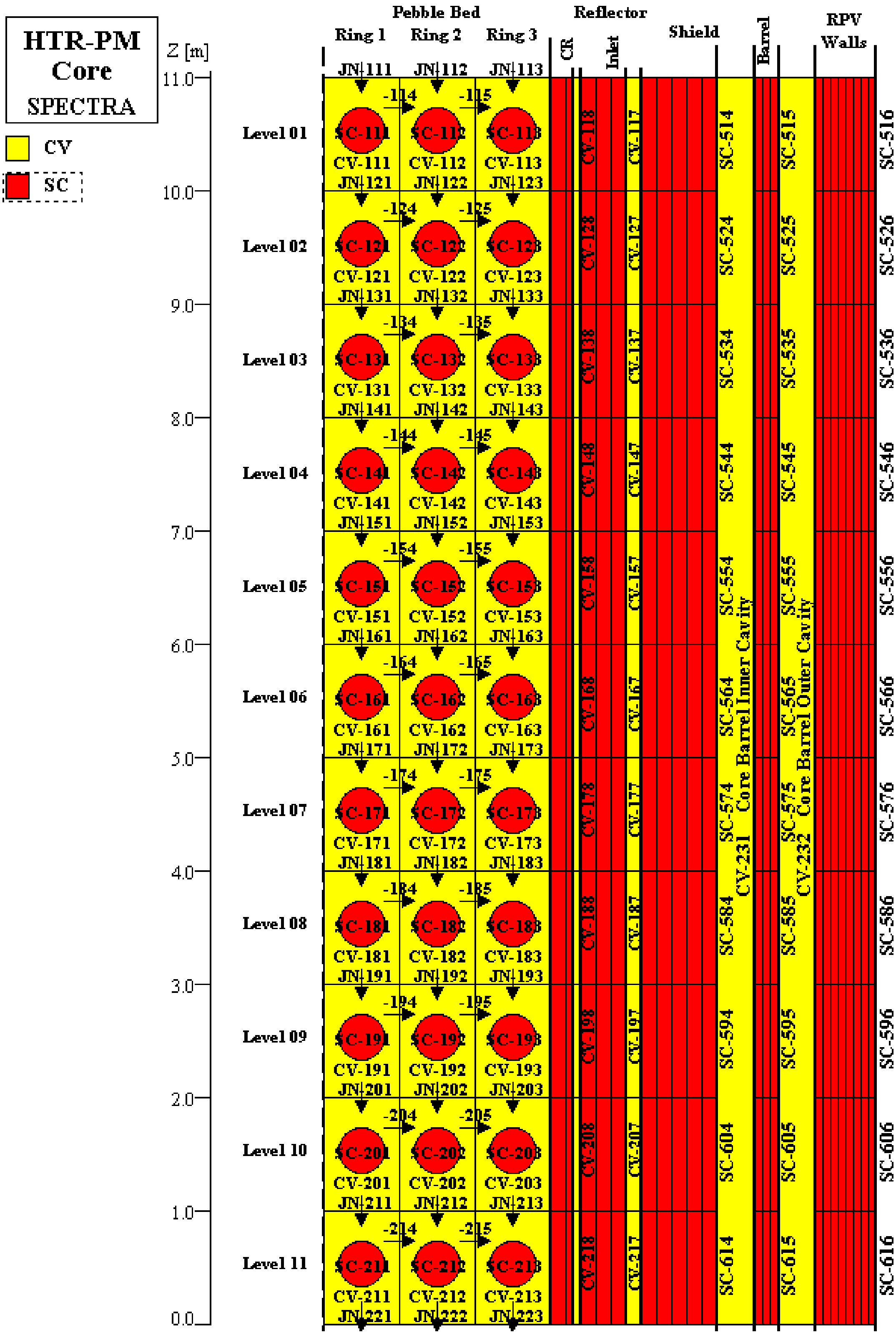

Figure 3-5 :

Nodalization of pebble bed, including reflector, thermal shield, core barrel, and RPV

The reactor kinetics model used is the point kinetics with six groups of delayed neutron precursors and reactivity feedbacks from fuel and moderator temperature changes. Additionally a reactivity feedback from steam was defined. The reactivity feedback was defined as a function of average steam density in the core. Relevant data was found in references [7], [8], [9], [10] and are shown in Figure 3-6. The most conservative data is given by van Bremen [8]. For the current model the data of INET has been applied [10].

Since the present model is based on point reactor kinetics, the steam density is averaged over the whole core to calculate reactivity feedback. This will lead to too optimistic reactivity effect. In reality the steam densities will larger in certain locations (closer to the place where steam enters the core). This will lead to local increase of reactivity and power. This effect cannot be captured with point reactor kinetics. A 3-D kinetics model is needed, with reactivity effects from local steam concentrations.

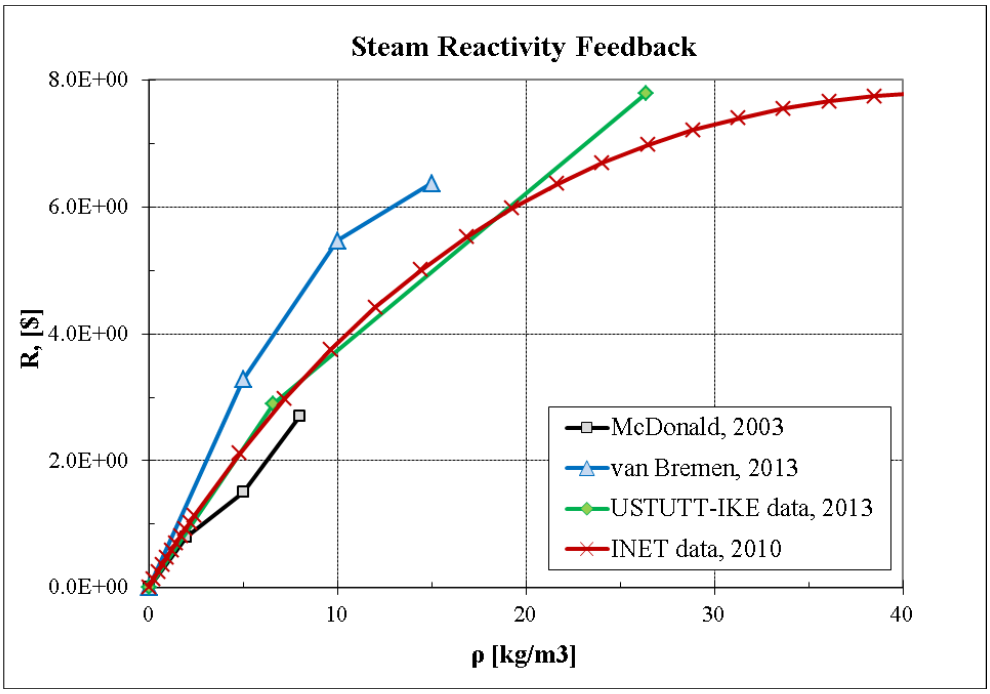

Figure 3-6 : Reactivity feedback from steam

3.2.3 Steam Generator and Blower

The steam generator vessel, including the main blower, is shown in Figure 3-7. The steam generator tubes are shown in Figure 3-8. The SG tubes are modeled using 20 nodes. The tube walls are modeled using 3 nodes in the radial direction - Figure 3-8.

The SG secondary side model includes the FW line, with the FW pump and the FW isolation valve, the Steam Line including the isolation valve, as well as the SG drain system. In case of SG tube break, the SG secondary side is isolated. This is done by closing the FW valve (the valve starts closing at the accident detection, closing time is 5 seconds) and the SL valve (the valve starts closing with the delay of 30 seconds, to avoid over-pressurization of the SG; the valve is closing time is 10 seconds)

The SG drain system is used in case of SG tube rupture to minimize the water ingress into the primary system by draining the SG water. The diameter of the drain line is: D_{drain} = 0.059 m. The drain line is assumed to open 10 seconds after SCRAM; the opening time is 3 seconds [11]. The drain valve is closed when the pressure in the SG drops to the design limit of 7.3 MPa [11]. This is done to prevent the secondary pressure from becoming lower than the primary pressure and therefore inflow of radioactive isotopes from the primary system into the secondary system.

At the inlet of the SG tubes (water side) there is an orifice. The orifice diameter was selected by trial and error to give approximately the desired pressure drop for the SG secondary side. It was found out that a good match was obtained using the orifice diameter of:

$$D_{orifice} = 0.0041 \text{ m}$$

The loss factors are obtained using thin orifice formula from [18]. For the normal operation this is based on contraction from a 'relatively large' flow area to the orifice diameter and expansion into the SG tube, diameter of 0.013 m. This gives:

$$K_{normal} = 2.584$$

This value is in the base model. For the case of broken tube, the loss factor is based on contraction from a 'relatively large' flow area (infinity) to the orifice diameter and expansion into a 'relatively large' area. This gives:

$$K_{broken} = 2.914$$

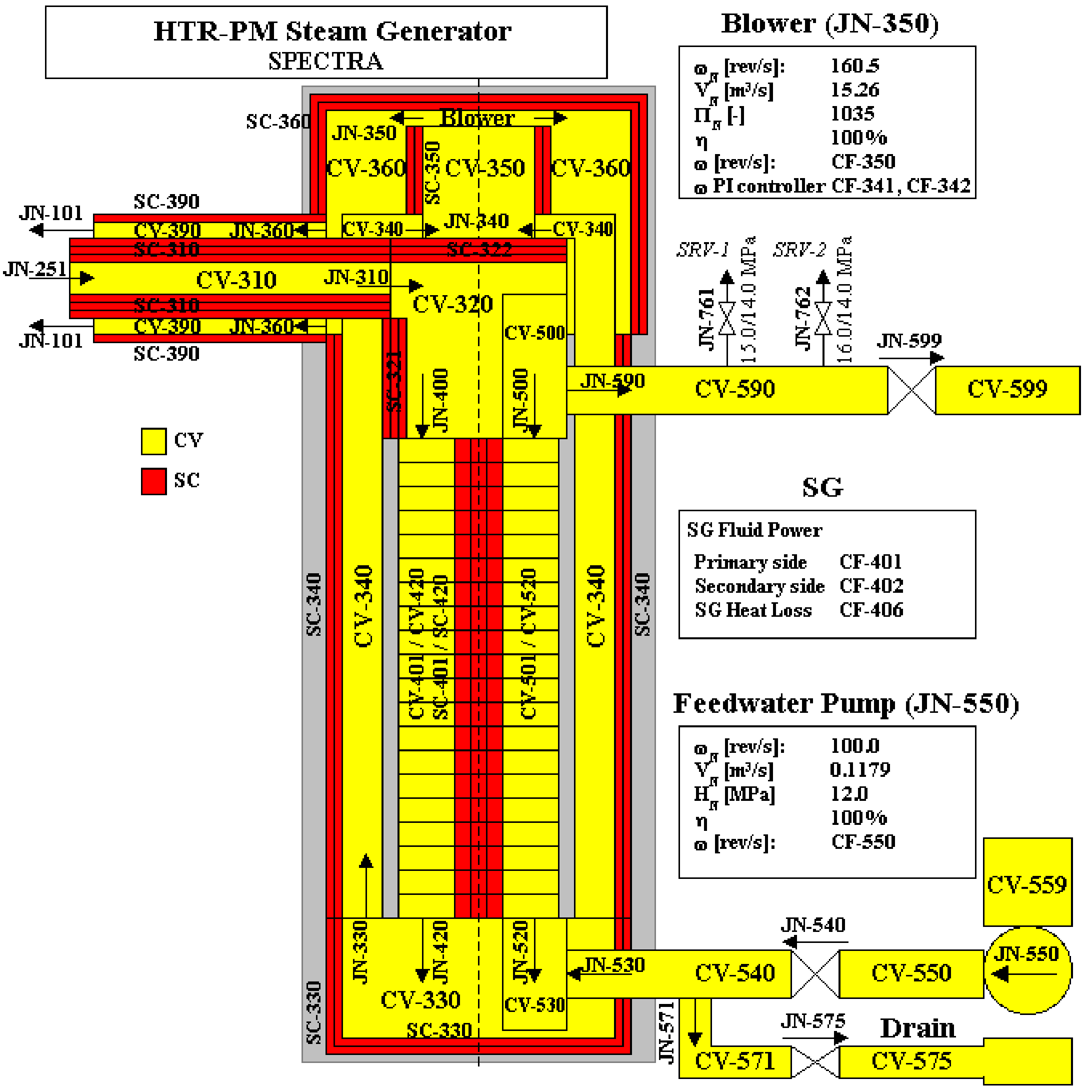

Figure 3-7 : Nodalization of Steam Generator

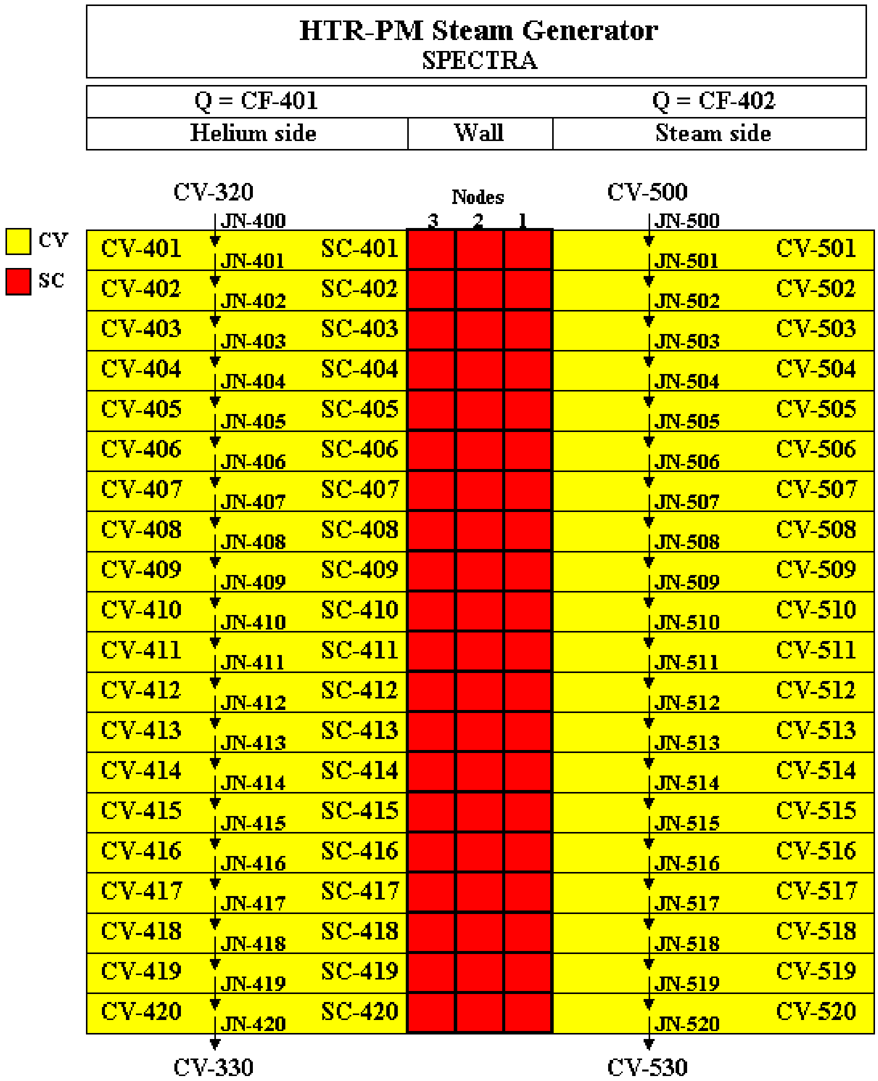

Figure 3-8 : Nodalization of Steam Generator tubes

3.2.4 Residual Heat Removal System

Nodalization of the Residual Heat Removal System is shown in Figure 3-9. The RHRS is modeled in a simplified way. The water side is replaced by boundary conditions defined by Tabular Functions. The following values are assumed for the current model: h = 1000 W/m^2-K and T = 360 K (87°C).

The energy exchange between RPV wall and RHRS wall is assumed to consist of convection and radiation. The default convection models are used with the hydraulic diameter assumed equal to 1.0 m (approximately the distance between RPV wall and RHRS wall). The emissivity of the RPV and RHRS walls is assumed to be 0.9.

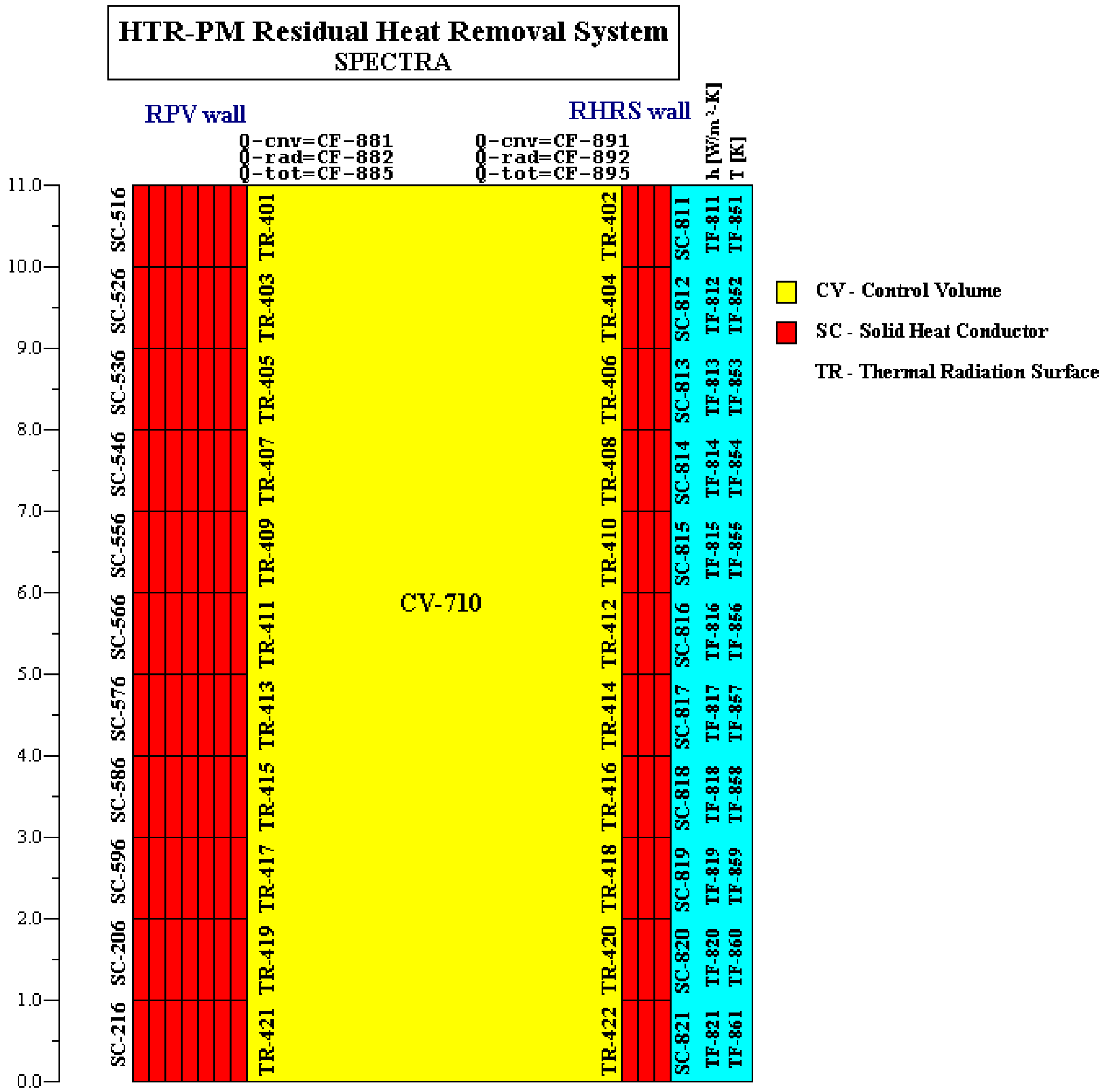

Figure 3-9 : Nodalization of Residual Heat Removal System

3.2.5 Sub-Systems

3.2.5.1 Primary Pressure Release System

Two safety valves are used: JN-751 and JN-752 - Figure 3-3. The opening Δ*P* for these valves are 7.8 and 8.15 MPa. (therefore the valves will open when the absolute pressure in the primary system is approximately 7.9 and 8.25 MPa respectively). The closing Δ*P* for these valves is 6.8 MPa. (therefore the valves will close when absolute pressure in the primary system is approximately 6.9 MPa). The flow areas of these valves were selected by trial and error to give the mass flows of 0.18 and 12 kg/s respectively (section 3.1.5.1) at their opening setpoint pressures.

3.2.5.2 Secondary Circuit Isolation System

The isolation valves on the feed-water line and the steam line are modeled as JN-540 and JN-599 respectively - Figure 3-7. The time required to close the valves from fully open position is 5 seconds for a FW valve and 10 seconds for the steam valve.

During the analyzed accident the feedwater valves closure is initiated 10 seconds after the accident starts. This is the time needed to detect the accident by the humidity sensors [10]. Therefore this valve is fully closed at 15 s after the tube break accident. Closure of the steam valve is delayed by 30 seconds. This delay is needed to avoid over-pressurization of the SG secondary side and opening of the SG relief valves. Therefore the steam valve starts closing at 40 s and is fully closed at 50 seconds after the tube break. The open fractions of the valves are shown in Table 3-1.

Table 3-1 : Isolation valve data

Feedwater valve JN-540		Steam valve JN-599	
t **[s]**	***A*****/*****A*****$_0$ [-]**	***t*** **[s]**	***A*****/*****A*****$_0$ [-]**
0.0	1.0	0.0	1.0
10.0	1.0	40.0	1.0
15.0	0.0	50.0	0.0

3.2.5.3 Steam Generator Emergency Draining System

The SG emergency draining system is modeled as CV-571, CV-575, JN-571 and JN-575 - Figure 3-7. If the system is taken into account, the time required to fully open the drain valve, JN-575, is assumed to be 10 seconds. The drain valve opens simultaneously with the FW valve, 10 seconds after the tube break.

3.2.5.4 Helium Purification Facility

The helium purification facility is not modeled. Analyses are done without taking that system into account for conservatism, the same as the water ingress analyses described in [10].

3.2.5.5 Confinement Sub-Pressure Ventilation System

The ventilation system is not modeled. Analyses are done without taking that system into account.

3.3 Validation of the SPECTRA Model

Validation of the model was done by analyzing accident scenarios including pressurized loss of forced circulation (PLOFC) and depressurized loss of forced circulation (DLOFC).

- PLOFC
- DLOFC, 65 mm break
- DLOFC, 10 mm break
- DLOFC, guillotine rupture of the co-axial duct.

Results were compared with the results reported in [15]. A good agreement with the reference data was found for the analyzed scenarios.

4 Water Ingress Analyses

A double-ended (2F) guillotine break of a steam generator heating tube represents the most serious design basis accident (DBA) for water ingress into the primary circuit [10]. This accident has been analyzed within the present work. Additionally, various assumptions concerning safety systems have been studied.

When a leakage of the steam generator occurs, the water and steam in the steam generator will spray into the primary circuit and flow into the reactor core along with the helium driven by the blower due to significantly higher pressure in the secondary loop (~140 bar) than in the primary loop (~70 bar). This accident can be detected by the humidity sensors within 10 s [10] and the following protective actions will be triggered by the signal of water vapor in the primary coolant:

- Drop of all control rods and small absorber spheres.
- Shutdown of the blower and closure of the blower flaps.
- Isolation of the steam generator and shutdown of the feedwater pump.
- Rapid drainage of steam generator through the SG drain.

For the current analysis, it is assumed that above actions will be initiated at 10 s. The duration of dropping all control rods is assumed to be 50 s, while the shutdown of the blower will be completed within 30 s. When the above protective actions are finished and the reactor is safely shut down, the helium purification facility can effectively remove the water and mitigate the accident. However, in the present analysis the water removal and pressure control functions of the helium purification facility are not taken into account for conservatism.

The following tube ruptures scenario was analyzed:

- Guillotine rupture of a single SG Tube.

Two break locations were considered:

- Bottom of SG,
- Top of SG.

The following availability of safety functions was considered:

- all available (except for the helium purification system),
- failure of SG drain,
- failure of SG drain and blower flaps closure.

The helium purification system was not taken into account in any of the analyzed cases.

The following modeling parameters were used:

- Best estimate oxidation model (section 2.2),
- Conservative oxidation model (section 2.2). The conservative oxidation was considered only with the cases when SG drain is not available, because with SG drain available oxidation is very low.

The initial condition for all analyses is steady state at 105% reactor power.

4.1 Guillotine Rupture at the Bottom of SG

A guillotine break at the bottom of the SG is considered. In order to model the guillotine break, the broken tube is modeled separately. The steam/water side of SG tubes is modeled with Control Volumes CV-501 ÷ CV-520 (Figure 3-7, Figure 3-8). These volumes represent 665 identical tubes. For the water ingress analyses Control Volumes CV-901 ÷ CV-920 were introduced to model the broken tube. These volumes represent the broken tube and therefore have a multiplicity equal to the number of the broken tubes (in current analyses 1). At the same time the multiplicity of CV-501 ÷ CV-520 has been decreased accordingly. The same was done with Junctions representing connections and Solid Heat Conductors representing the tube walls. Nodalization is shown in Figure 4-1. The guillotine break is modeled as follows.

- JN-920, representing the normal inlet to the SG tubes, is closed at the time of break (note that in the model the positive direction of all junctions was assumed downwards, therefore in normal situation the flow on the secondary side is negative).
- JN-921, connecting CV-920 with CV-330 rather than CV-530, is opened at the time of break. Geometry of this junction is the same as JN-920.
- JN-922, connecting the secondary side inlet (CV-530) to the primary side outlet plenum (CV-330), is opened at the time of break. Geometrical data is the same for JN-920 and JN-922 except for the flow length which was set to a small value and the *K*-factor (see section 3.2.3).

Separate calculations were performed to achieve steady state with the model extended by the broken tube. Accident simulation was performed as follows:

- 100 seconds of steady state, starting at *t*=–100. seconds.
- 100 hours (4 days and 4 hours) of accident simulation, starting at *t*=0.0s, ending at *t*=360,000 s.

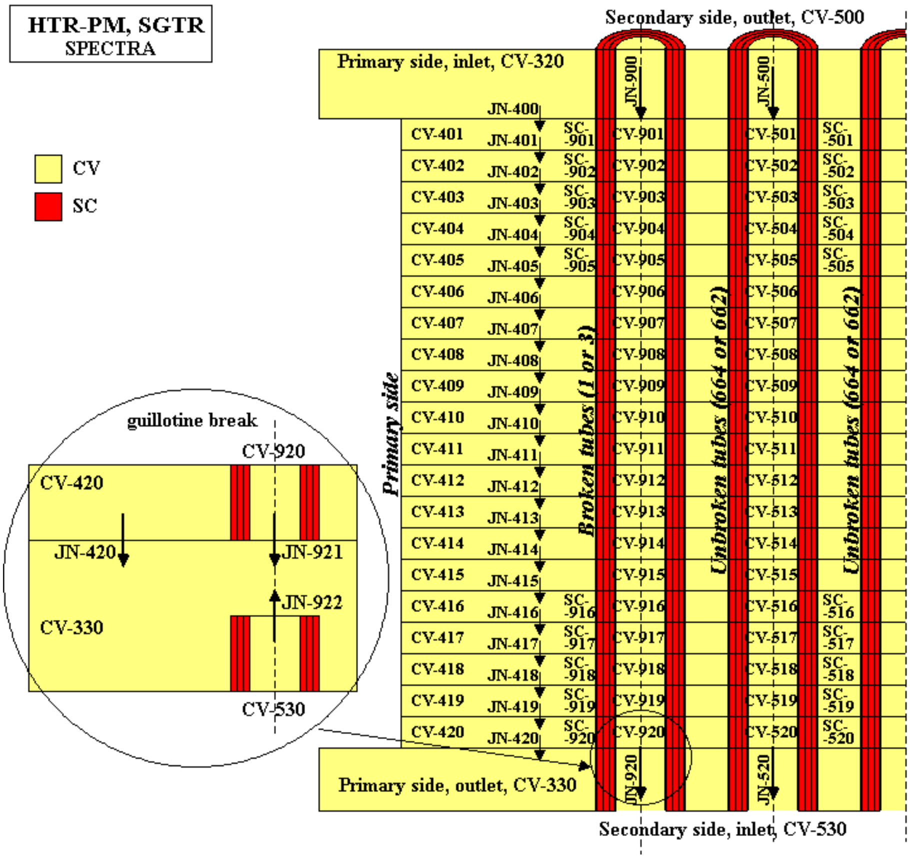

Figure 4-1 : Nodalization of broken tube(s) and the guillotine break at the bottom

4.1.1 1-Tube Rupture, Safety Systems Available

This section presents results of a break of single tube at the bottom of SG, with safety systems available (except for the helium purification system, which is not taken into account in any of the analyses presented in this report). Results are shown in Figure 4-2 through Figure 4-17 and Table 4-1 through Table 4-3.

The mass flow through the break is shown in Figure 4-2. The flow from the broken tube has a short peak with a maximum value of about 1.7 kg/s. On the plenum side the flow (through the orifice) is somewhat below 1 kg/s. The break flow lasts about 65 seconds. Afterwards pressures equilibrate due to quick opening of the SG drain valve. The SG drain is initiated at 20 seconds [11]. The drain valve is fully open at 23 s. The drain valve starts closing when the SG pressure drops to 7.3 MPa, at 63 s, and is fully closed at 66 s.

Figure 4-12 and Figure 4-13 show the state of the system at 20 seconds, when the drain valve begins to open. Figure 4-14 and Figure 4-15 show the state of the system at 65 seconds, at the end of the blowdown phase (when primary and secondary pressures equilibrate). At the end of the blowdown phase the masses of steam/water mixtures that have entered the primary system are shown below.

End of blowdown:

- tube side (JN-921): 17 kg
- plenum side (JN-922): 35 kg
- **total 52 kg**

After the blowdown is terminated, there is a very small flow through the break. Positive flow through JN-921 is approximately balanced by negative flow through JN-922. Over the analyzed part of accident the integrated flow through this break is **224 kg** Figure 4-3, Table 4-3.

The humidity detectors are assumed to initiate safety actions at 10 seconds. The reactor SCRAM is initiated with a 2 seconds delay. The total drop time of the control rods is 50 seconds [10]. Additionally, small absorber spheres are dropped 5 hours after SCRAM to ensure long term sub-criticality [10]. Maximum reactor power, about 106% or 265 MW is observed at 12 seconds - Figure 4-4. At this time the amount of steam and water in the primary system is about 18 kg, 4.0 kg of steam and 14.3 kg of liquid. In the analysis presented in [10] it was conservatively assumed that 600 kg entered the primary system instantaneously and in the form of steam. Therefore the power increase was much more significant (about 16 MW compared to only about 2 MW in the present analysis). The relatively small power increase is a consequence of small amount of steam reaching the core before the SCRAM is initiated - Figure 4-6. Maximum reactivity due to steam ingress is 0.021 $, corresponding to the steam density of 0.036 kg/m^3. This value is based on an average steam density in the core. Local density and therefore reactivity may be larger. At the time of SCRAM the maximum steam density in the upper part of the core is about 0.012 kg/m^3, while the average value is 0.007 kg/m^3. With the point kinetics used, the power increase is small - only about 1%. The local effect will increase the power somewhat but it is expected to be within few percent. To study the local effect in detail, a 3-D kinetics model is needed.

The maximum and average fuel temperatures are shown in Figure 4-7. The maximum fuel temperature is 1314 K (1041°C). Natural convection in the core results in a shift of the core maximum temperatures (Figure 4-16) and consequently the maximum corrosion (Figure 4-17) to the upper part of the core.

The system pressures are shown in Figure 4-8 and Figure 4-9. The blowdown is finished within about 65 seconds. In the long term, the primary pressure never reaches the setpoint of the primary pressure release system, 7.9 MPa.

Graphite corrosion is shown in Figure 4-10 and Table 4-1. After 100 hours the total mass of carbon reacted is 4.9 kg. The maximum corrosion depth is 0.007 mm, corresponding to the oxidation density (oxidized mass per unit volume of core) of 67.9 mol/m^3. This will not result in any damage of the fuel elements - the thickness of the graphite layer around the fuel zone is 5 mm. Such is the critical oxidation depth in case of uniform oxidation. The oxidized volume would in such case be 42% of the total pebble volume. In reality the pebbles will always be subjected to anisotropic oxidation. Reference [10] provides estimation of critical oxidation depth in case of a non-uniform oxidation. A non-uniform corrosion factor of 6 was assumed. Therefore the critical volume is estimated as 7% (=42/6).

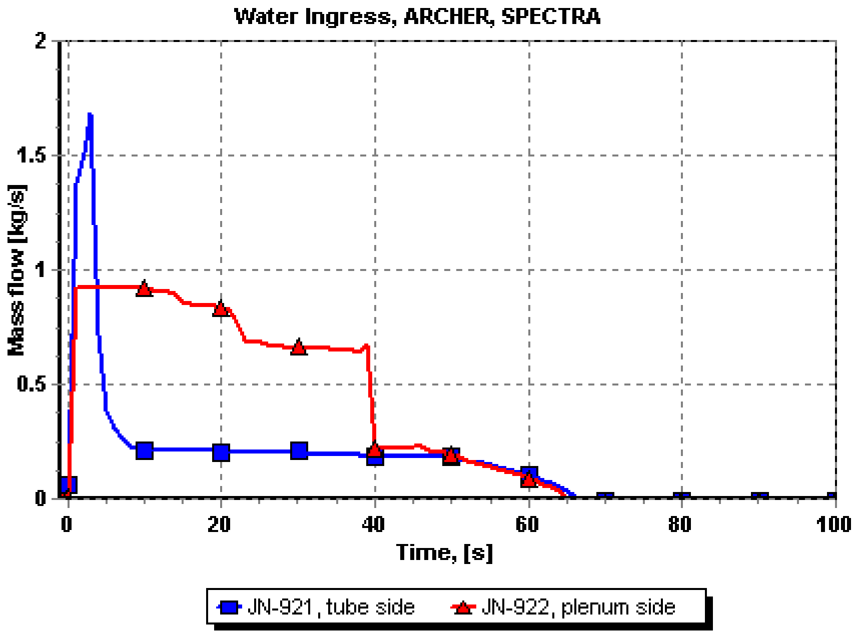

Figure 4-2 :
Break flows (1-tube, bottom of SG, safety systems available)

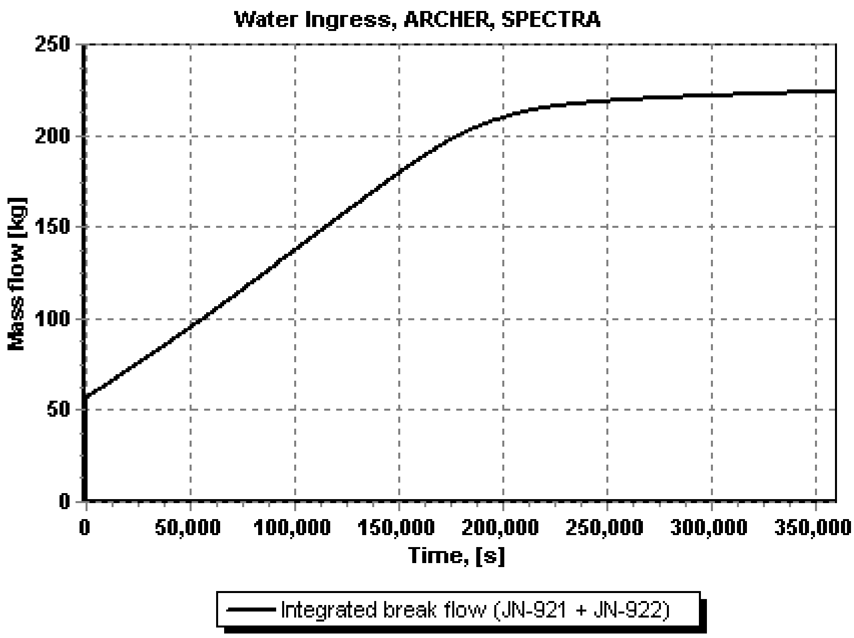

Figure 4-3 :
Integrated break flow (1-tube, bottom of SG, safety systems available)

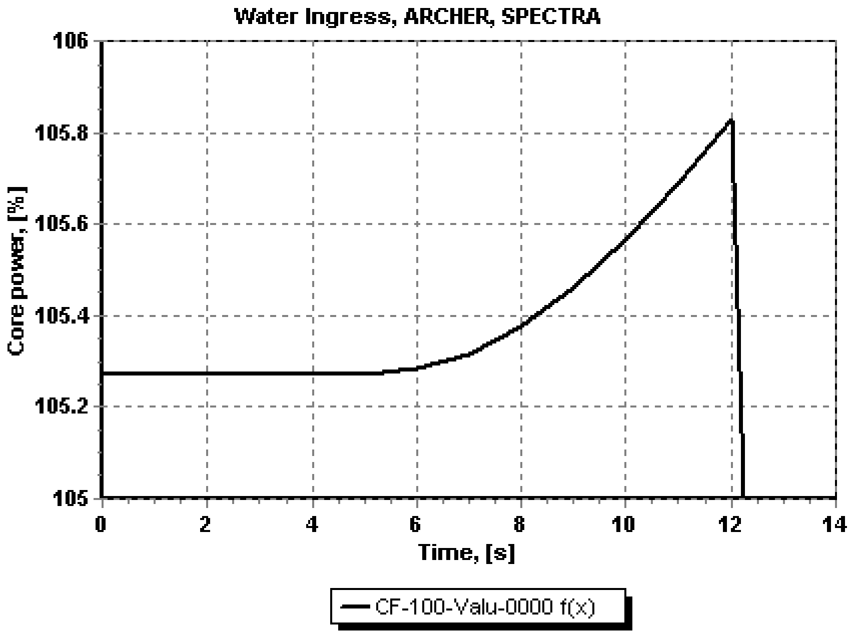

Figure 4-4 :
Relative core power (1-tube, bottom of SG, safety systems available)

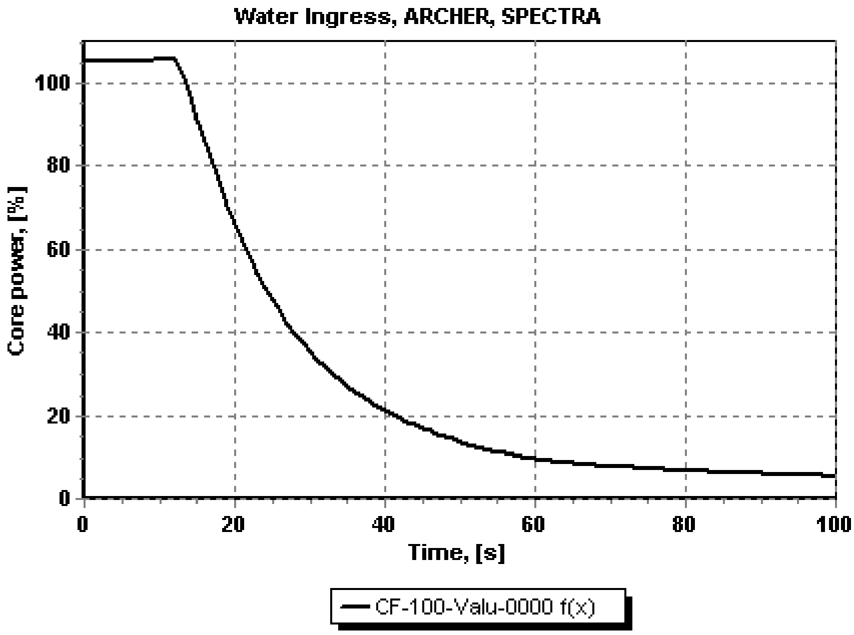

Figure 4-5 :
Relative core power (1-tube, bottom of SG, safety systems available)

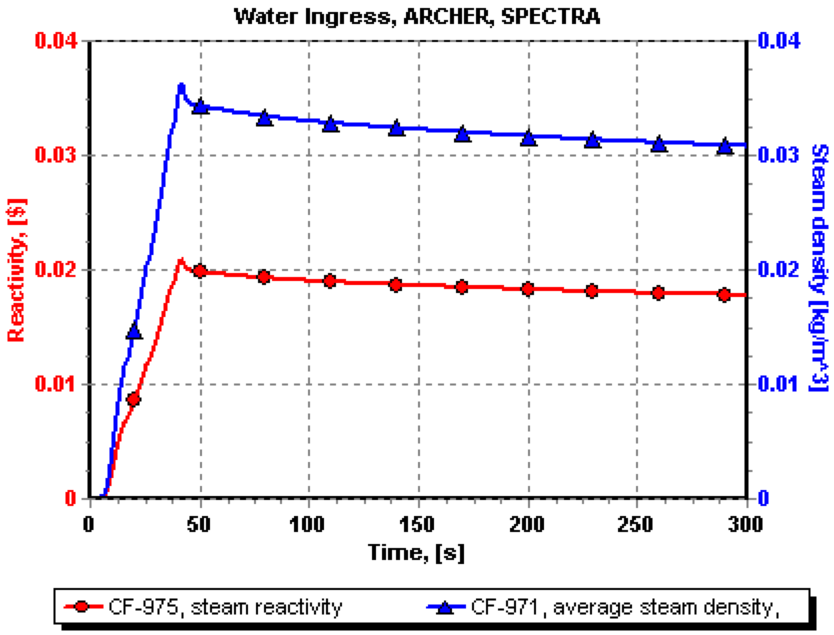

Figure 4-6 :
Steam density and reactivity (1-tube, bottom of SG, safety systems available)

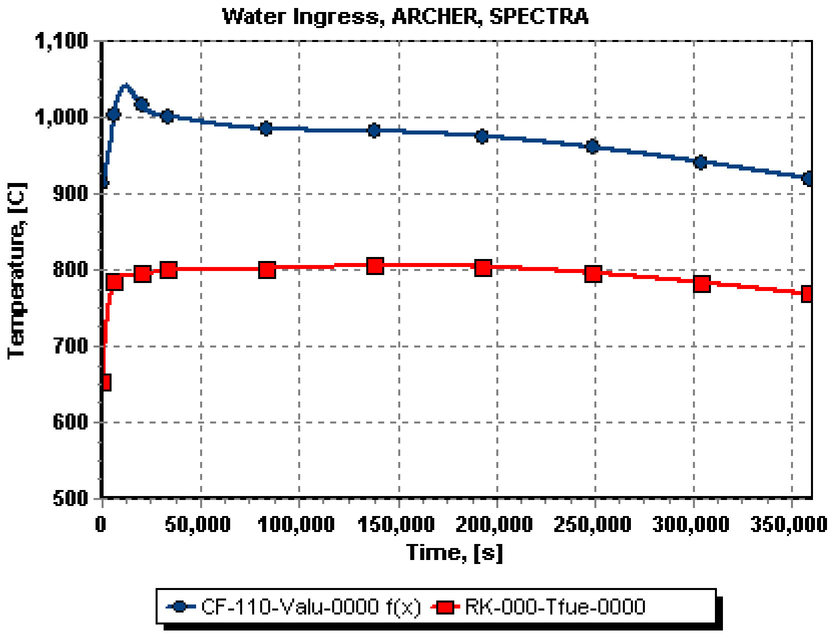

Figure 4-7 :
Fuel temperatures (1-tube, bottom of SG, safety systems available)

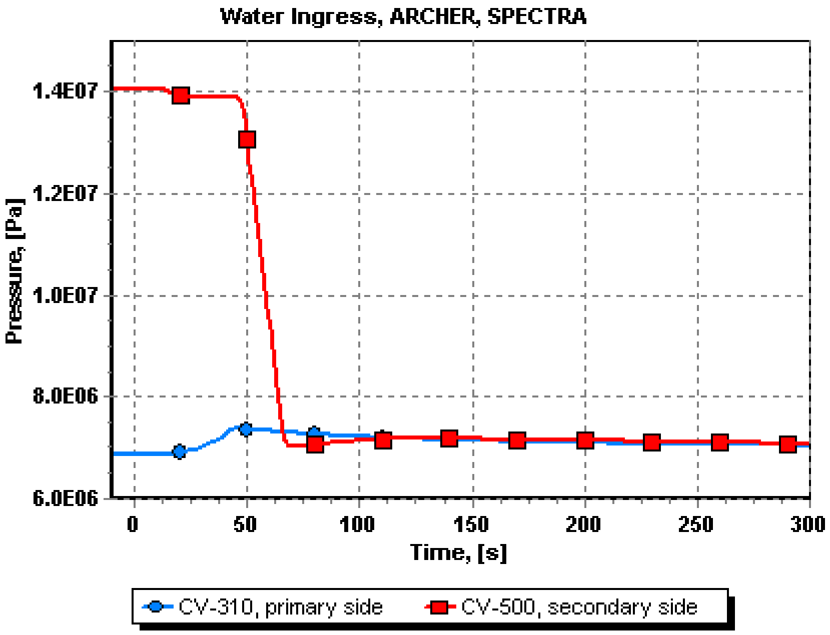

Figure 4-8 :
Pressures - short term (1-tube, bottom of SG, safety systems available)

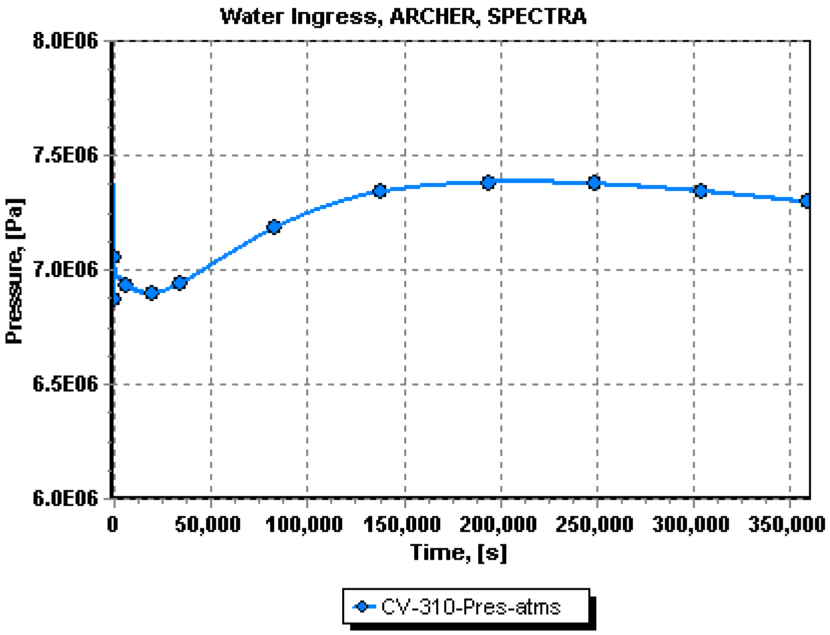

Figure 4-9 :
Primary pressure - long term (1-tube, bottom of SG, safety systems available)

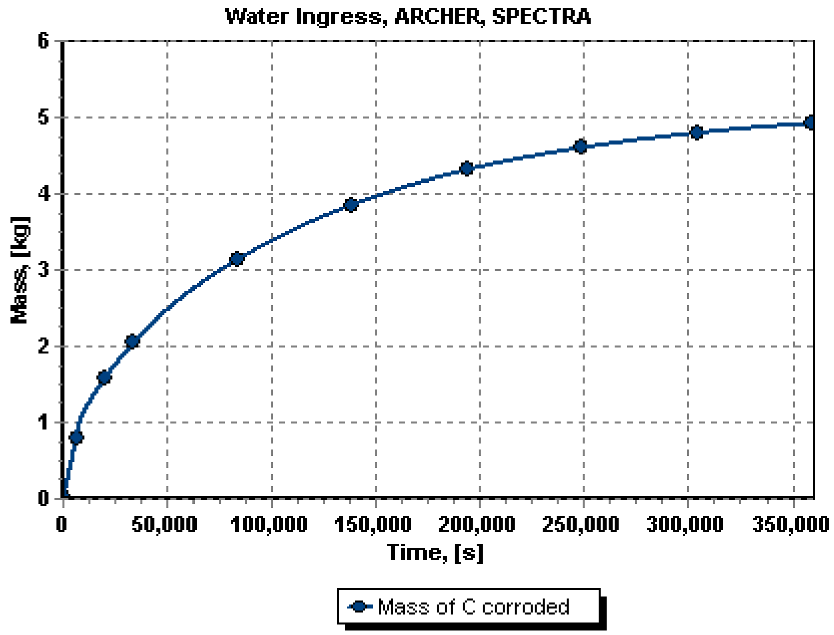

Figure 4-10 :
Graphite corrosion mass (1-tube, bottom of SG, safety systems available)

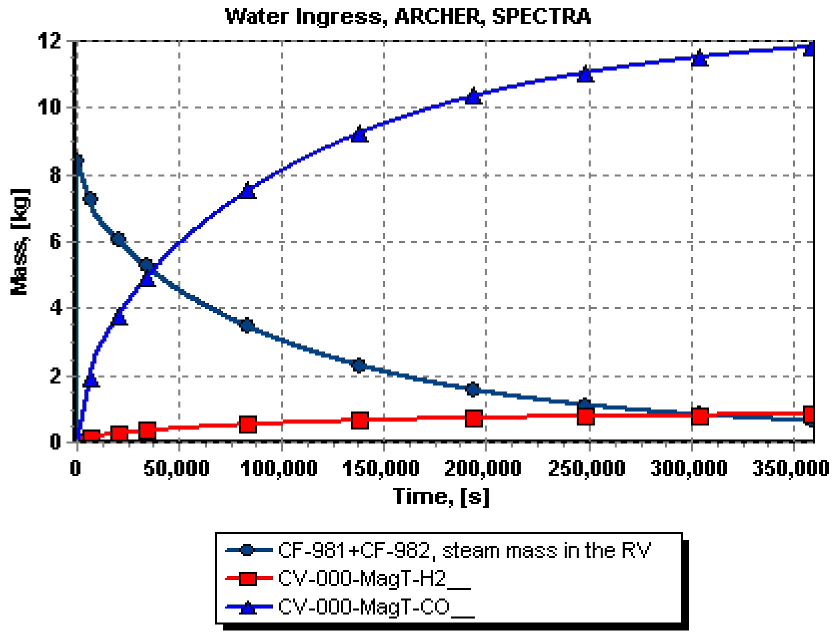

Figure 4-11 :
Mass of steam in RV and total mass of generated H_2 and CO
(1-tube, bottom of SG, safety systems available)

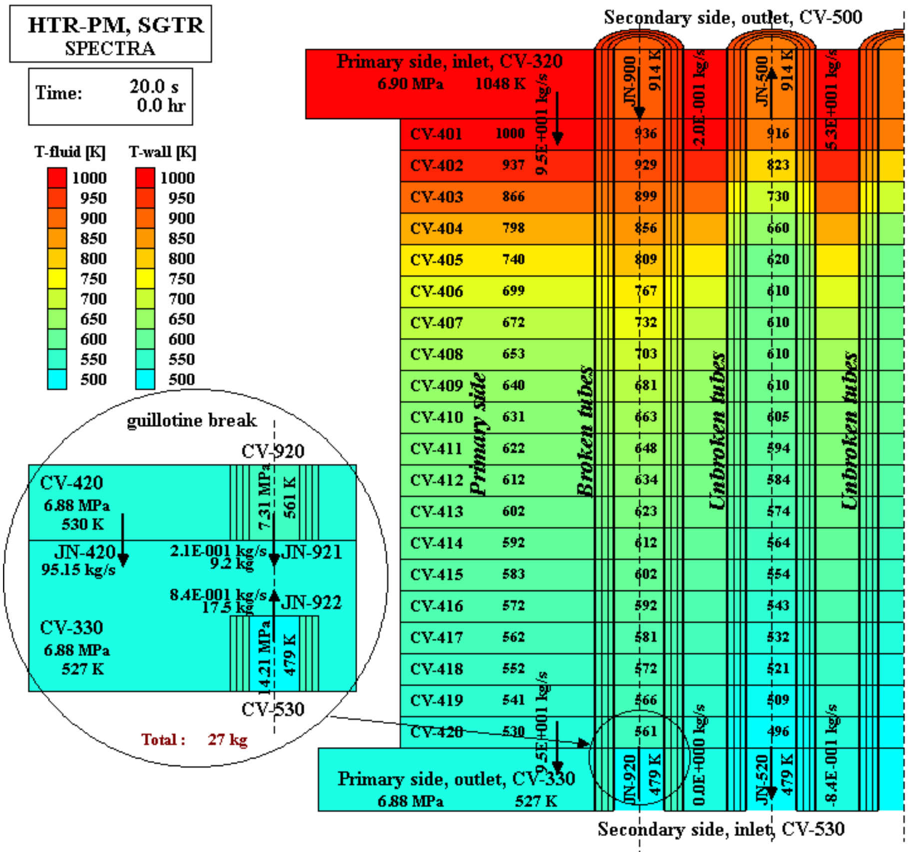

Figure 4-12 :

Break at *t*=20 s (1-tube, bottom of SG, safety systems available)

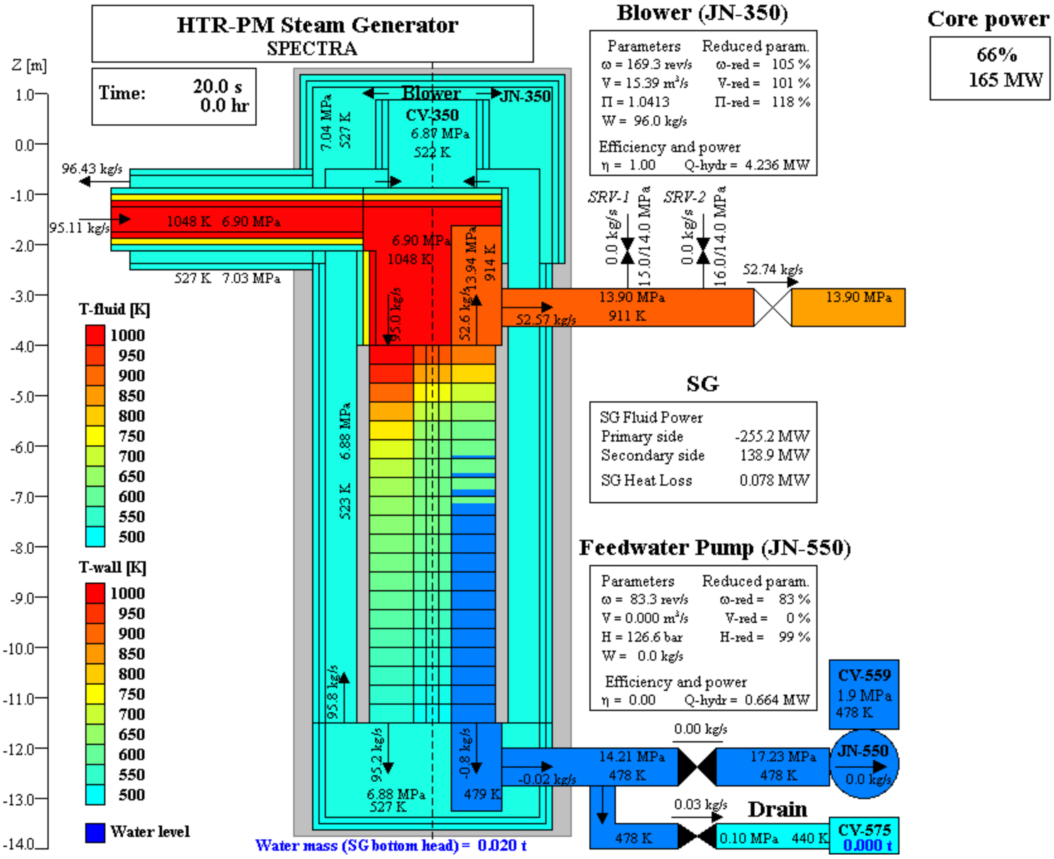

Figure 4-13 :

SG vessel at *t*=20 s (1-tube, bottom of SG, safety systems available)

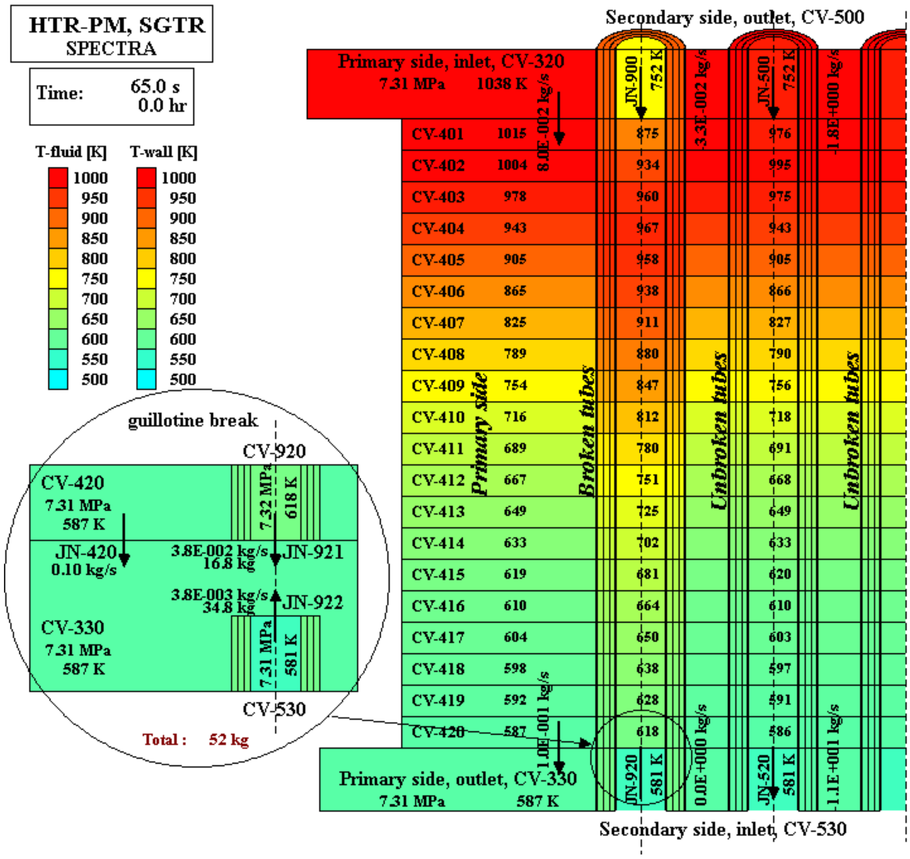

Figure 4-14 :

Break at *t*=65 s (1-tube, bottom of SG, safety systems available)

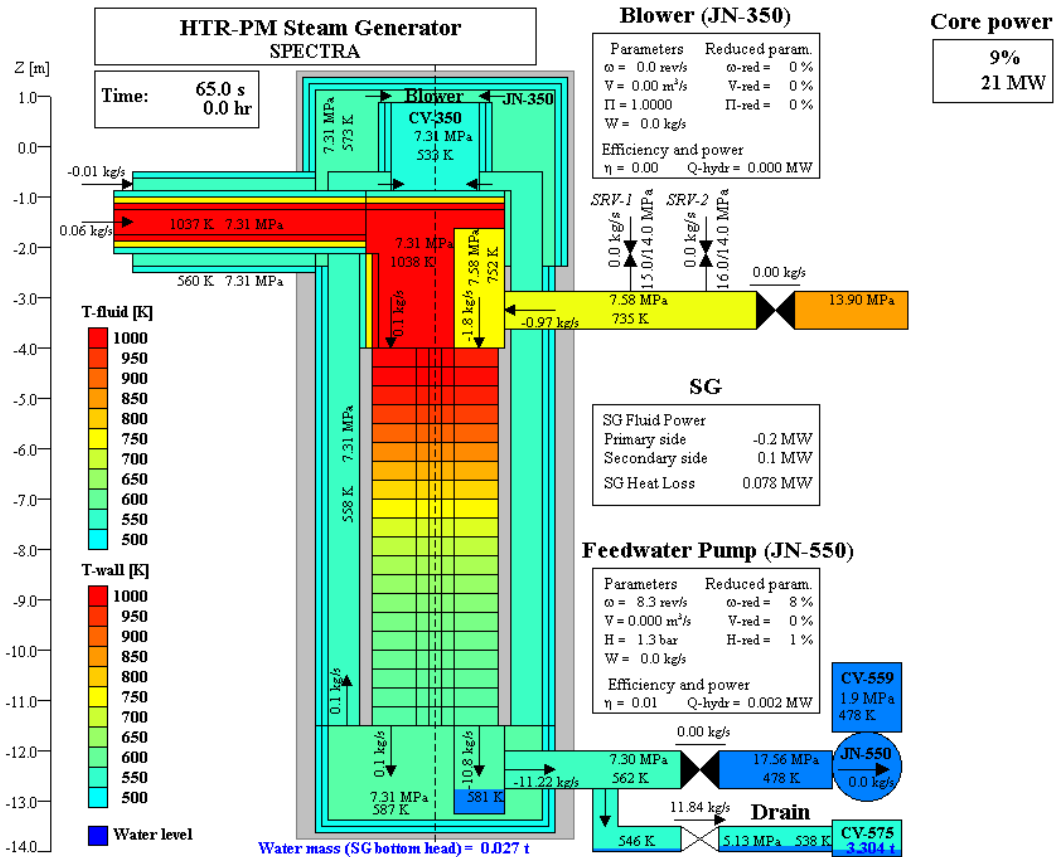

Figure 4-15 :

SG vessel at *t*=65 s (1-tube, bottom of SG, safety systems available)

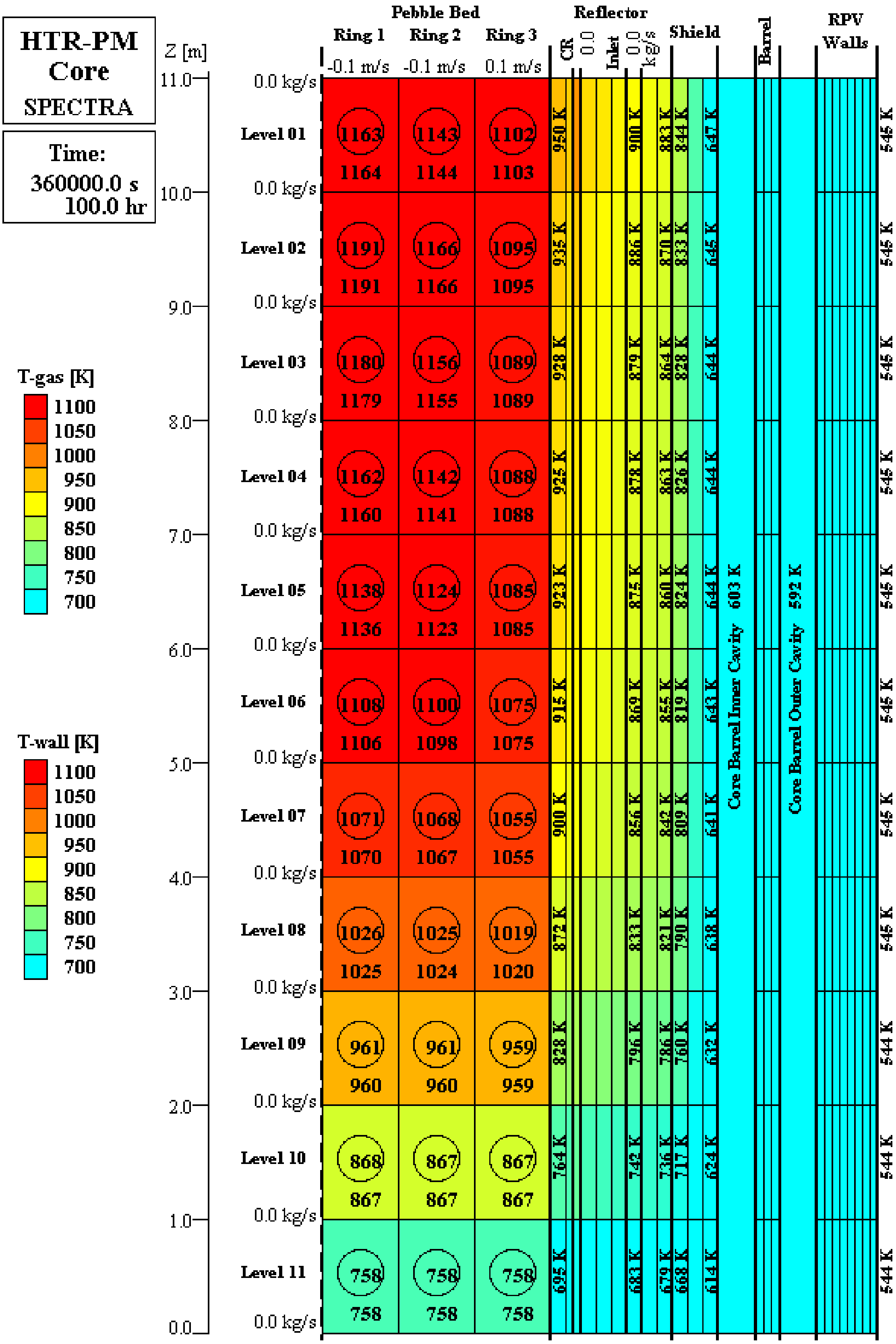

Figure 4-16 :

Temperatures at *t*=100 hr (1-tube, bottom of SG, safety systems available)

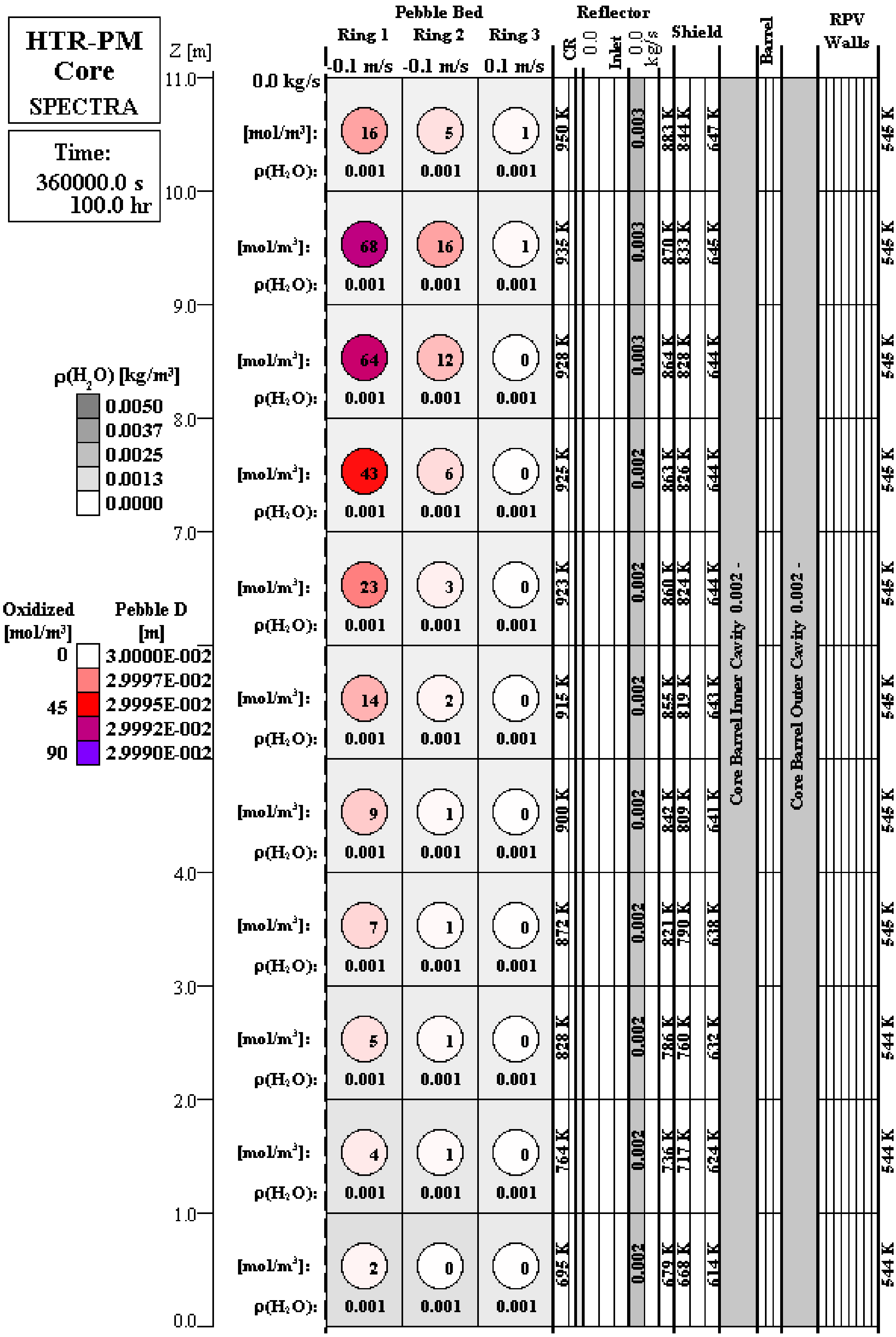

Figure 4-17 :

Oxidation at *t*=100 hr (1-tube, bottom of SG, safety systems available)

Table 4-1 : Oxidation at *t*= 100 hr (1-tube, bottom of SG, safety systems available)

HTR-PM Oxidation Summary
SPECTRA

Time: 3.60E+005 s, 1.00E+002 hr

	Oxidation depth, [mm]			Oxidized mass, [mol/m³]		
	Ring 1	Ring 2	Ring 3	Ring 1	Ring 2	Ring 3
01	0.002	0.001	0.000	16.3	5.4	0.9
02	0.007	0.002	0.000	67.9	16.3	0.9
03	0.007	0.001	0.000	64.2	11.8	0.0
04	0.005	0.001	0.000	42.5	6.3	0.0
05	0.003	0.000	0.000	22.6	2.7	0.0
06	0.002	0.000	0.000	13.6	1.8	0.0
07	0.001	0.000	0.000	9.1	0.9	0.0
08	0.001	0.000	0.000	7.2	0.9	0.0
09	0.001	0.000	0.000	5.4	0.9	0.0
10	0.000	0.000	0.000	3.6	0.9	0.0
11	0.000	0.000	0.000	1.8	0.0	0.0

Table 4-2 : State at *t*= 20 s (1-tube, bottom of SG, safety systems available)

HTR-PM Water Ingress Summary
SPECTRA

Time: 2.00E+001 s, 5.56E-003 hr

Steam masses	abs. [kg]	rel. [%]	Water masses	abs. [kg]	rel. [%]
RV, pebble bed:	3.0	44.6%	RV, pebble bed:	0.0	0.0%
RV, other:	0.5	6.8%	RV, other:	0.0	0.0%
SG primary side:	3.1	46.1%	SG primary side:	20.2	100.0%
SG tubes, primary:	0.2	2.4%	SG tubes, primary:	0.0	0.0%
Primary system, total:	6.6	100.0%	Primary system, total:	20.2	100.0%

Total masses [kg]		Drained mass [kg]	
Liquid:	4176.5	CV-575:	0.0
Gases:		**Reacted C [kg]**	
He:	3045.6	Measur. 1:	0.0
H_2:	0.0	Measur. 2:	0.0
CO:	0.0		

Integrated flow through the break [kg]	
Integrated flow, total:	26.7

Table 4-3 : State at *t*= 100 hr (1-tube, bottom of SG, safety systems available)

HTR-PM Water Ingress Summary
SPECTRA

Time: 3.60E+005 s, 1.00E+002 hr

Steam masses	abs. [kg]	rel. [%]	Water masses	abs. [kg]	rel. [%]
RV, pebble bed:	0.4	1.2%	RV, pebble bed:	0.0	0.0%
RV, other:	0.2	0.7%	RV, other:	0.0	0.0%
SG primary side:	33.6	97.5%	SG primary side:	142.1	100.0%
SG tubes, primary:	0.2	0.6%	SG tubes, primary:	0.0	0.0%
Primary system, total:	34.5	100.0%	Primary system, total:	142.1	100.0%

Total masses [kg]		Drained mass [kg]	
Liquid:	3635.3	CV-575:	3215.1
Gases:		**Reacted C [kg]**	
He:	3045.6	Measur. 1:	4.9
H_2:	0.8	Measur. 2:	4.9
CO:	11.8		

Integrated flow through the break [kg]	
Integrated flow, total:	224.0

This means that with this estimation of non-uniformity, the Estimated Critical Depth (ECD) of oxidation (corresponding to oxidized volume of 7 vol.%) is 0.72 mm. In the present case the maximum oxidation depth is 0.007 mm, or 0.07 vol.%. This means the maximum corrosion is 1.0% of ECD.

maximum corrosion = 0.07 vol.% = 1.0% of ECD

Gas masses are shown in Figure 4-11, including the mass of steam in the reactor vessel and the total amounts of the gases generated due to corrosion: H_2 and CO. The mass of steam in the RV, equal to 8.5 kg soon after the break, slowly decreases as the corrosion proceeds. At the same time the mass of reaction products increases. At 100 hours there is still 0.6 kg of steam in the RV (Figure 4-11, Table 4-3).

4.1.2 1-Tube Rupture, Failure of SG Drain

This section presents results of a break of single tube at the bottom of SG, with simultaneous failure of the SG drain system. Results are shown in Figure 4-18 through Figure 4-31 and Table 4-4 through Table 4-6.

The mass flow through the break is shown in Figure 4-18. At the end of blowdown (about 4000 s) - Figure 4-28 - about **1906 kg** of steam/water mixture has entered the primary system, most of it through the plenum side of the break (JN-922: about 1562 kg). Most of the water remains at the SG lower head as liquid. At the end of blowdown the mass of liquid in the lower head is about 1445 kg - Figure 4-29. At the end of the calculations it is equal to 2646 kg (Table 4-6). The total amount of water/steam entering the primary system in this scenario is **2659 kg** (Table 4-6). Most of it remains as liquid at the SG lower head and never enters the core.

The humidity detectors are assumed to initiate safety actions at 10 seconds. The reactor SCRAM is initiated with a 2 seconds delay. The total drop time of the control rods is 50 seconds [10]. Additionally small absorber spheres are dropped to ensure long term subcriticality [10]. Maximum reactor power, about 106% or 265 MW is observed at 12 seconds. The maximum reactivity due to steam ingress is below 0.02 $, corresponding to the steam density of about 0.034 kg/m^3 - Figure 4-20.

The SG drain system is not used in this scenario. Consequently there is more liquid entering the primary system. The mass flow through the break decreases slowly until pressures equilibrate at about 4000 s - Figure 4-18, Figure 4-22.

In contrast to the previous case where steam was flowing at the later phase, there is practically pure liquid flowing through the break all the time. Some of that liquid evaporates due to flashing, but still the amount of steam reaching the reactor vessel is somewhat smaller than in the case when drain is active. Therefore, **when the break is at the bottom of the SG tubes, the amount of steam entering the core is not larger when the SG drain system fails**. Failure of the SG drain keeps the break under a “protective” layer of water.

The maximum and average fuel temperatures are shown in Figure 4-21. The maximum fuel temperature is 1309 K (1036°C). Natural convection in the core results in a shift of the core maximum temperatures (Figure 4-30) and consequently the maximum corrosion (Figure 4-31) to the upper part of the core.

The system pressures are shown in Figure 4-22 and Figure 4-23. The blowdown is finished within about 4000 seconds. In the long term, the primary pressure never reaches the setpoint of the primary pressure release system, 7.9 MPa.

Graphite corrosion is shown in Figure 4-24 and Table 4-4. After 100 hours the total mass of carbon reacted is about 6.0 kg. The maximum corrosion depth is about 0.010 mm, corresponding to the oxidation density of about 93 mol/m^3. The maximum oxidation depth of 0.010 mm corresponds to the oxidized volume of 0.10 vol.%. This means the maximum corrosion is 1.4% of ECD.

maximum corrosion = 0.10 vol.% = 1.4% of ECD

Gas masses are shown in Figure 4-25, including the mass of steam in the reactor vessel and the total amounts of the gases generated due to corrosion: H_2 and CO. The mass of steam in the RV, equal to about

10.8 kg soon after the break, slowly decreases as the corrosion proceeds. At the same time the mass of reaction products increases. At 100 hours there is still about 0.8 kg of steam in the RV (Figure 4-25, Table 4-6).

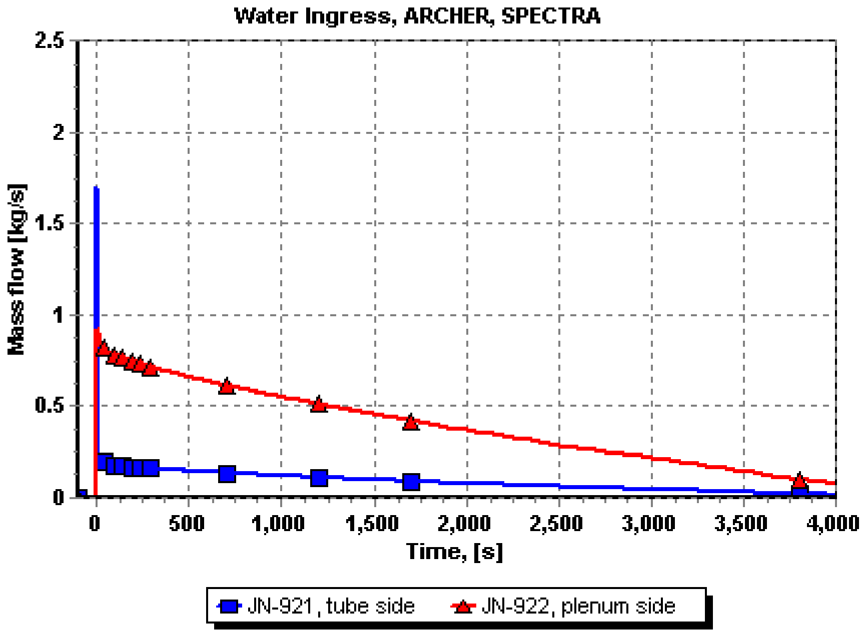

Figure 4-18 :
Break flows (1-tube, bottom of SG, failure of SG drain)

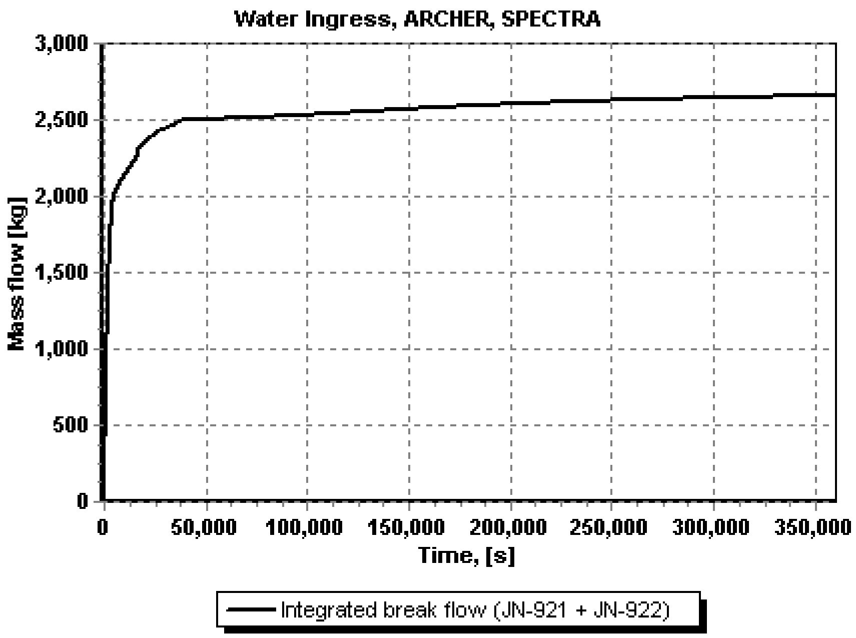

Figure 4-19 :
Integrated break flow (1-tube, bottom of SG, failure of SG drain)

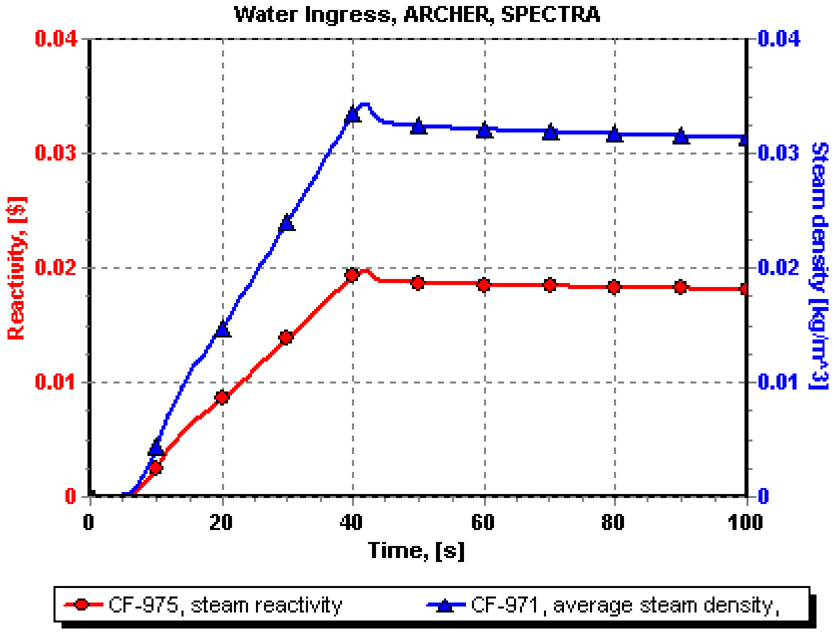

Figure 4-20 :
Steam density and reactivity (1-tube, bottom of SG, failure of SG drain)

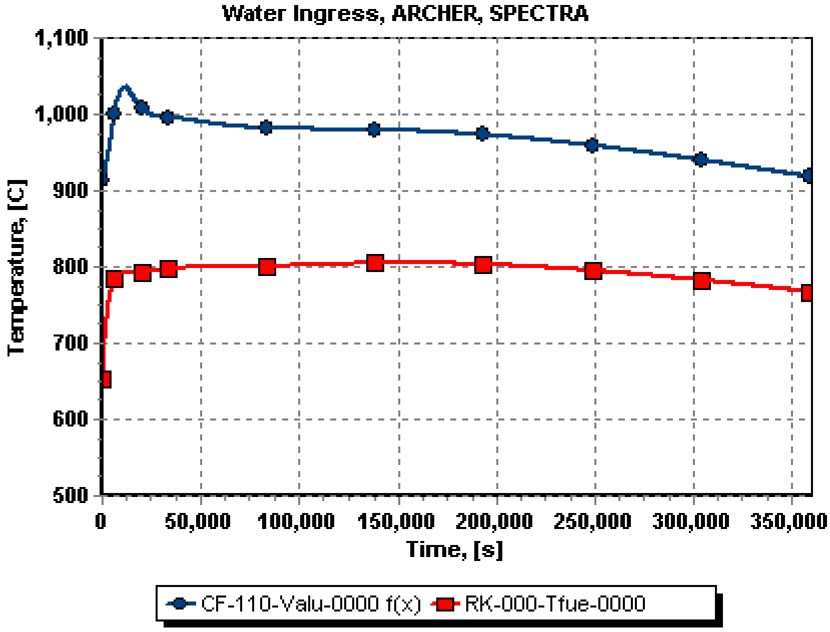

Figure 4-21 :
Fuel temperatures (1-tube, bottom of SG, failure of SG drain)

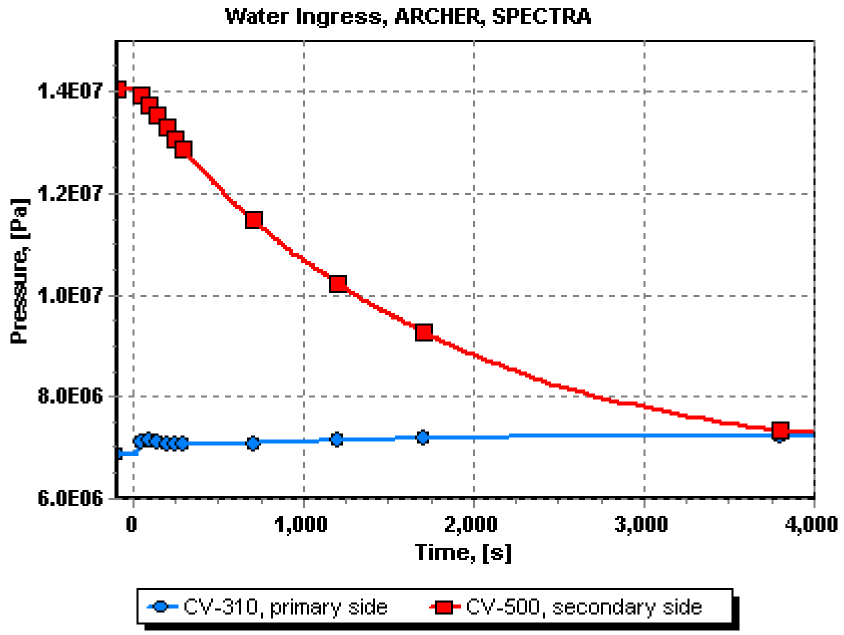

Figure 4-22 :
Pressures - short term (1-tube, bottom of SG, failure of SG drain)

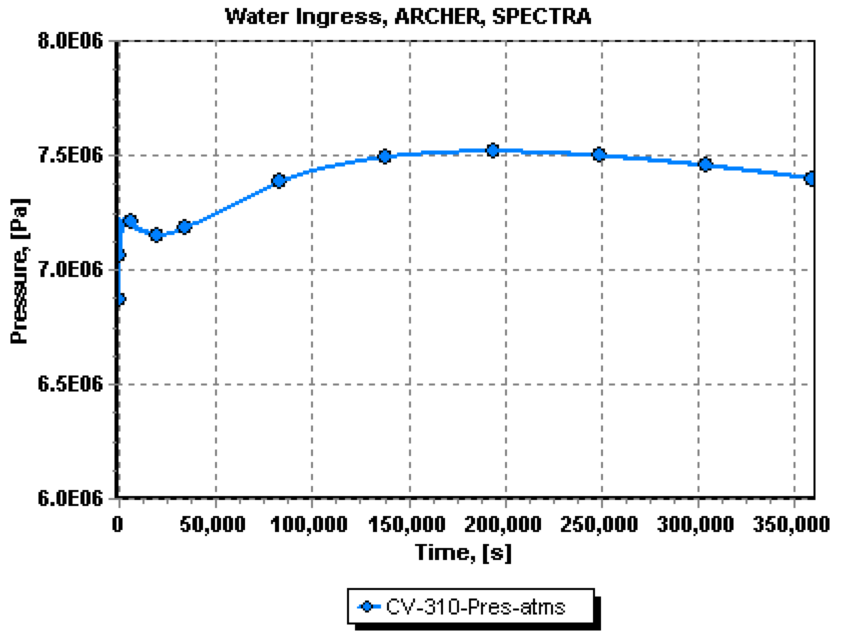

Figure 4-23 :
Primary pressure - long term (1-tube, bottom of SG, failure of SG drain)

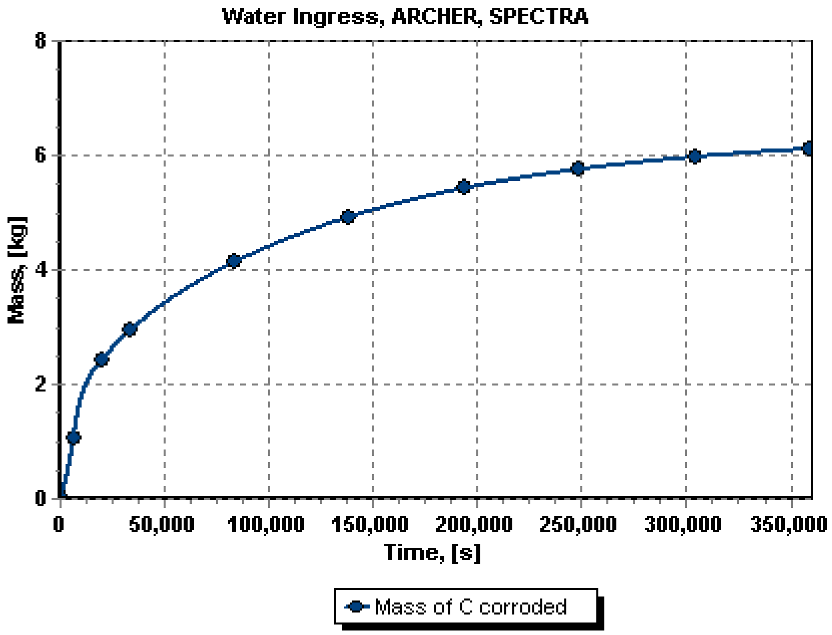

Figure 4-24 :
Graphite corrosion mass (1-tube, bottom of SG, failure of SG drain)

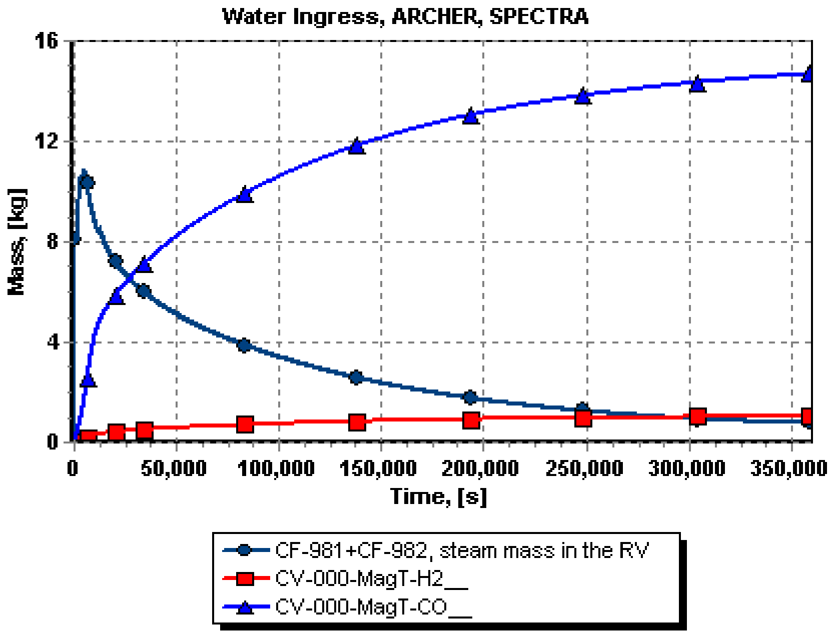

Figure 4-25 :
Mass of steam in RV and total mass of generated H_2 and CO
(1-tube, bottom of SG, failure of SG drain)

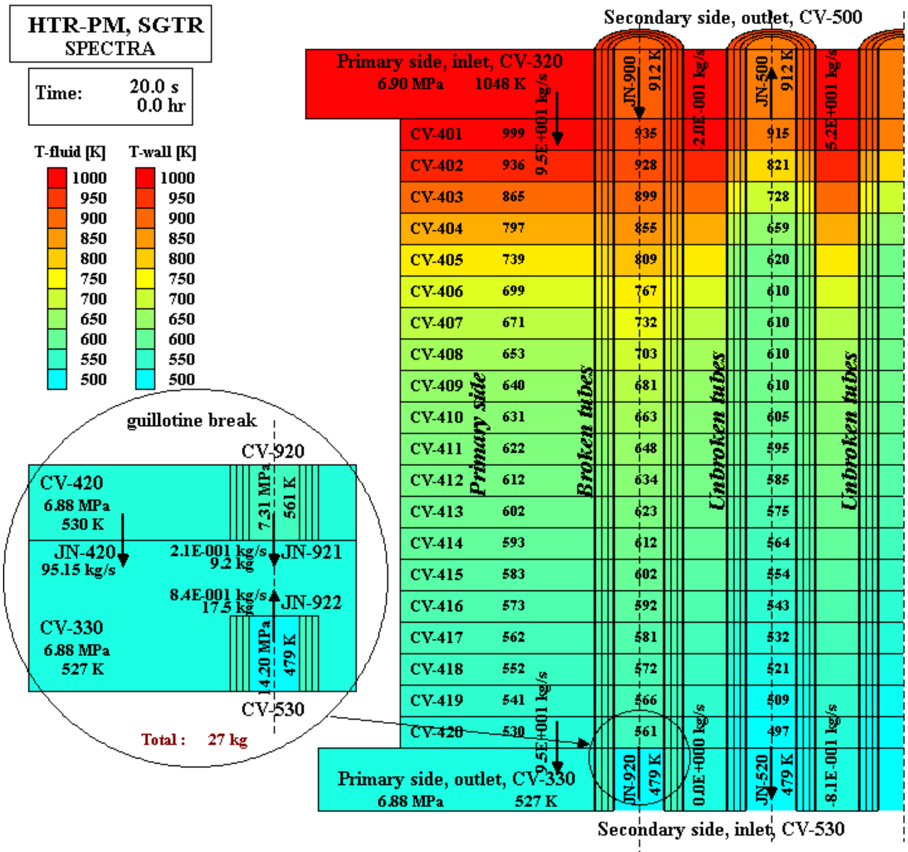

Figure 4-26 :
Break at *t*=20 s (1-tube, bottom of SG, failure of SG drain)

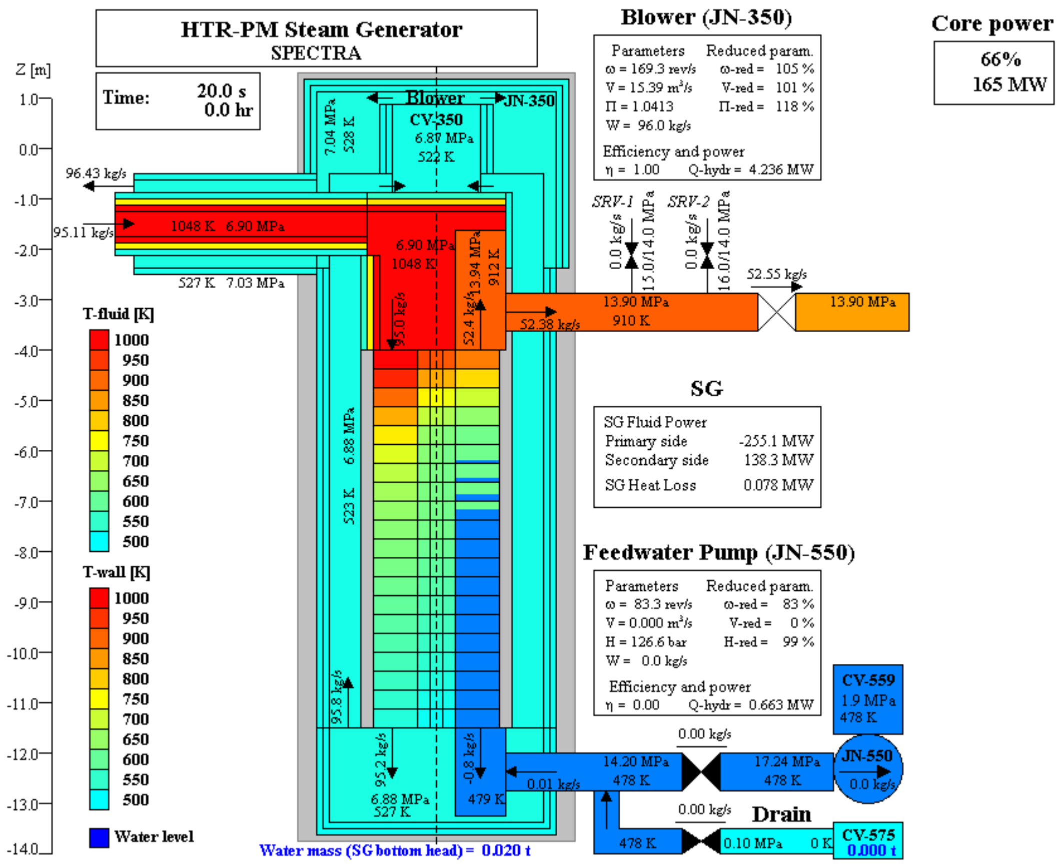

Figure 4-27 :
SG vessel at *t*=20 s (1-tube, bottom of SG, failure of SG drain)

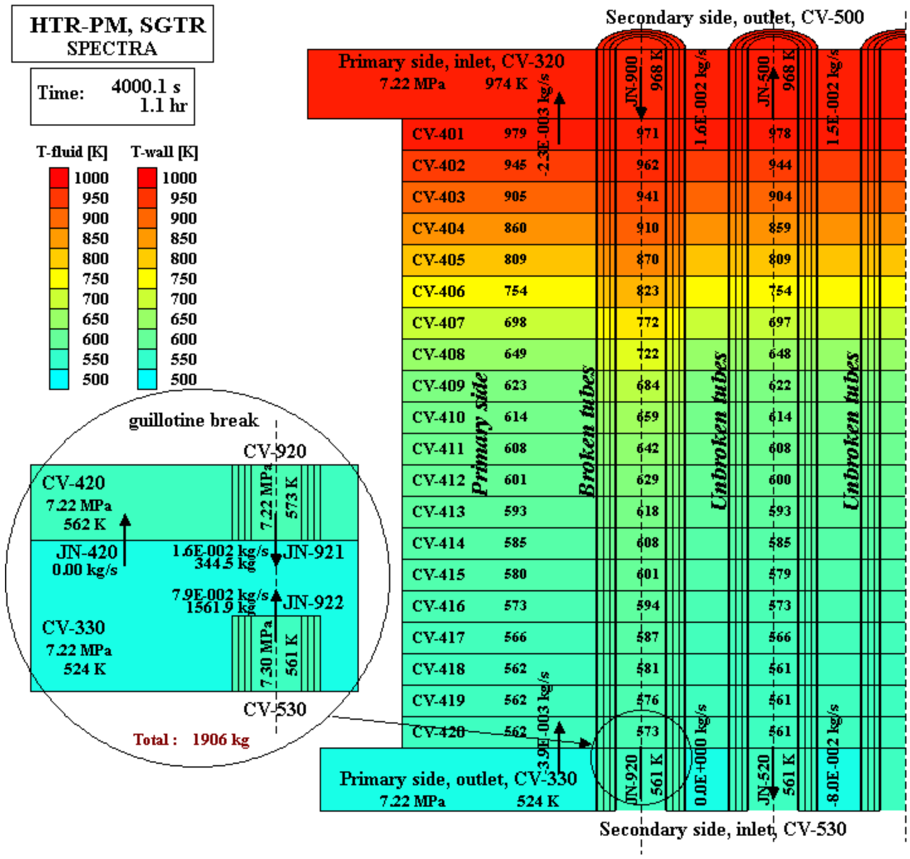

Figure 4-28 :

Break at *t*=4000 s (1-tube, bottom of SG, failure of SG drain)

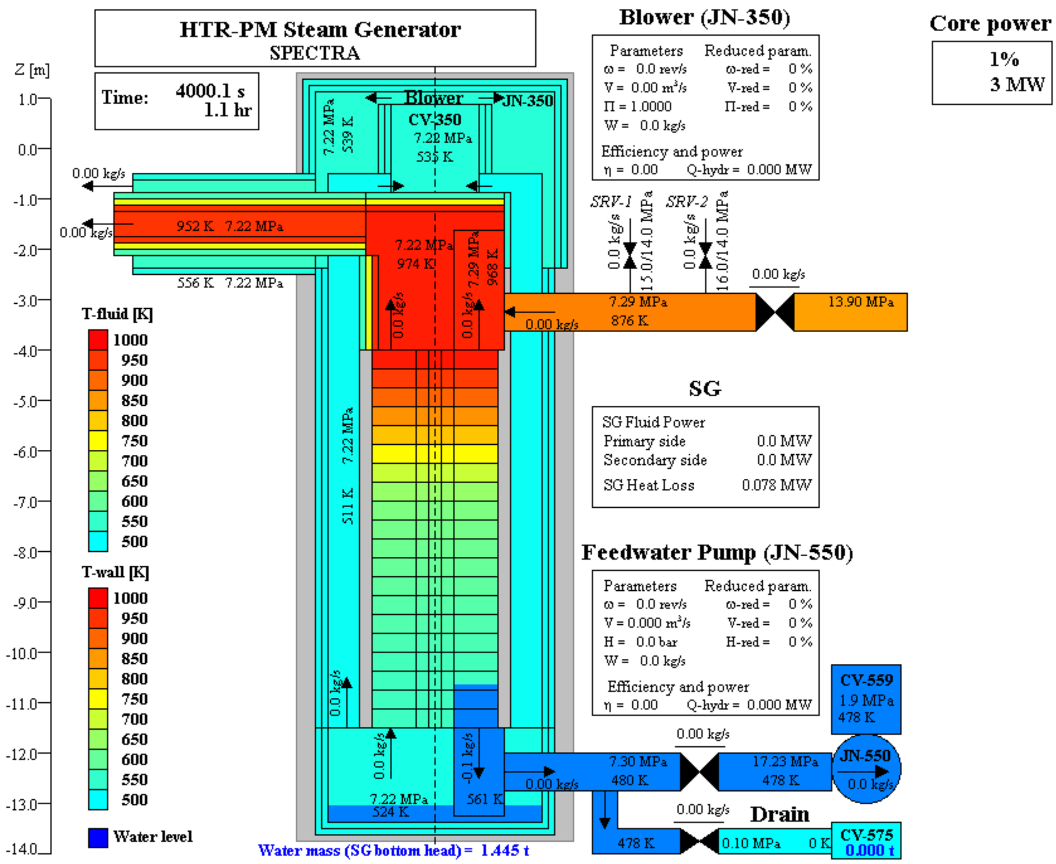

Figure 4-29 :

SG vessel at *t*=4000 s (1-tube, bottom of SG, failure of SG drain)

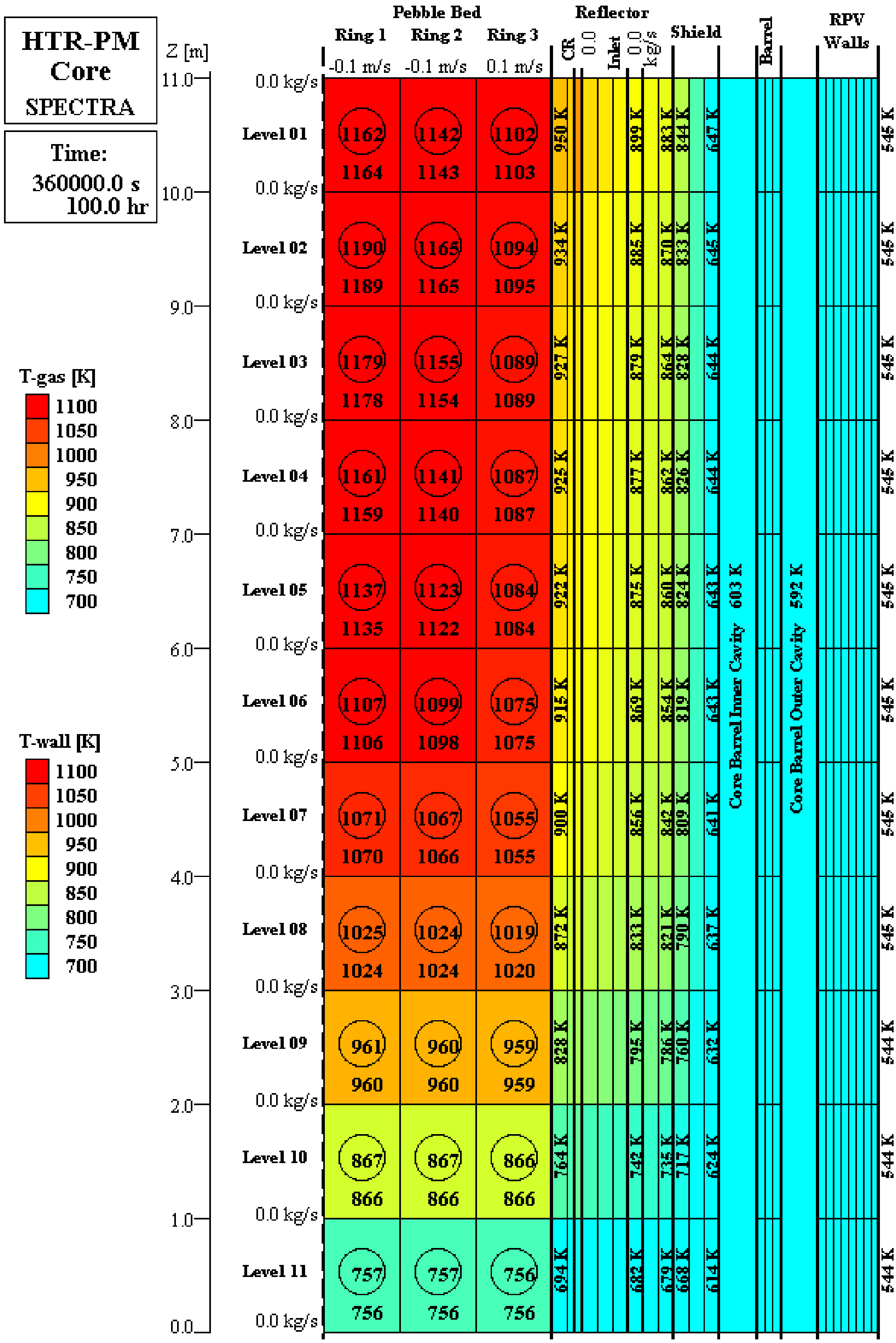

Figure 4-30 :

Temperatures at *t*=100 hr (1-tube, bottom of SG, failure of SG drain)

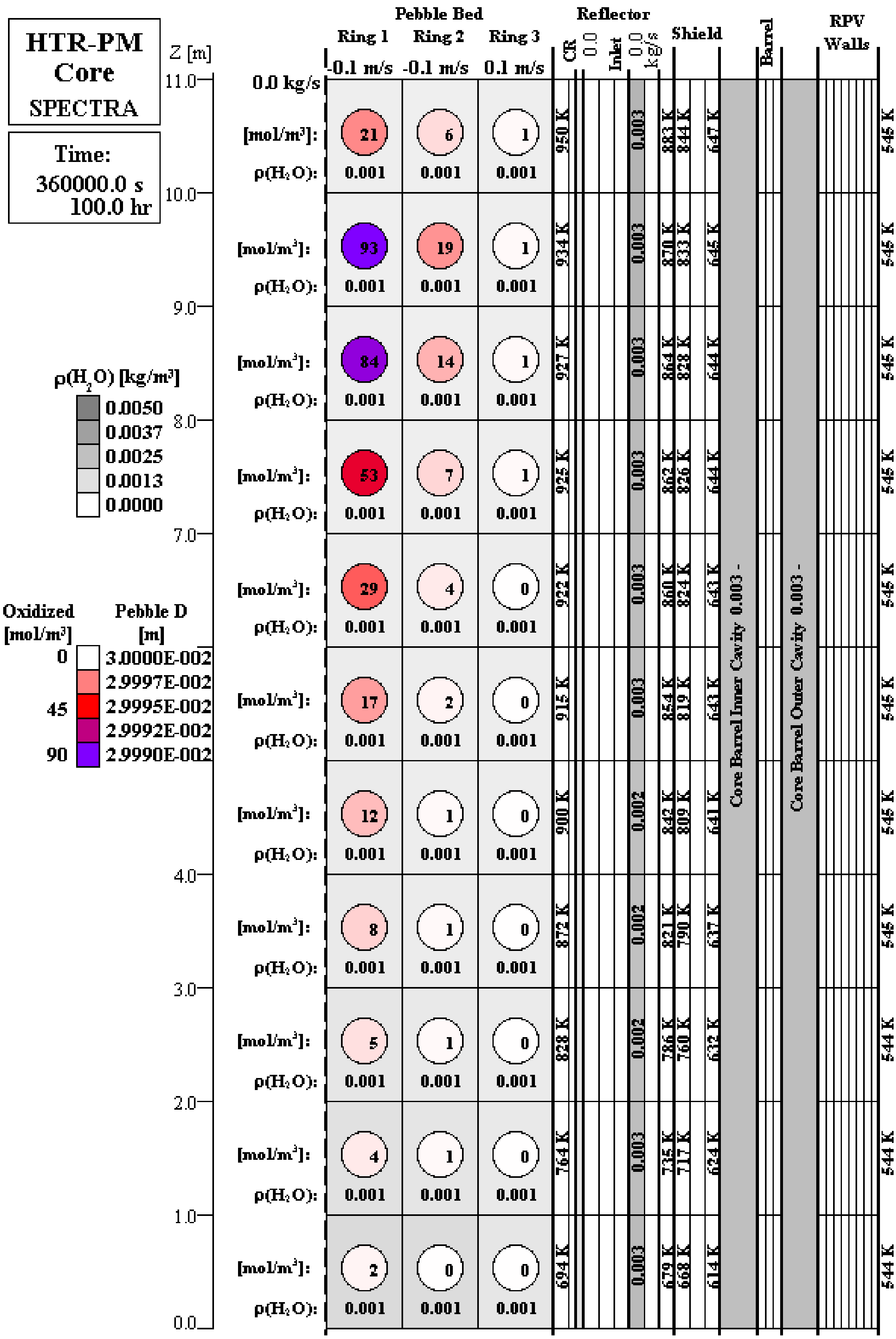

Figure 4-31 :

Oxidation at *t*=100 hr (1-tube, bottom of SG, failure of SG drain)

Table 4-4 : Oxidation at *t*= 100 hr (1-tube, bottom of SG, failure of SG drain)

HTR-PM Oxidation Summary
SPECTRA

Time: 3.60E+005 s, 1.00E+002 hr

	Oxidation depth, [mm]				Oxidized mass, [mol/m³]		
	Ring 1	Ring 2	Ring 3		Ring 1	Ring 2	Ring 3
01	0.002	0.001	0.000	01	20.8	6.3	0.9
02	0.010	0.002	0.000	02	93.2	19.0	0.9
03	0.009	0.002	0.000	03	84.2	13.6	0.9
04	0.006	0.001	0.000	04	53.4	7.2	0.9
05	0.003	0.000	0.000	05	29.0	3.6	0.0
06	0.002	0.000	0.000	06	17.2	1.8	0.0
07	0.001	0.000	0.000	07	11.8	0.9	0.0
08	0.001	0.000	0.000	08	8.2	0.9	0.0
09	0.001	0.000	0.000	09	5.4	0.9	0.0
10	0.000	0.000	0.000	10	3.6	0.9	0.0
11	0.000	0.000	0.000	11	1.8	0.0	0.0

Table 4-5 : State at *t*= 20 s (1-tube, bottom of SG, failure of SG drain)

HTR-PM Water Ingress Summary
SPECTRA

Time: 2.00E+001 s, 5.56E-003 hr

Steam masses	abs. [kg]	rel. [%]	Water masses	abs. [kg]	rel. [%]
RV, pebble bed:	3.0	44.6%	RV, pebble bed:	0.0	0.0%
RV, other:	0.5	6.8%	RV, other:	0.0	0.0%
SG primary side:	3.1	46.1%	SG primary side:	20.2	100.0%
SG tubes, primary:	0.2	2.4%	SG tubes, primary:	0.0	0.0%
Primary system, total:	6.6	100.0%	Primary system, total:	20.2	100.0%

Total masses [kg]		Drained mass [kg]		Integrated flow through the break [kg]	
Liquid:	4176.5	CV-575:	0.0	Integrated flow, total:	26.7
Gases:		Reacted C [kg]			
He:	3045.6				
H_2:	0.0	Measur. 1:	0.0		
CO:	0.0	Measur. 2:	0.0		

Table 4-6 : State at *t*= 100 hr (1-tube, bottom of SG, failure of SG drain)

HTR-PM Water Ingress Summary
SPECTRA

Time: 3.60E+005 s, 1.00E+002 hr

Steam masses	abs. [kg]	rel. [%]	Water masses	abs. [kg]	rel. [%]
RV, pebble bed:	0.5	0.6%	RV, pebble bed:	0.0	0.0%
RV, other:	0.3	0.4%	RV, other:	0.0	0.0%
SG primary side:	76.4	95.7%	SG primary side:	2646.5	100.0%
SG tubes, primary:	2.6	3.3%	SG tubes, primary:	0.0	0.0%
Primary system, total:	79.8	100.0%	Primary system, total:	2646.5	100.0%

Total masses [kg]		Drained mass [kg]		Integrated flow through the break [kg]	
Liquid:	3267.1	CV-575:	0.0	Integrated flow, total:	2659.4
Gases:		Reacted C [kg]			
He:	3045.6				
H_2:	1.0	Measur. 1:	6.0		
CO:	14.5	Measur. 2:	6.0		

4.1.3 1-Tube Rupture, Failure of SG Drain and Blower Flaps Closure

This section presents results of a break of single tube at the bottom of SG, with simultaneous failure of the SG drain system and failure to close the blower flaps. Results are shown in Figure 4-32 through Figure 4-45 and Table 4-7 through Table 4-9.

The mass flow through the break is shown in Figure 4-32. At the end of blowdown (about 1200 s) - Figure 4-42 - about **650 kg** of steam/water mixture has entered the primary system, most of it through the plenum side of the break (JN-922: 526 kg). Most of the water remains at the SG lower head as liquid. At the end of blowdown the mass of liquid in the lower head is 401 kg - Figure 4-43. The total amount of water/steam entering the primary system is about **2648 kg** - Table 4-9. As will be shown below, a large part of this water evaporates slowly and is transported to the core.

The humidity detectors are assumed to initiate safety actions at 10 seconds. The reactor SCRAM is initiated with a 2 seconds delay. The total drop time of the control rods is 50 seconds [10]. Additionally small absorber spheres are dropped to ensure long term sub-criticality [10]. Maximum reactor power, about 106% or 265 MW is observed as 12 seconds. Maximum reactivity due to steam ingress is about 1.1 $, corresponding to the steam density of about 2.4 kg/m^3 - Figure 4-34. It is much higher than in previous cases because of larger amount of steam in the core, which is explained below.

The SG drain system and the blower flaps closure are assumed to fail in this scenario. As a consequence of the open blower flaps, there is a continuous natural circulation flow through the steam generator. The circulation flow is shown in Figure 4-33, showing the mass flow at JN-251 (Figure 3-7) with the reverse sign. The circulation flow is in reverse direction compared to the normal flow. As a consequence of this flow there is a slow evaporation of water located at the SG lower head. The steam is transported into the core where it causes significantly larger corrosion than in the previous cases. Therefore, **when the break is at the bottom of the SG tubes, failure to close blower flaps causes significant corrosion due to evaporation of water in the SG lower head and transport of the steam into the reactor vessel**.

The maximum and average fuel temperatures are shown in Figure 4-35. The maximum fuel temperature is 1261 K (988°C). Natural convection in the core results in a shift of the core maximum temperatures (Figure 4-44) and consequently the maximum corrosion (Figure 4-45) to the upper part of the core.

The system pressures are shown in Figure 4-36 and Figure 4-37. The blowdown is finished within about 1200 seconds. The primary pressure reaches the setpoint of the primary pressure release system, 7.9 MPa, at about 81,000 s.

Graphite corrosion is shown in Figure 4-38 and Table 4-7. After 100 hours the total mass of carbon reacted is about 254 kg. The maximum corrosion depth is about 0.466 mm, corresponding to the oxidation density of 4214 mol/m^3. The maximum oxidation depth of 0.466 mm corresponds to the oxidized volume of 4.59 vol.%. This means the maximum corrosion is 64.7% of ECD.

maximum corrosion = 4.59 vol.% = 64.7% of ECD

Gas masses are shown in Figure 4-39, including the mass of steam in the reactor vessel and the total amounts of the gases generated due to corrosion: H_2 and CO. The mass of steam in the RV is increasing during the first 150,000 s (except for a short drop during the safety valve opening) due to continuous transport of steam evaporated from the SG lower head. After this time the amount of steam is approximately constant. At 100 hours there is about 1000 kg of steam in the RV (Figure 4-39, Table 4-9).

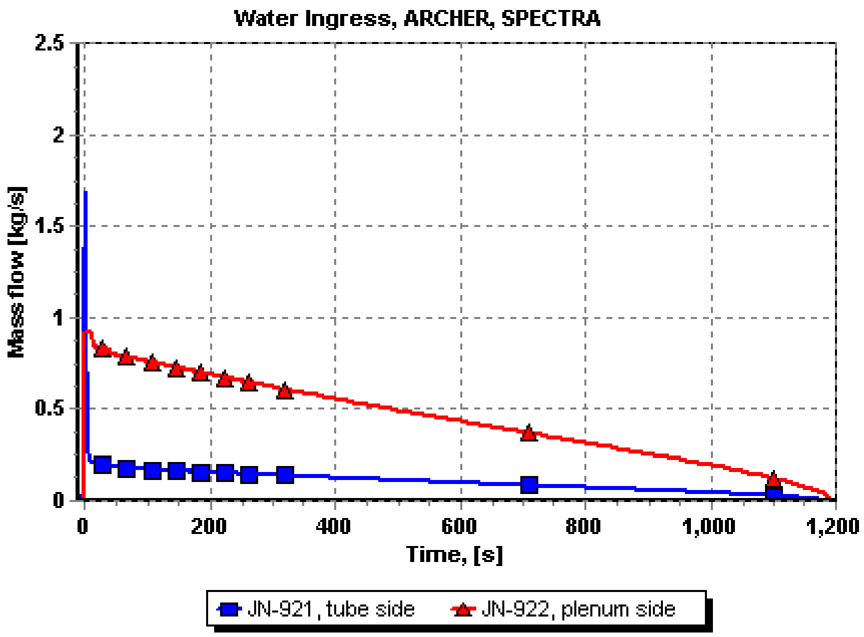

Figure 4-32 :

Break flows (1-tube, bottom of SG, failure of SG drain and blower flaps closure)

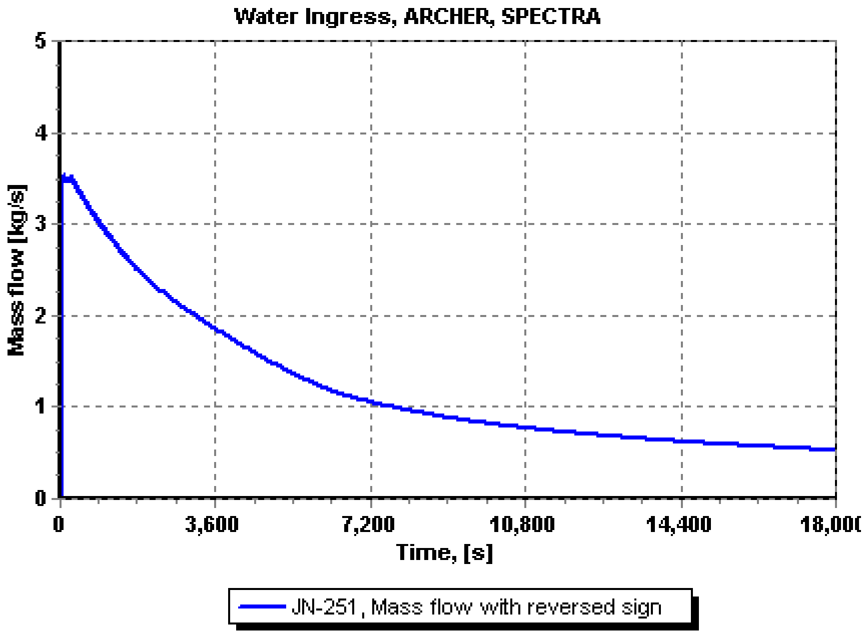

Figure 4-33 :

Natural circulation flow (1-tube, bottom of SG, failure of SG drain and blower flaps closure)

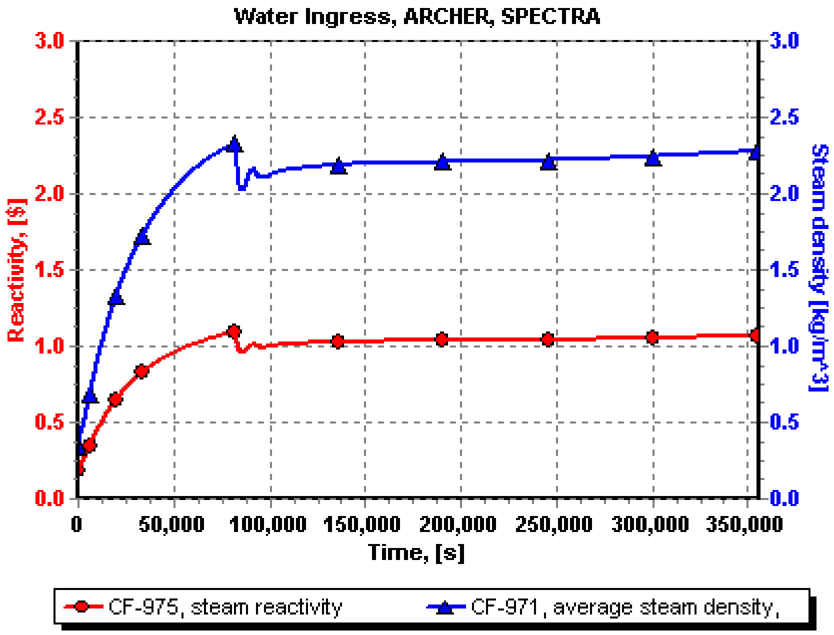

Figure 4-34 :
Steam density and reactivity (1-tube, bottom of SG, failure of SG drain and blower flaps closure)

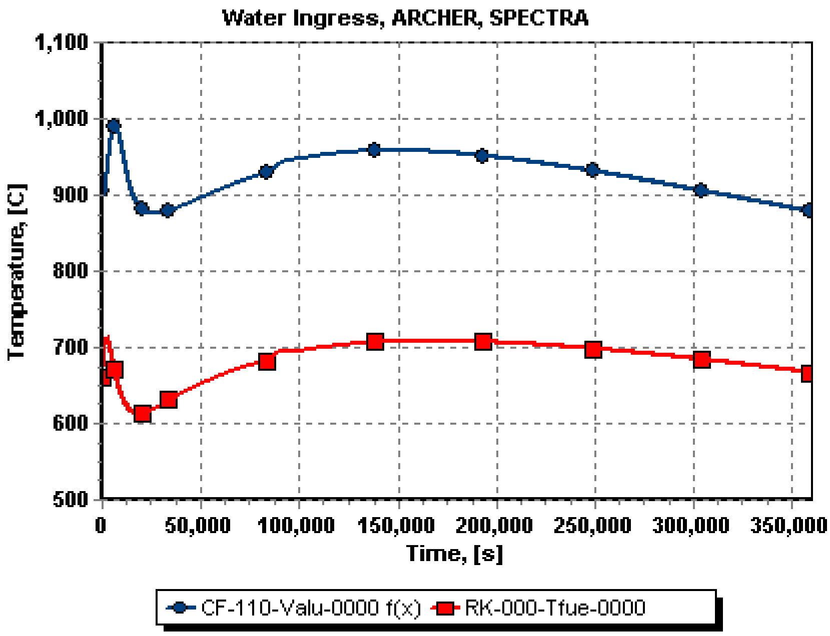

Figure 4-35 :
Fuel temperatures (1-tube, bottom of SG, failure of SG drain and blower flaps closure)

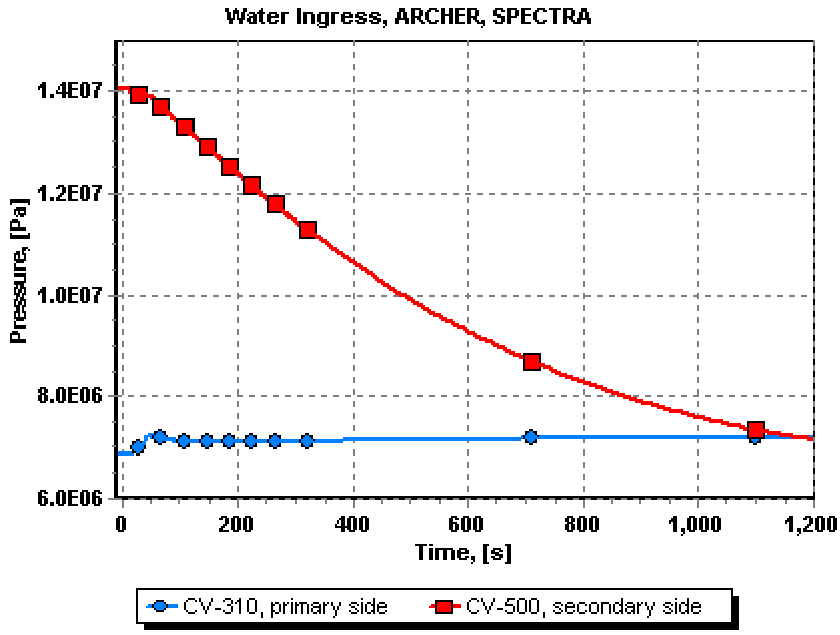

Figure 4-36 :
Pressures - short term (1-tube, bottom of SG, failure of SG drain and blower flaps closure)

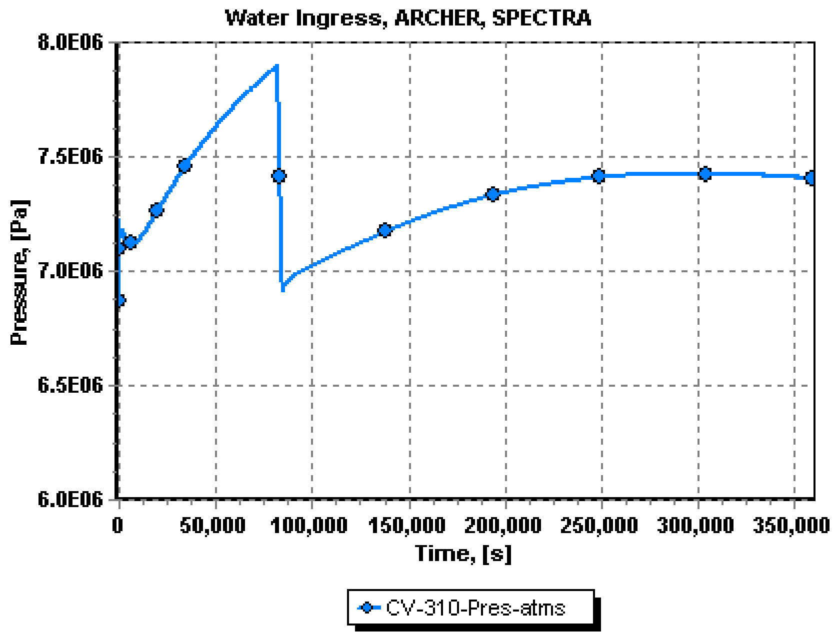

Figure 4-37 :
Primary pressure - long term (1-tube, bottom of SG, failure of SG drain and blower flaps closure)

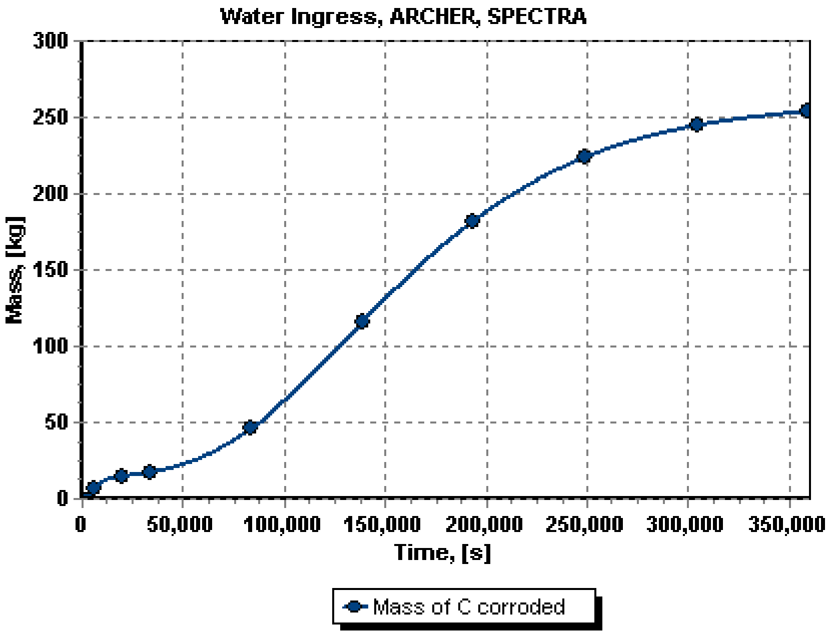

Figure 4-38 :
Graphite corrosion mass (1-tube, bottom of SG, failure of SG drain and blower flaps closure)

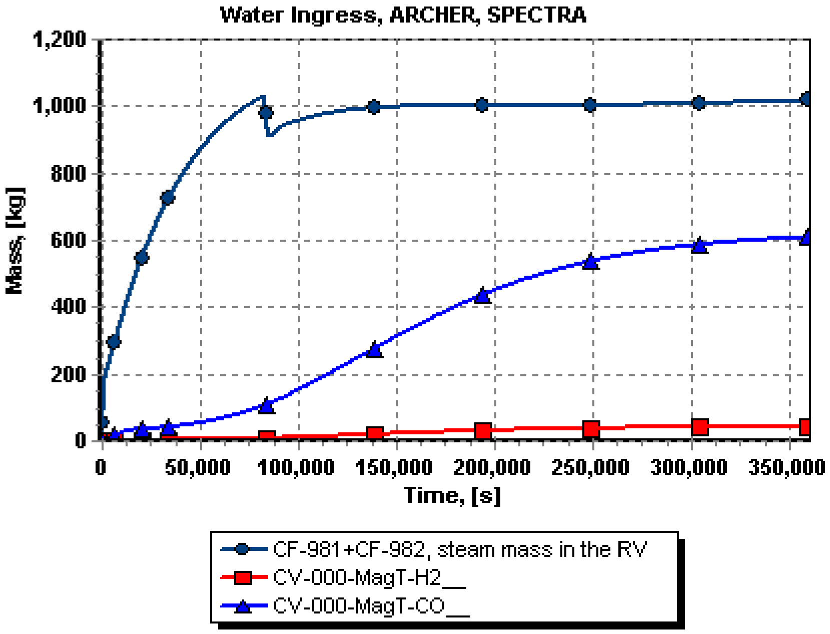

Figure 4-39 :
Mass of steam in RV and total mass of generated H_2 and CO
(1-tube, bottom of SG, failure of SG drain and blower flaps closure)

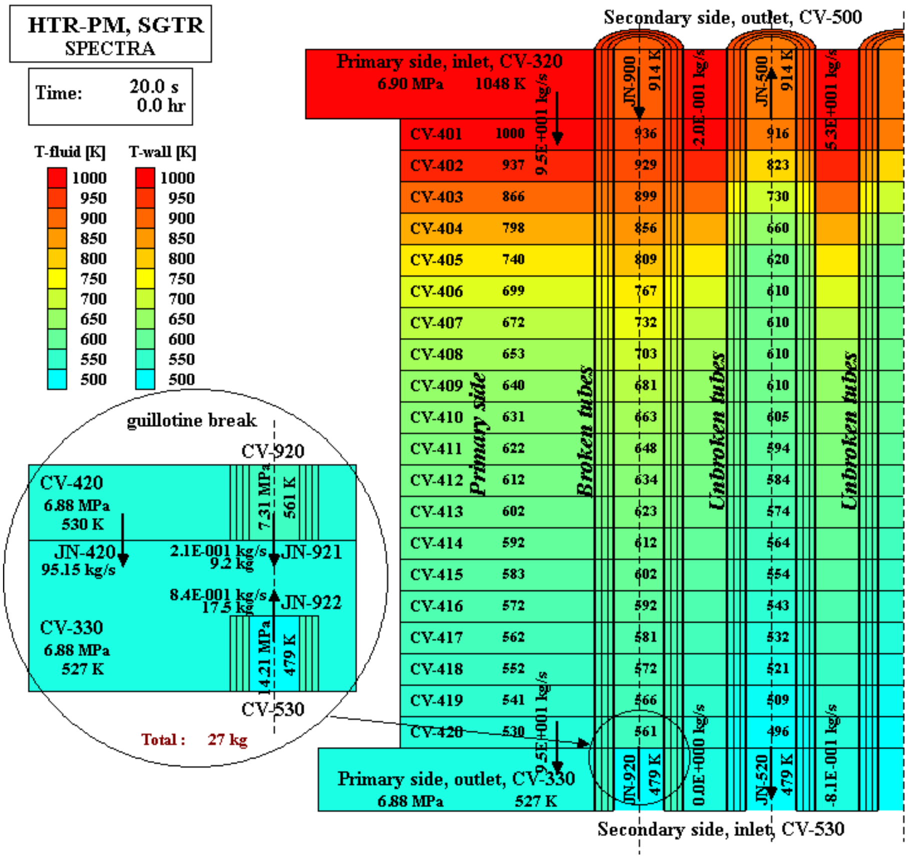

Figure 4-40 :
Break at *t*=20 s (1-tube, bottom of SG, failure of SG drain and blower flaps closure)

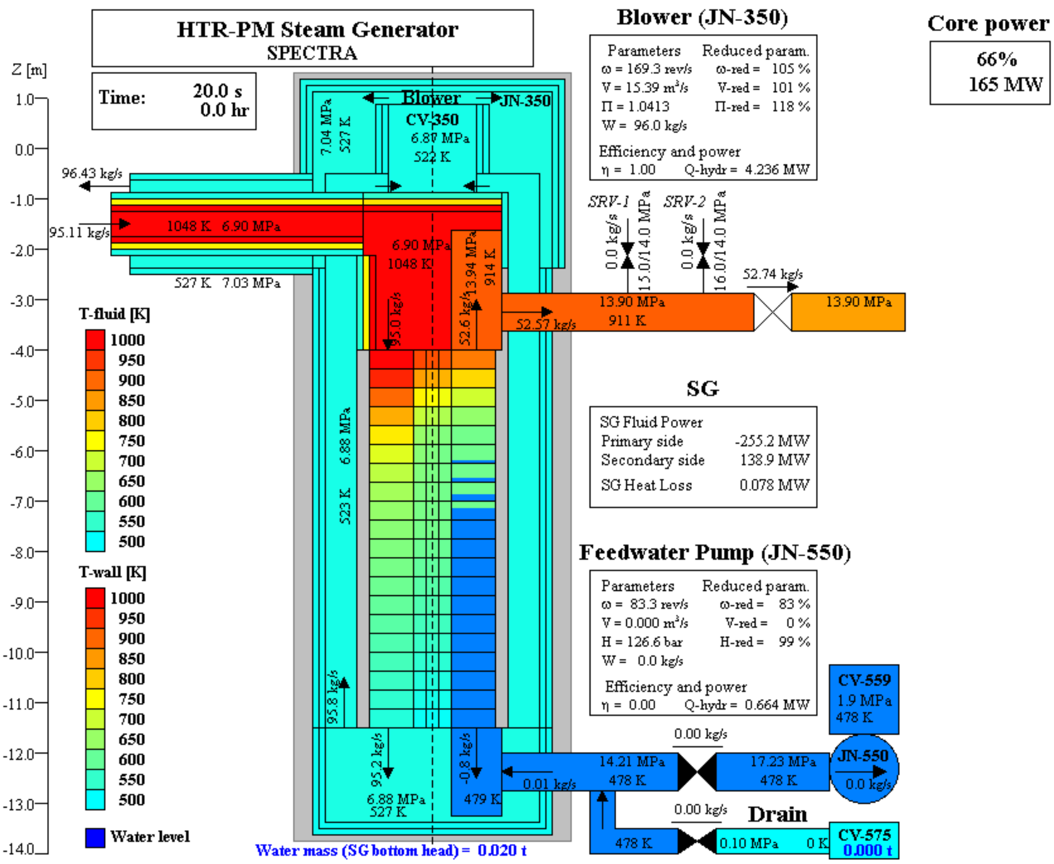

Figure 4-41 :
SG vessel at *t*=20 s (1-tube, bottom of SG, failure of SG drain and blower flaps closure)

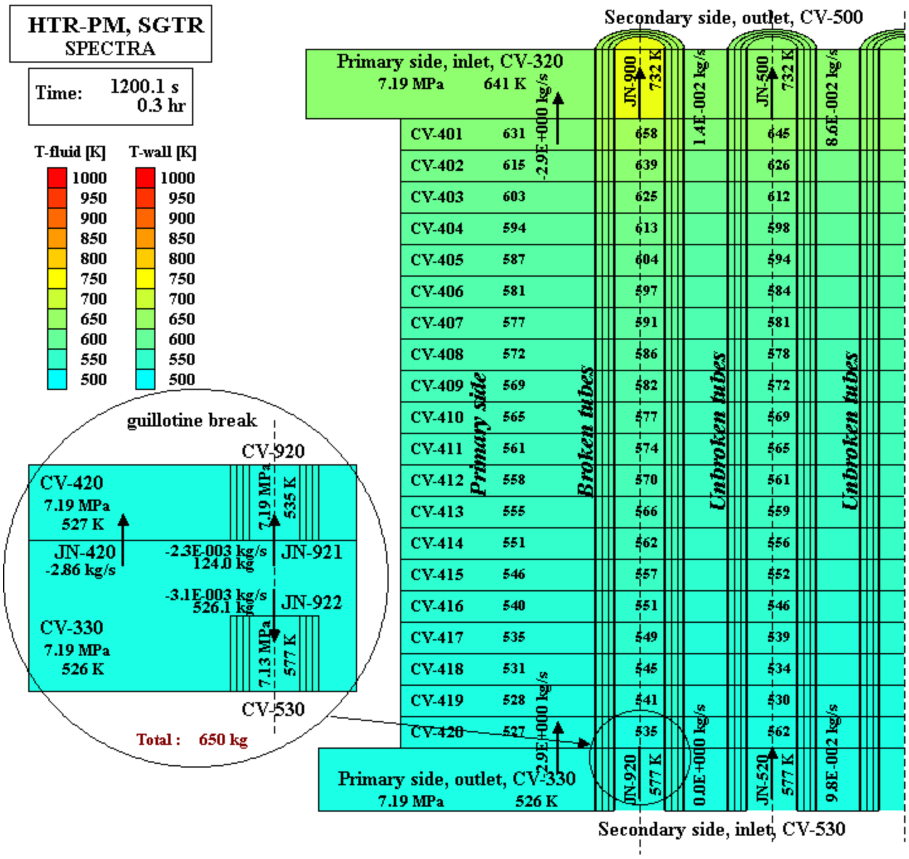

Figure 4-42 :

Break at *t*=1200 s (1-tube, bottom of SG, failure of SG drain and blower flaps closure)

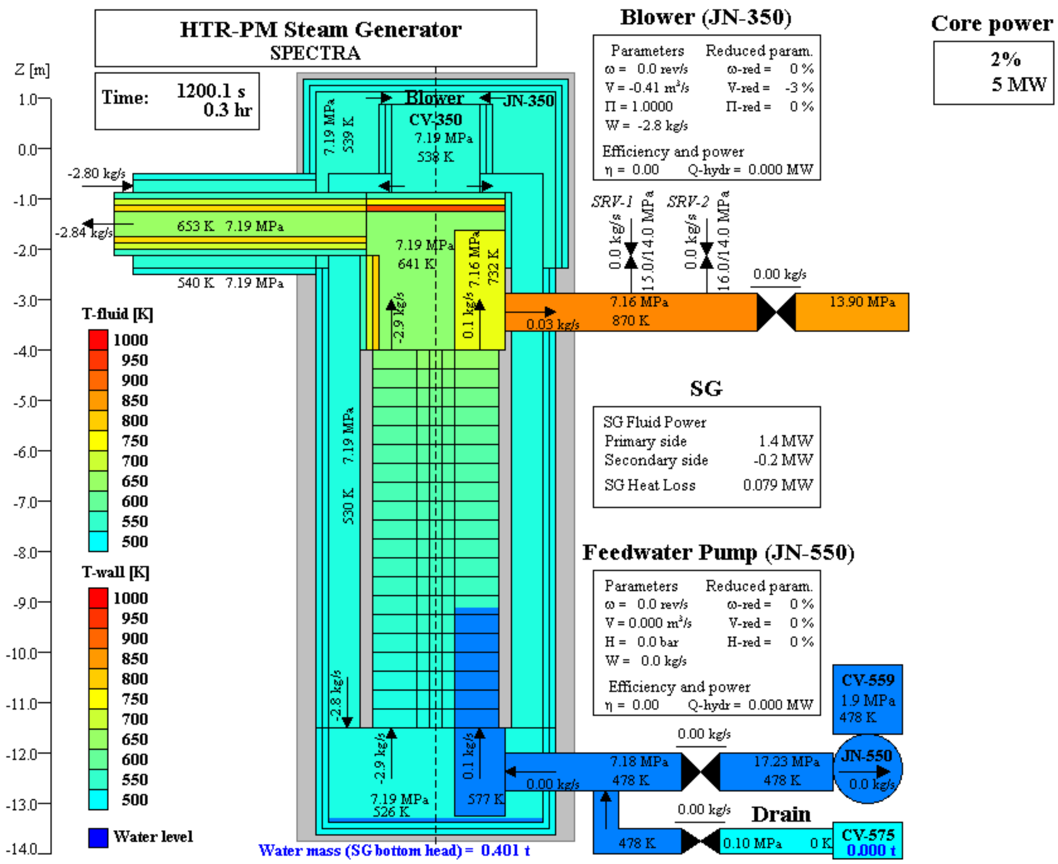

Figure 4-43 :

SG vessel at *t*=1200 s (1-tube, bottom of SG, failure of SG drain and flaps closure)

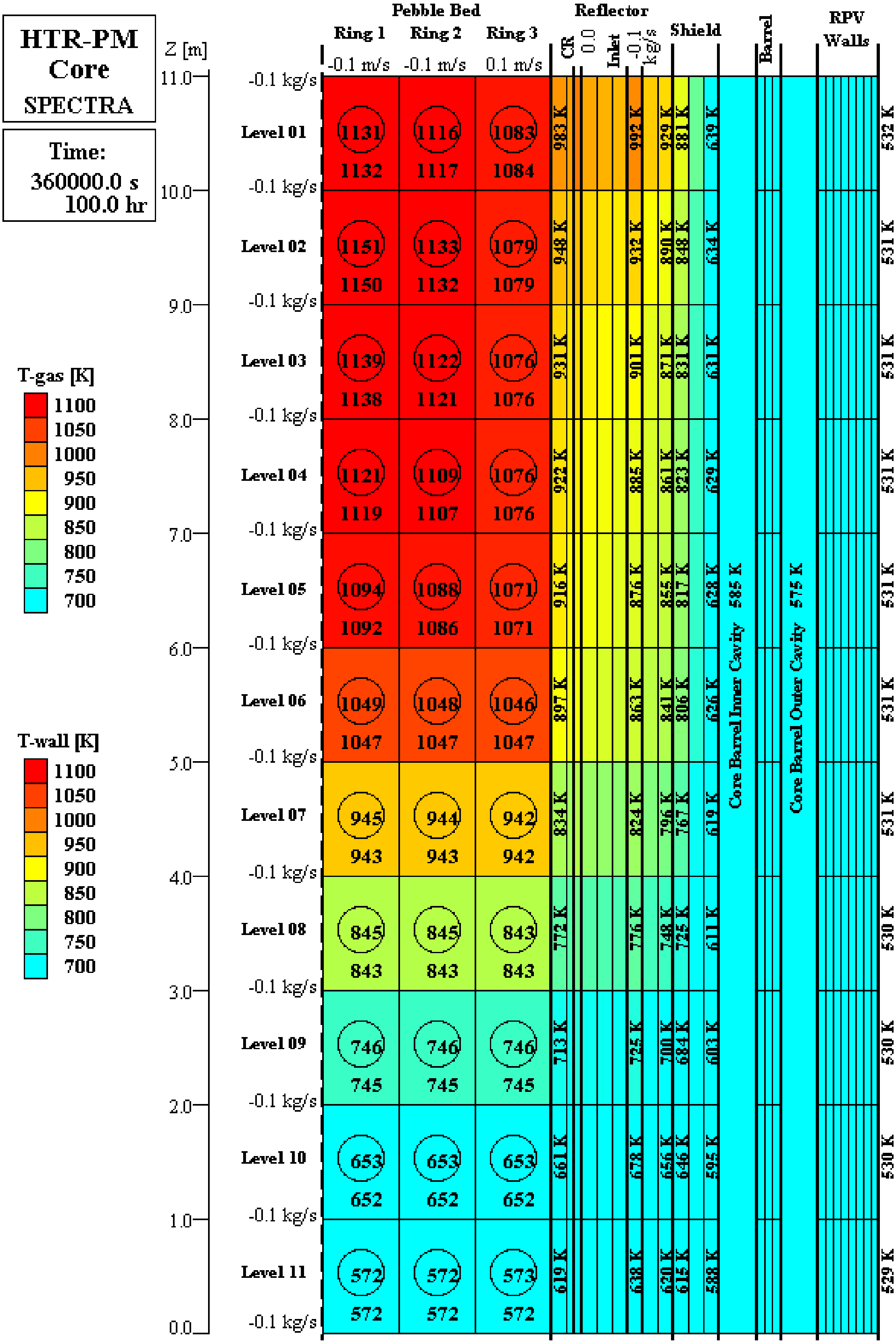

Figure 4-44 :

Temperatures at *t*=100 hr (1-tube, bottom of SG, failure of SG drain and blower flaps closure)

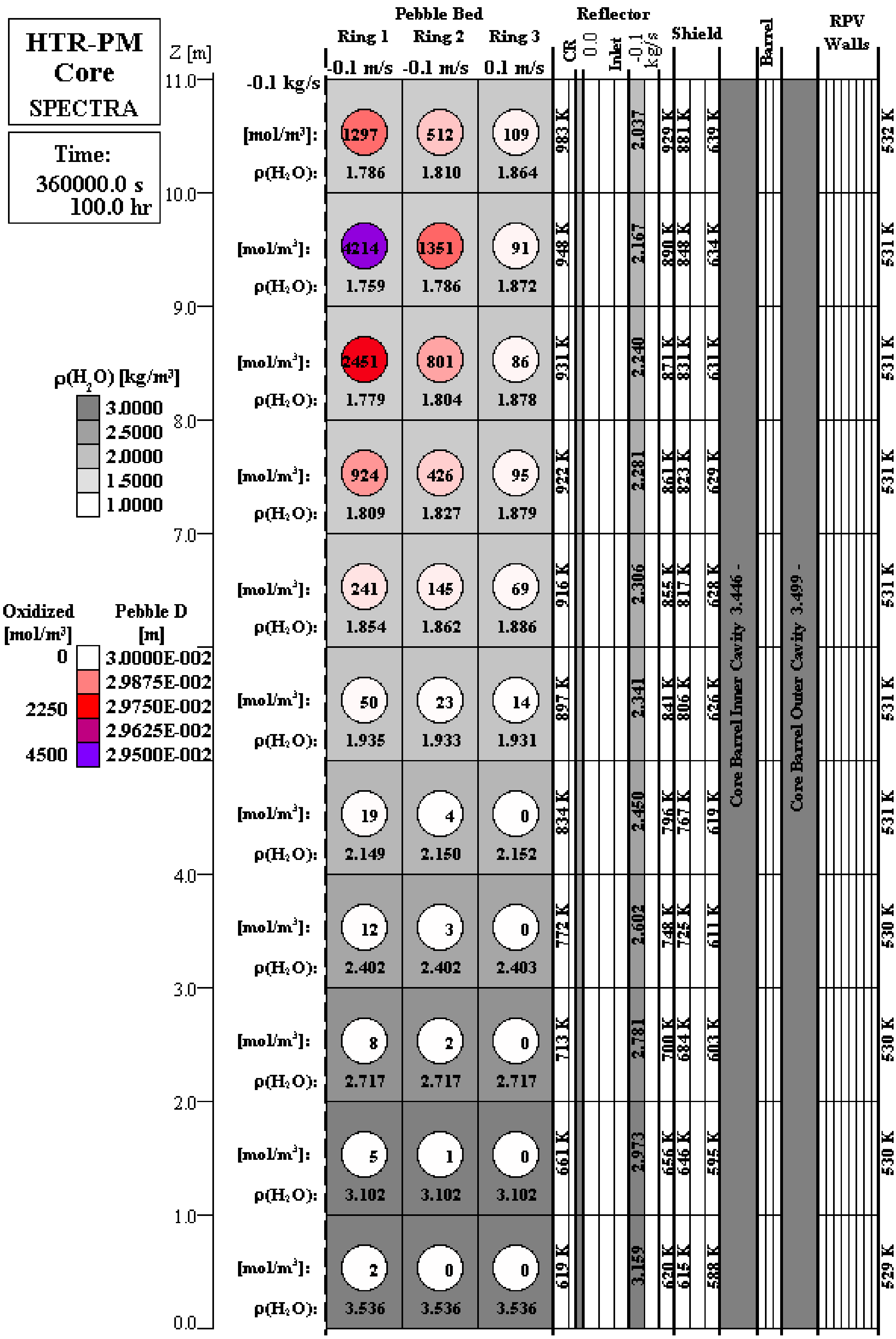

Figure 4-45 :

Oxidation at *t*=100 hr (1-tube, bottom of SG, failure of SG drain and blower flaps closure)

Table 4-7 : Oxidation at *t*= 100 hr (1-tube, bottom of SG, failure of SG drain and blower flaps closure)

HTR-PM Oxidation Summary SPECTRA							Time: 3.60E+005 s 1.00E+002 hr
Oxidation depth, [mm]				Oxidized mass, [mol/m³]			
	Ring 1	Ring 2	Ring 3		Ring 1	Ring 2	Ring 3
01	0.143	0.057	0.012	01	1296.6	512.2	109.5
02	0.466	0.149	0.010	02	4213.8	1350.9	91.4
03	0.271	0.089	0.010	03	2451.2	800.8	86.0
04	0.102	0.047	0.011	04	923.8	426.2	95.0
05	0.027	0.016	0.008	05	240.7	144.8	68.8
06	0.005	0.003	0.002	06	49.8	22.6	13.6
07	0.002	0.000	0.000	07	19.0	3.6	0.0
08	0.001	0.000	0.000	08	11.8	2.7	0.0
09	0.001	0.000	0.000	09	8.2	1.8	0.0
10	0.000	0.000	0.000	10	4.5	0.9	0.0
11	0.000	0.000	0.000	11	1.8	0.0	0.0

Table 4-8 : State at *t*= 20 s (1-tube, bottom of SG, failure of SG drain and blower flaps closure)

HTR-PM Water Ingress Summary SPECTRA — Time: 2.00E+001 s 5.56E-003 hr

Steam masses	abs. [kg]	rel. [%]	Water masses	abs. [kg]	rel. [%]
RV, pebble bed:	3.0	44.6%	RV, pebble bed:	0.0	0.0%
RV, other:	0.5	6.8%	RV, other:	0.0	0.0%
SG primary side:	3.1	46.1%	SG primary side:	20.2	100.0%
SG tubes, primary:	0.2	2.4%	SG tubes, primary:	0.0	0.0%
Primary system, total:	6.6	100.0%	Primary system, total:	20.2	100.0%

Total masses [kg]		Drained mass [kg]		Integrated flow through the break [kg]	
Liquid:	4176.5	CV-575:	0.0	Integrated flow, total:	26.7
Gases:		Reacted C [kg]			
He:	3045.6	Measur. 1:	0.0		
H_2:	0.0	Measur. 2:	0.0		
CO:	0.0				

Table 4-9 : State at *t*= 100 hr (1-tube, bottom of SG, failure of SG drain and blower flaps closure)

HTR-PM Water Ingress Summary SPECTRA — Time: 3.60E+005 s 1.00E+002 hr

Steam masses	abs. [kg]	rel. [%]	Water masses	abs. [kg]	rel. [%]
RV, pebble bed:	657.3	45.2%	RV, pebble bed:	0.0	0.0%
RV, other:	360.0	24.8%	RV, other:	0.0	0.0%
SG primary side:	390.9	26.9%	SG primary side:	687.0	100.0%
SG tubes, primary:	45.2	3.1%	SG tubes, primary:	0.0	0.0%
Primary system, total:	1453.4	100.0%	Primary system, total:	687.0	100.0%

Total masses [kg]		Drained mass [kg]		Integrated flow through the break [kg]	
Liquid:	1360.6	CV-575:	0.0	Integrated flow, total:	2647.7
Gases:		Reacted C [kg]			
He:	3041.3	Measur. 1:	253.5		
H_2:	42.7	Measur. 2:	254.0		
CO:	609.7				

4.2 Guillotine Rupture at the Top of SG

A guillotine break at the top of the SG is considered. In order to model the guillotine break, the broken tube is modeled separately. The steam/water side of SG tubes is modeled with Control Volumes CV-501 ÷ CV-520 (Figure 3-7, Figure 3-8). These volumes represent 665 identical tubes. For the water ingress analyses Control Volumes CV-901 ÷ CV-920 were introduced to model the broken tube. These volumes represent the broken tubes and therefore have a multiplicity equal to the number of the broken tubes (in current analyses 1). At the same time the multiplicity of CV-501 ÷ CV-520 has been decreased accordingly. The same was done with Junctions representing connections and Solid Heat Conductors representing the tube walls. Nodalization is shown in Figure 4-46. The guillotine break is modeled as follows.

- JN-901, representing the normal outlet from the SG tubes, is closed at the time of break (note that in the model the positive direction of all junctions was assumed downwards, therefore in normal situation the flow on the secondary side is negative).
- JN-921, connecting to CV-901 with CV-320 rather than CV-500, is opened at the time of break. Geometry of this junction is the same as JN-901, only the flow direction was reversed.
- JN-922, connecting the secondary side outlet (CV-500) to the primary side inlet plenum (CV-320), is opened at the time of break. Geometrical data is the same as for JN-921 except for the flow length which was set to a small value.

Separate calculations were performed to achieve steady state with the model extended by the broken tube. Accident simulation was performed as follows:

- 100 seconds of steady state, starting at *t*=–100.0 seconds.
- 100 hours (4 days and 2 hours) of accident simulation, starting at *t*=0.0s, ending at *t*=360,000 s.

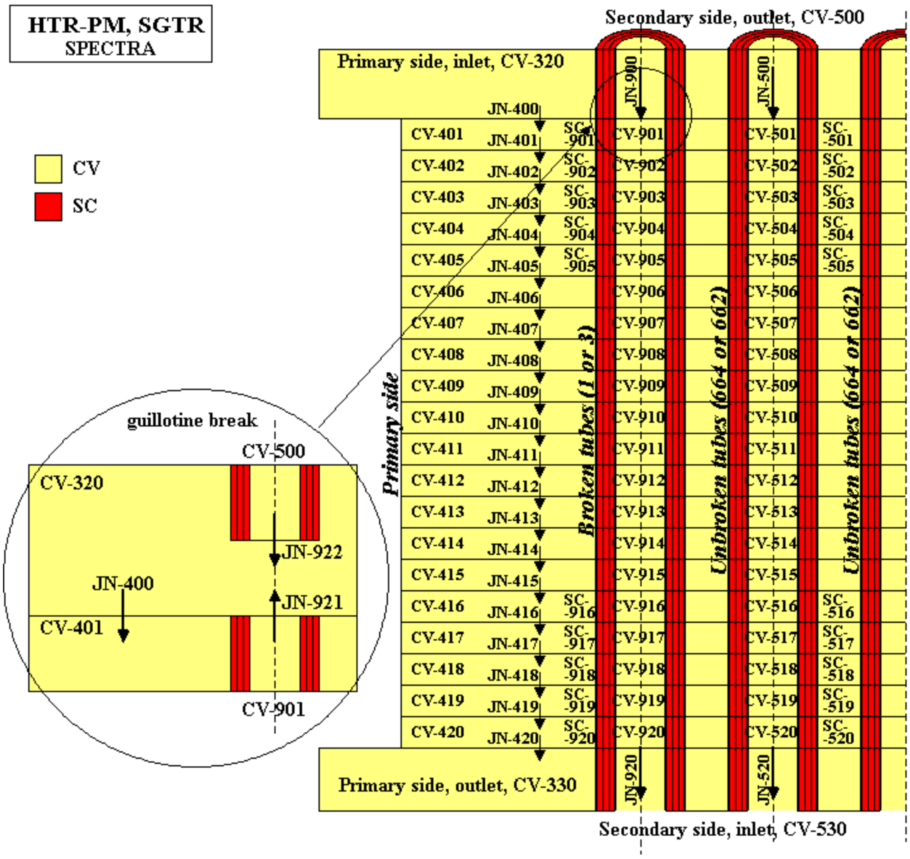

Figure 4-46 : Nodalization of broken tube(s) and the guillotine break at the top

4.2.1 1-Tube Rupture, Safety Systems Available

This section presents results of a break of single tube at the top of SG, with safety systems available (except for the helium purification system, which is not taken into account in any of the analyses presented in this report). Results are shown in Figure 4-47 through Figure 4-60 and Table 4-10 through Table 4-12.

The mass flow through the break is shown in Figure 4-47. Since the break is at the top of SG tube, the flow is practically pure steam. The flow from the tube side of the break is smaller due to large friction resistance. After 20 seconds - Figure 4-55 - about 44 kg of steam has entered the primary system, most of it through the plenum side of the break (JN-922: 38 kg). In contrast to the break at the bottom of SG tubes, where some water is deposited in the SG lower head (27 kg - Figure 4-15), in the present case there is practically no water in the SG head - Figure 4-56. The SG drain is initiated at 20 seconds. The drain valve is fully open at 23 s. The drain valve starts closing when the SG pressure drops to 7.3 MPa, at 65 s, and is fully closed at 68 s.

Figure 4-55 and Figure 4-56 show the state of the system at 20 seconds, when the drain valve begins to open. Figure 4-57 and Figure 4-58 show the state of the system at 65 seconds, when the break flow is practically terminated. At the end of the blowdown phase the masses of steam/water mixtures that have entered the primary system are shown below.

End of blowdown:

- tube side (JN-921): 118.5 kg
- plenum side (JN-922): 16.6 kg
- **total 135 kg**

After the blowdown is terminated, there is a very small flow through the break, which lasts for about 100,000 s. Positive flow through JN-921 is approximately balanced by negative flow through JN-922. Over the analyzed part of accident the integrated flow through this break is **171 kg** - Figure 4-48, Table 4-12.

The humidity detectors are assumed to initiate safety actions at 10 seconds. The reactor SCRAM is initiated with a 2 seconds delay. The total drop time of the control rods is 50 seconds [10]. Additionally small absorber spheres are dropped to ensure long term subcriticality [10]. Maximum reactor power, about 109% or 272 MW is observed at 12 seconds. At this time, the amount of steam ingress into the primary system is about 26 kg. Maximum reactivity due to steam ingress is about 0.13 $, corresponding to the steam density of about 0.22 kg/m^3 - Figure 4-49.

The maximum and average fuel temperatures are shown in Figure 4-50. Maximum fuel temperature is 1318 K (1045°C). Natural convection in the core results in a shift of the core maximum temperatures (Figure 4-59) and consequently the maximum corrosion (Figure 4-60) to the upper part of the core.

The system pressures are shown in Figure 4-51 and Figure 4-52. The blowdown is finished within about 65 s. In the long term, the primary pressure never reaches the setpoint of the primary pressure release system, 7.9 MPa.

Graphite corrosion is shown in Figure 4-53 and Table 4-10. After 100 hours the total mass of carbon reacted is about 27.5 kg. The maximum corrosion depth is about 0.055 mm, corresponding to the oxidation density of 501 mol/m^3. The maximum oxidation depth of 0.055 mm corresponds to the oxidized volume of 0.55 vol.%. This means the maximum corrosion is 7.6% of ECD.

maximum corrosion = 0.55 vol.% = 7.6% of ECD

Gas masses are shown in Figure 4-54, including the mass of steam in the reactor vessel and the total amounts of the gases generated due to corrosion: H_2 and CO. The mass of steam in the RV, equal to about 52 kg soon after the break, slowly decreases as the corrosion proceeds. At the same time, the mass of reaction products increases. At 100 hours there is still about 7 kg of steam in the RV (Figure 4-54, Table 4-12).

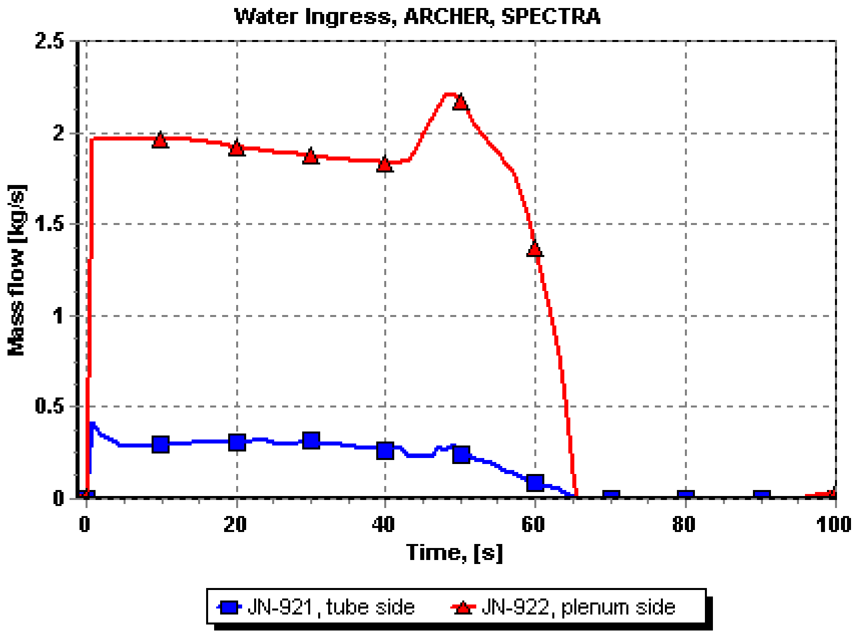

Figure 4-47 :
Break flows (1-tube, top of SG, safety systems available)

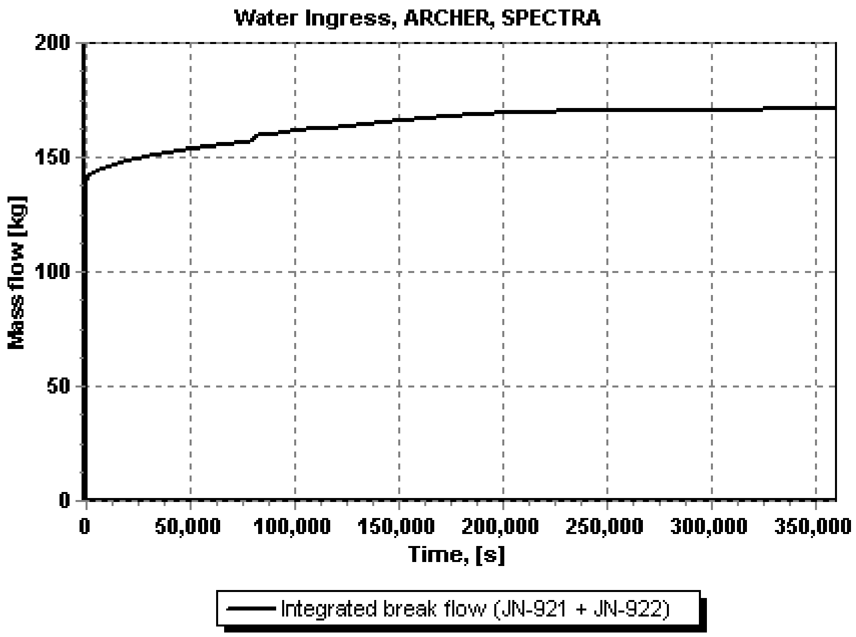

Figure 4-48 :
Integrated break flow (1-tube, top of SG, safety systems available)

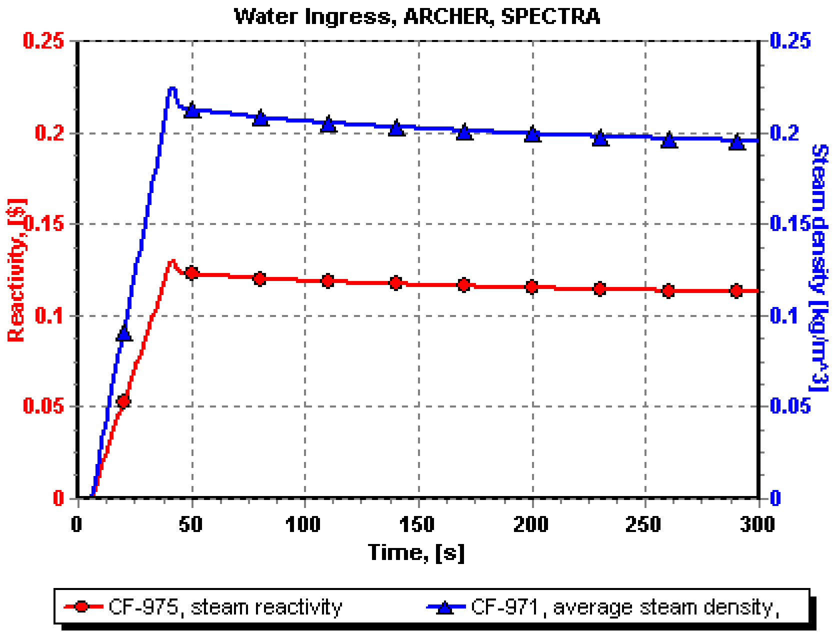

Figure 4-49 :
Steam density and reactivity (1-tube, top of SG, safety systems available)

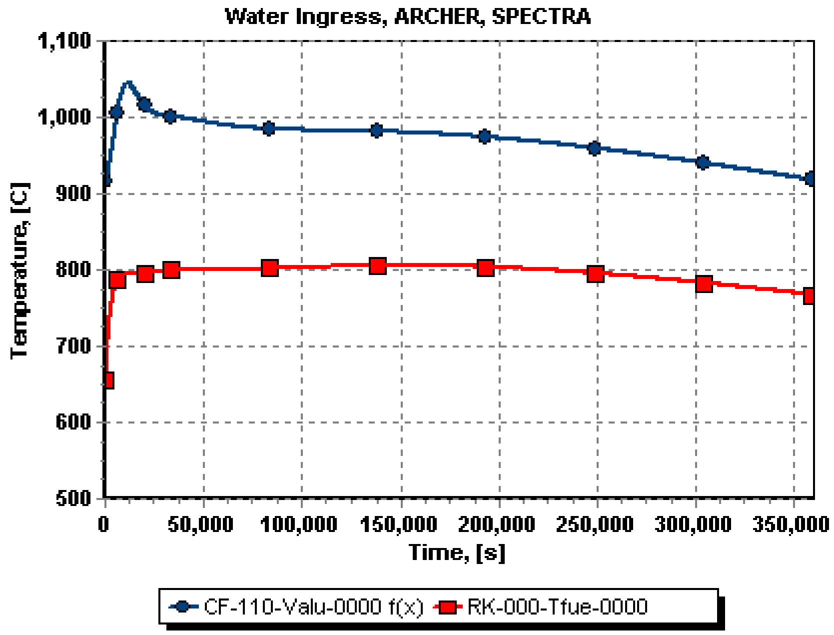

Figure 4-50 :
Fuel temperatures (1-tube, top of SG, safety systems available)

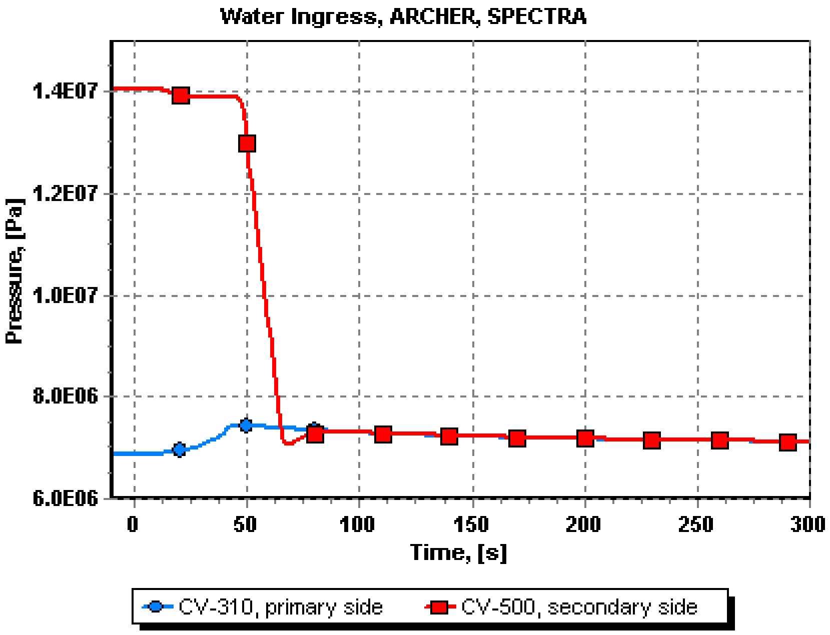

Figure 4-51 :
Pressures - short term (1-tube, top of SG, safety systems available)

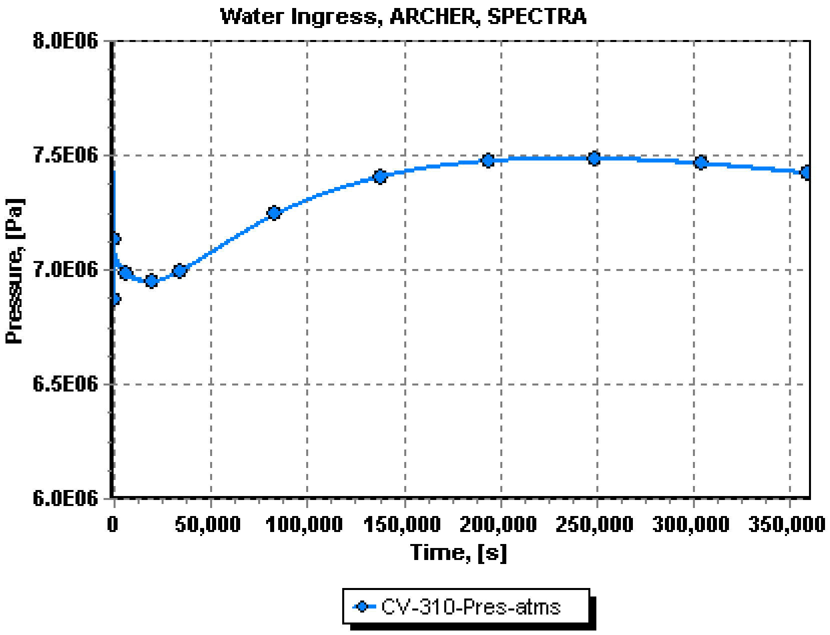

Figure 4-52 :
Primary pressure - long term (1-tube, top of SG, safety systems available)

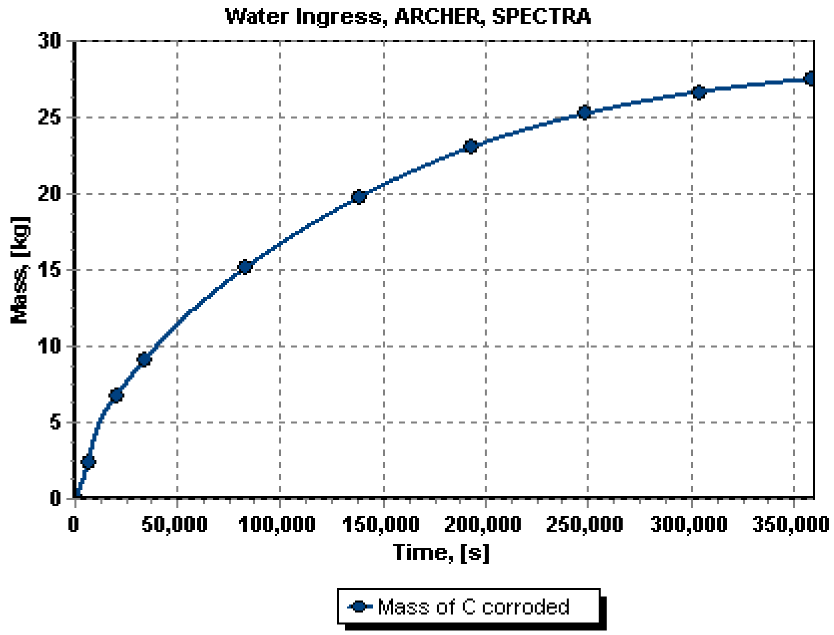

Figure 4-53 :
Graphite corrosion mass (1-tube, top of SG, safety systems available)

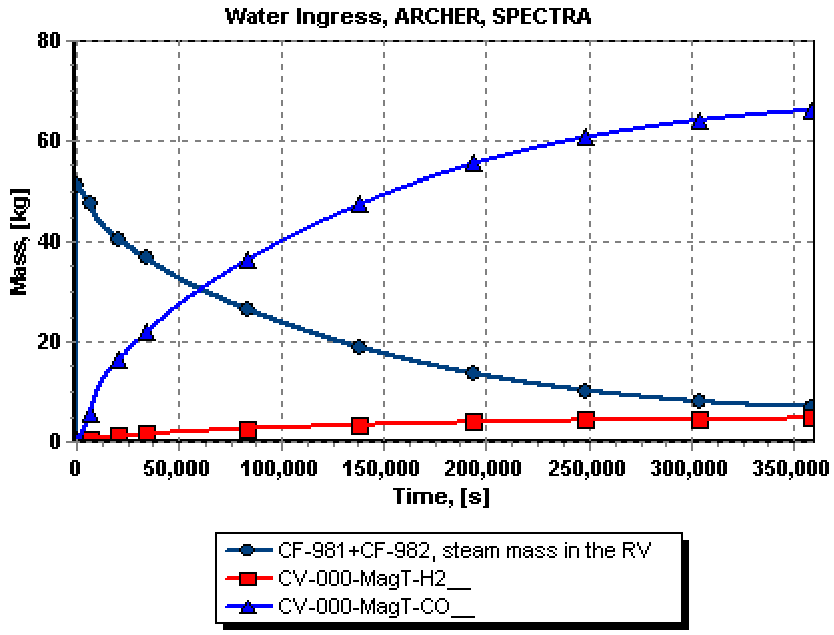

Figure 4-54 :
Mass of steam in RV and total mass of generated H_2 and CO (1-tube, top of SG, safety systems available)

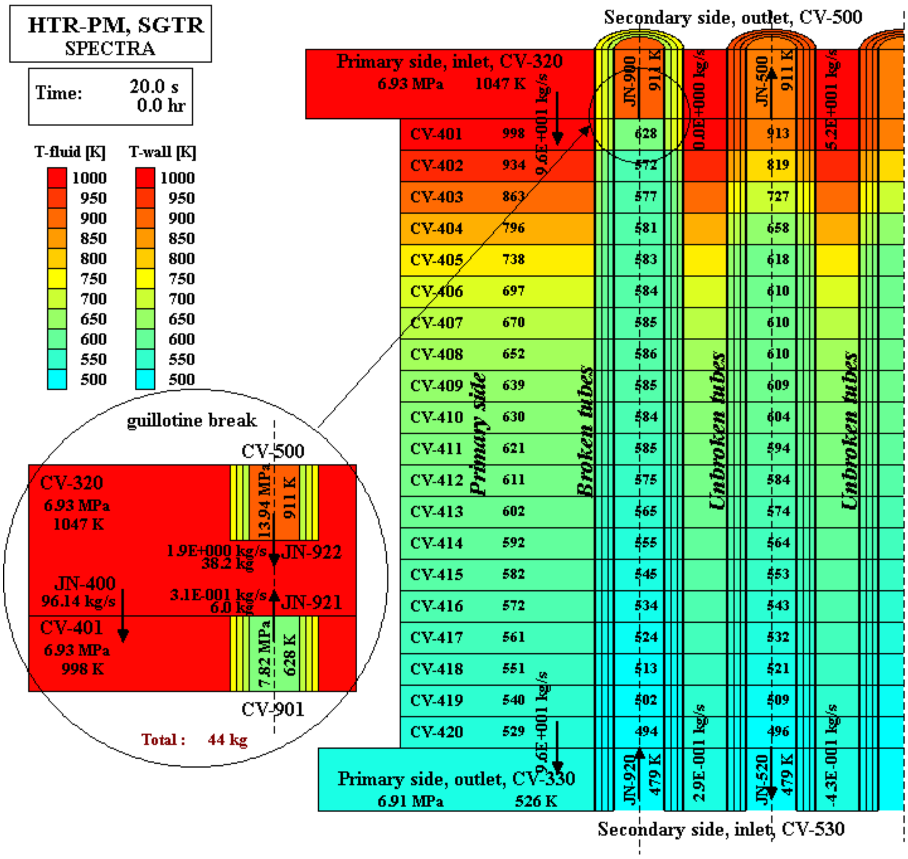

Figure 4-55 :

Break at *t*=20 s (1-tube, top of SG, safety systems available)

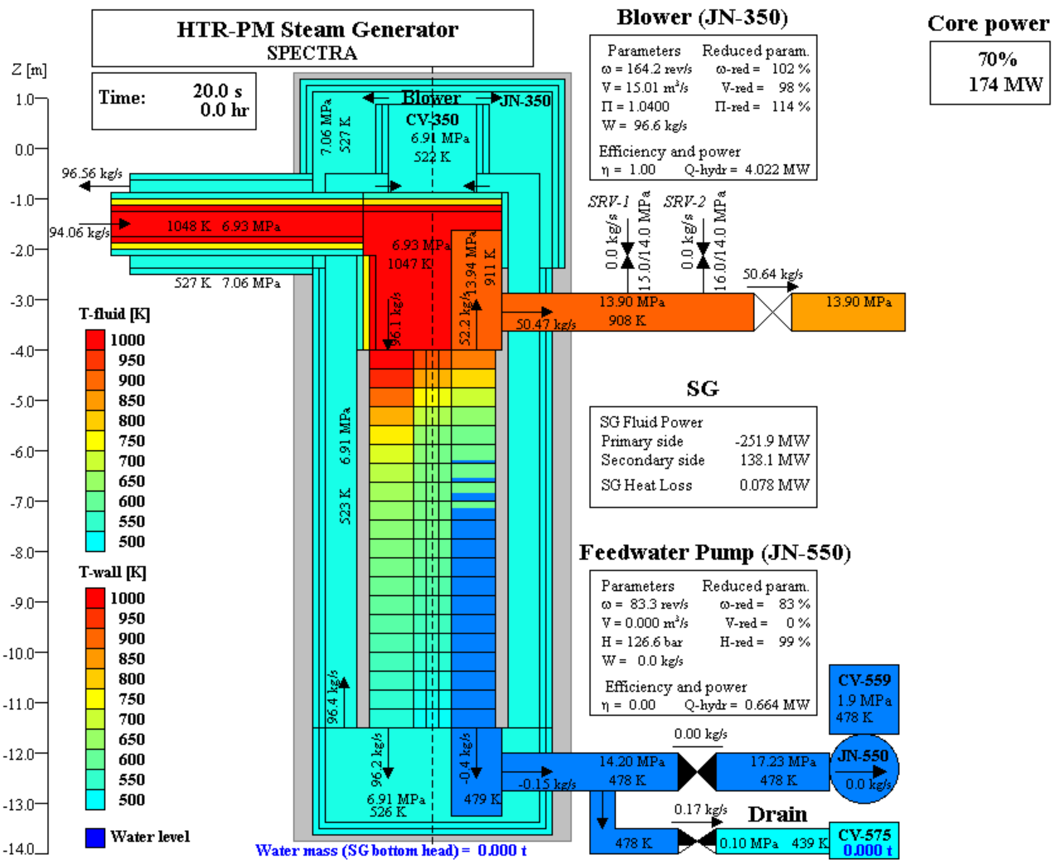

Figure 4-56 :

SG vessel at *t*=20 s (1-tube, top of SG, safety systems available)

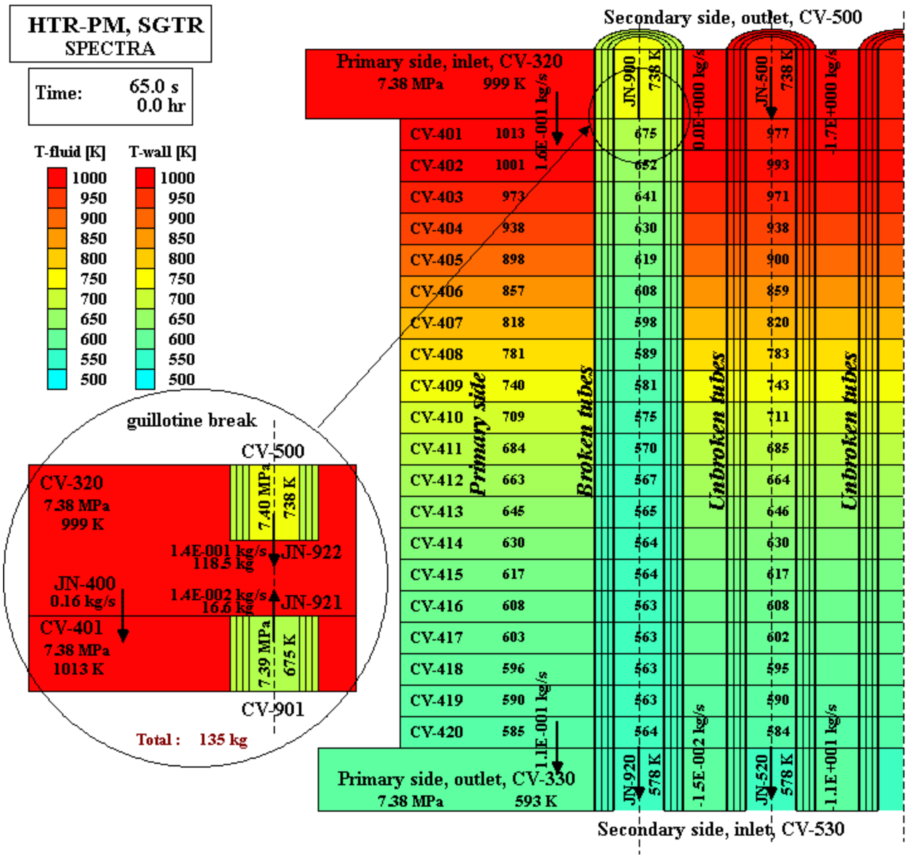

Figure 4-57 :
Break at t=65 s (1-tube, top of SG, safety systems available)

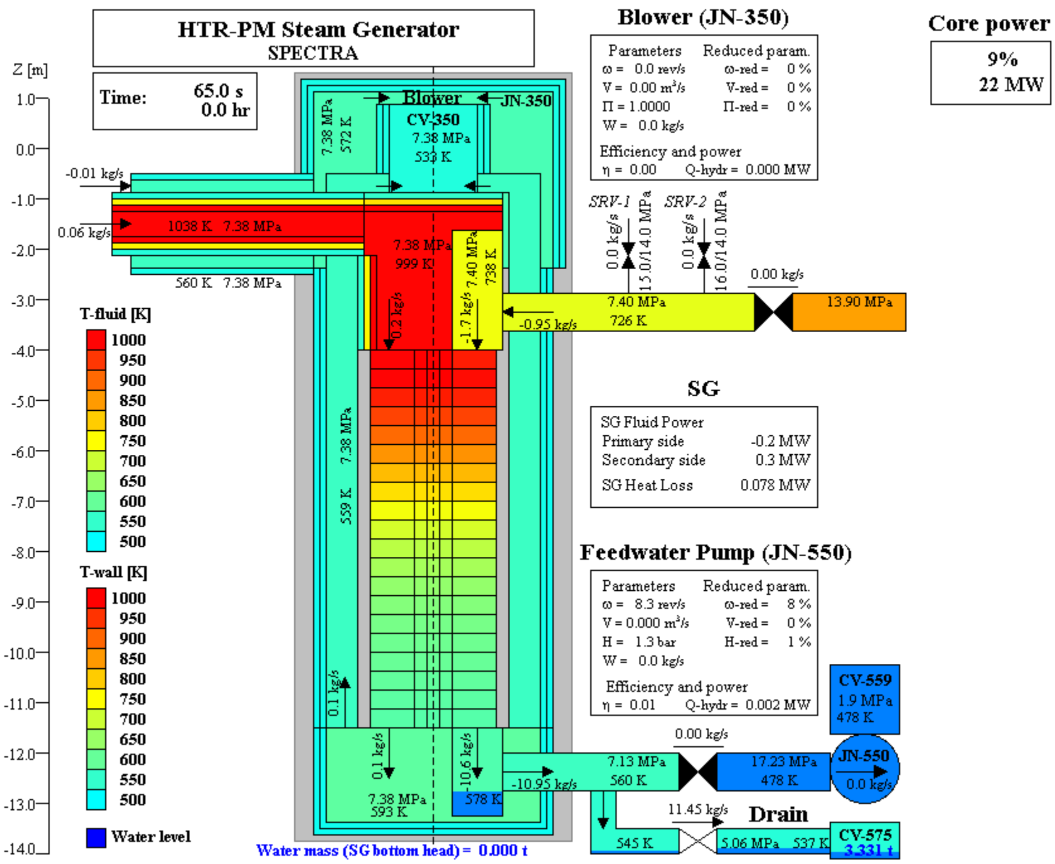

Figure 4-58 :
SG vessel at t=65 s (1-tube, top of SG, safety systems available)

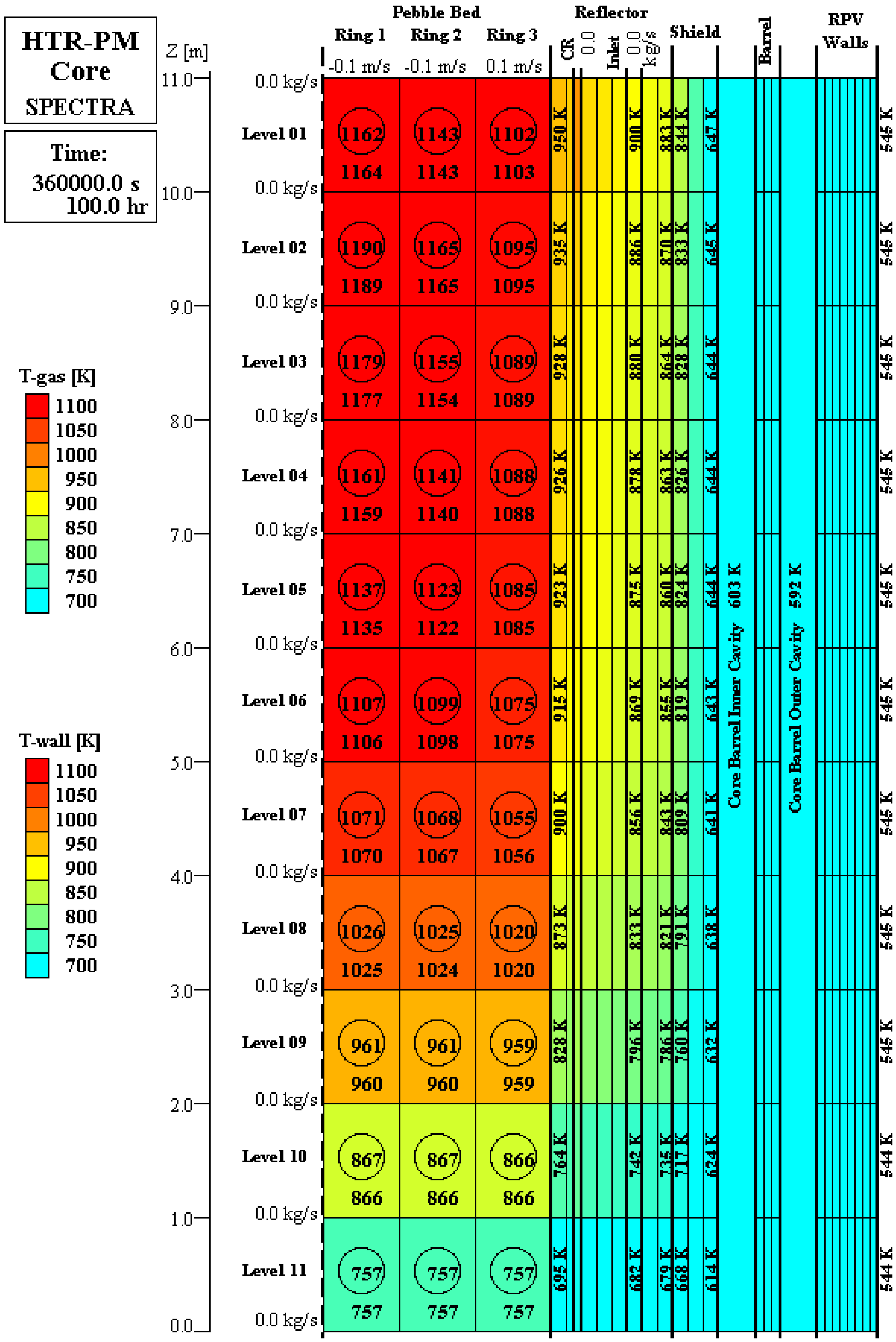

Figure 4-59 :

Temperatures at *t*=100 hr (1-tube, top of SG, safety systems available)

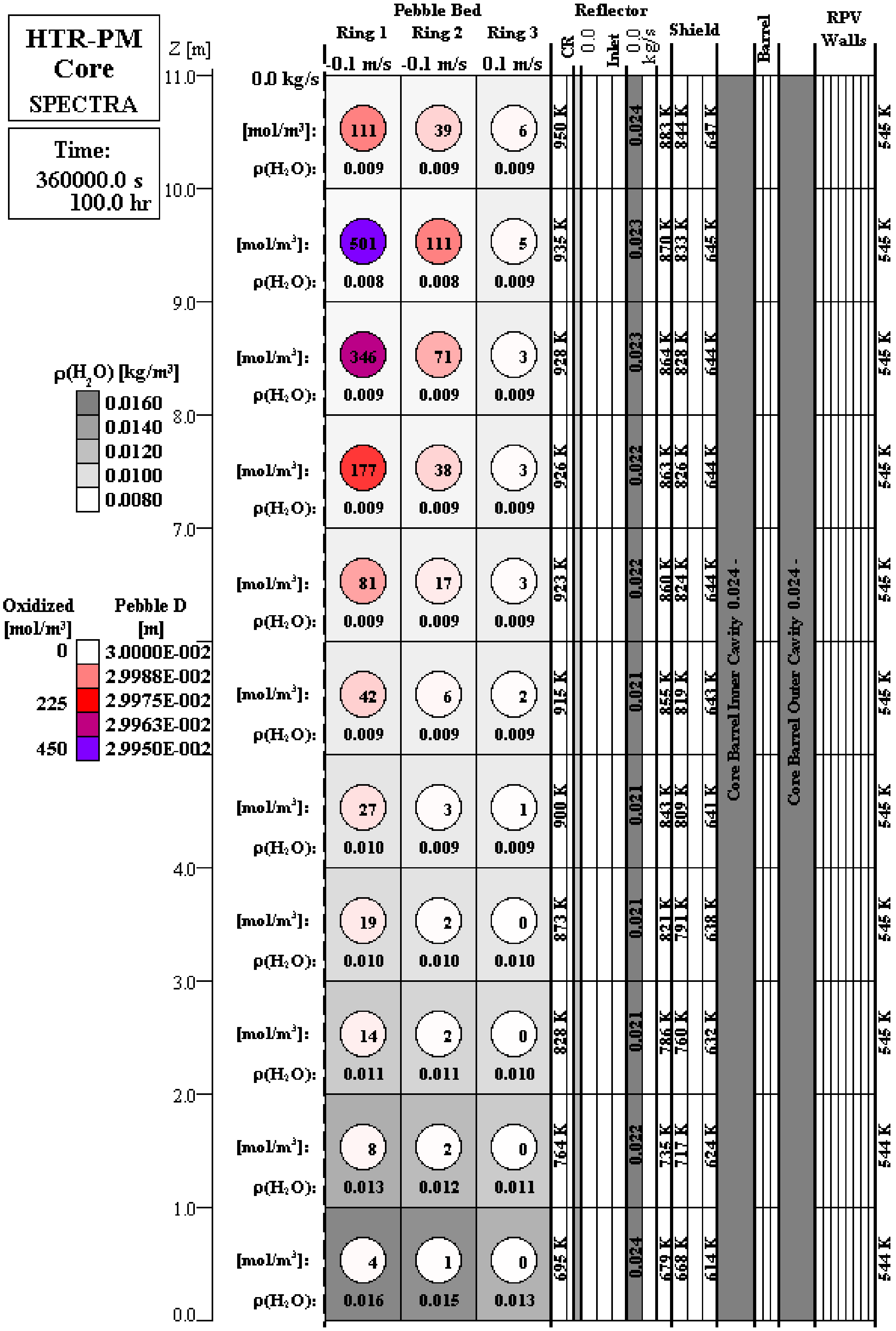

Figure 4-60 :

Oxidation at *t*=100 hr (1-tube, top of SG, safety systems available)

Table 4-10 : Oxidation at *t*= 100 hr (1-tube, top of SG, safety systems available)

HTR-PM Oxidation Summary
SPECTRA

Time: 3.60E+005 s / 1.00E+002 hr

Oxidation depth, [mm]	Ring 1	Ring 2	Ring 3	Oxidized mass, [mol/m³]	Ring 1	Ring 2	Ring 3
01	0.012	0.004	0.001	01	111.3	38.9	6.3
02	0.055	0.012	0.000	02	501.3	111.3	4.5
03	0.038	0.008	0.000	03	345.7	71.5	2.7
04	0.020	0.004	0.000	04	177.4	38.0	2.7
05	0.009	0.002	0.000	05	81.4	17.2	2.7
06	0.005	0.001	0.000	06	41.6	6.3	1.8
07	0.003	0.000	0.000	07	27.2	2.7	0.9
08	0.002	0.000	0.000	08	19.0	1.8	0.0
09	0.002	0.000	0.000	09	13.6	1.8	0.0
10	0.001	0.000	0.000	10	8.2	1.8	0.0
11	0.000	0.000	0.000	11	3.6	0.9	0.0

Table 4-11 : State at *t*= 20 s (1-tube, top of SG, safety systems available)

HTR-PM Water Ingress Summary
SPECTRA

Time: 2.00E+001 s / 5.56E-003 hr

Steam masses	abs. [kg]	rel. [%]	Water masses	abs. [kg]	rel. [%]
RV, pebble bed:	18.5	41.8%	RV, pebble bed:	0.0	0.0%
RV, other:	2.7	6.2%	RV, other:	0.0	0.0%
SG primary side:	20.9	47.1%	SG primary side:	0.0	0.0%
SG tubes, primary:	2.2	4.9%	SG tubes, primary:	0.0	0.0%
Primary system, total:	44.3	100.0%	Primary system, total:	0.0	0.0%

Total masses [kg]		Drained mass [kg]		Integrated flow through the break [kg]	
Liquid:	4177.2	CV-575:	0.0	Integrated flow, total:	44.2
Gases:		Reacted C [kg]			
He:	3045.6				
H_2:	0.0	Measur. 1:	0.0		
CO:	0.0	Measur. 2:	0.0		

Table 4-12 : State at *t*= 100 hr (1-tube, top of SG, safety systems available)

HTR-PM Water Ingress Summary
SPECTRA

Time: 3.60E+005 s / 1.00E+002 hr

Steam masses	abs. [kg]	rel. [%]	Water masses	abs. [kg]	rel. [%]
RV, pebble bed:	4.4	5.5%	RV, pebble bed:	0.0	0.0%
RV, other:	2.6	3.3%	RV, other:	0.0	0.0%
SG primary side:	61.0	76.6%	SG primary side:	15.0	100.0%
SG tubes, primary:	11.6	14.6%	SG tubes, primary:	0.0	0.0%
Primary system, total:	79.6	100.0%	Primary system, total:	15.0	100.0%

Total masses [kg]		Drained mass [kg]		Integrated flow through the break [kg]	
Liquid:	3540.4	CV-575:	3240.1	Integrated flow, total:	171.0
Gases:		Reacted C [kg]			
He:	3045.6				
H_2:	4.6	Measur. 1:	27.5		
CO:	66.1	Measur. 2:	27.6		

4.2.2 1-Tube Rupture, Failure of SG Drain

This section presents results of a break of single tube at the top of SG, with simultaneous failure of the SG drain system. Results are shown in Figure 4-61 through Figure 4-74 and Table 4-13 through Table 4-15.

The mass flow through the break is shown in Figure 4-61. At the end of blowdown (about 700 s) - Figure 4-71 - about **781 kg** of steam has entered the primary system, most of it through the plenum side of the break (JN-922: 664 kg). In contrast to the break at the bottom of SG tubes, where a lot of water is deposited in the SG lower head (1445 kg - Figure 4-29), in the present case there is practically no water in the SG head - Figure 4-72. The total amount of steam entering the primary system in this scenario is about **892 kg** - Table 4-15. A significant part (about 588 kg) is condensed in SG and remains as liquid in the SG lower head.

The humidity detectors are assumed to initiate safety actions at 10 seconds. The reactor SCRAM is assumed is initiated with a 2 seconds delay. The total drop time of the control rods is 50 seconds [10]. Additionally small absorber spheres are dropped to ensure long term subcriticality [10]. Maximum reactor power, about 109% or 272 MW is observed at 12 seconds - Figure 4-62. Maximum reactivity due to steam ingress is about 0.32 $, corresponding to the steam density of about 0.63 kg/m^3 - Figure 4-63.

The SG drain system is not used in this scenario. Consequently there is more steam entering the primary system than in the previous case. The mass flow through the break decreases slowly until pressures equilibrate at about 700 s - Figure 4-61, Figure 4-65.

The maximum and average fuel temperatures are shown in Figure 4-64. Maximum fuel temperature is 1310 K (1037°C). Natural convection in the core results in a shift of the core maximum temperatures (Figure 4-73) and consequently the maximum corrosion (Figure 4-74) to the upper part of the core.

The system pressures are shown in Figure 4-65 and Figure 4-66. The blowdown is finished within about 700 seconds. In the long term, the primary pressure never reaches the setpoint of the primary pressure release system, 7.9 MPa.

Graphite corrosion is shown in Figure 4-67 and Table 4-13. After 100 hours the total mass of carbon reacted is about 40 kg. The maximum corrosion depth is about 0.083 mm, corresponding to the oxidation density of about 747 mol/m^3. The maximum oxidation depth of 0.083 mm corresponds to the oxidized volume of 0.83 vol.%. This means the maximum corrosion is 11.5% of ECD.

maximum corrosion = 0.83 vol.% = 11.5% of ECD

Gas masses are shown in Figure 4-68, including the mass of steam in the reactor vessel and the total amounts of the gases generated due to corrosion: H_2 and CO. It is seen that the mass of steam in the RV, equal to about 80 kg soon after the break, slowly decreases as the corrosion proceeds. At the same time the mass of reaction products increases. At 100 hours there is still about 22 kg of steam in the RV (Figure 4-68, Table 4-15).

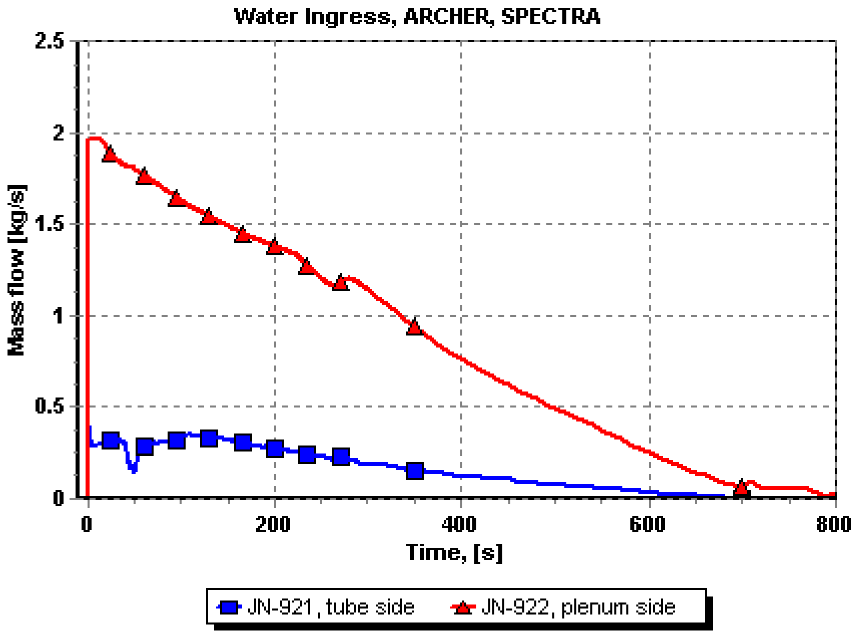

Figure 4-61 :
Break flows (1-tube, top of SG, failure of SG drain)

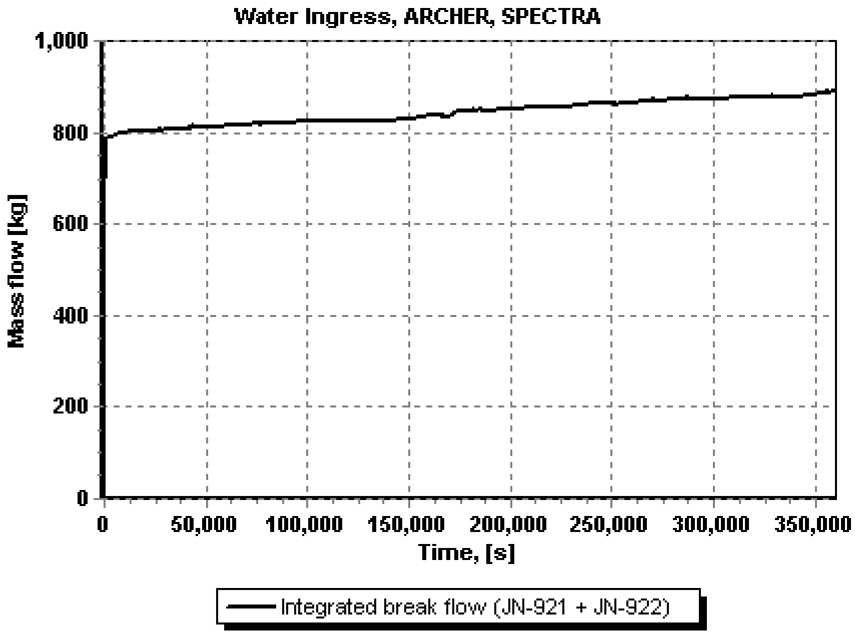

Figure 4-62 :
Integrated break flow (1-tube, top of SG, failure of SG drain)

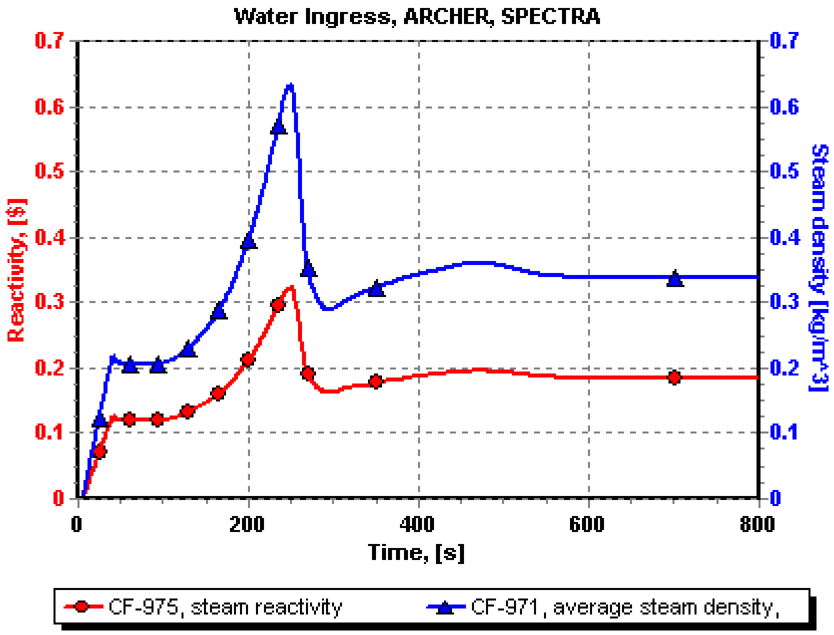

Figure 4-63 :
Steam density and reactivity (1-tube, top of SG, failure of SG drain)

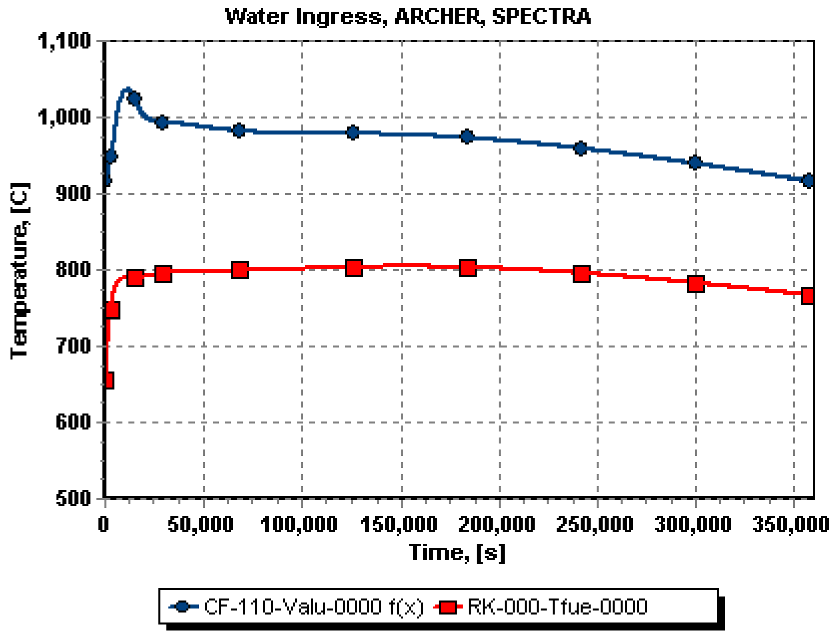

Figure 4-64 :
Fuel temperatures (1-tube, top of SG, failure of SG drain)

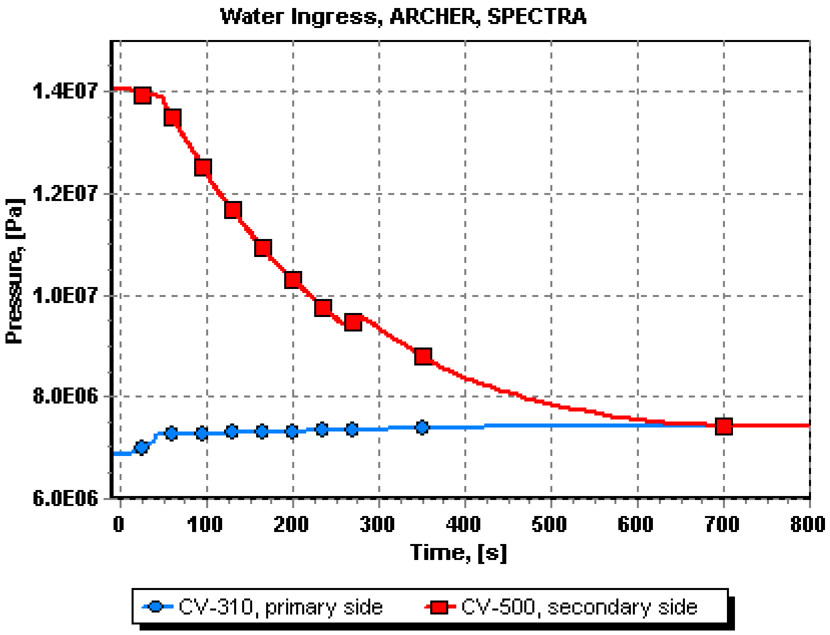

Figure 4-65 :
Pressures - short term (1-tube, top of SG, failure of SG drain)

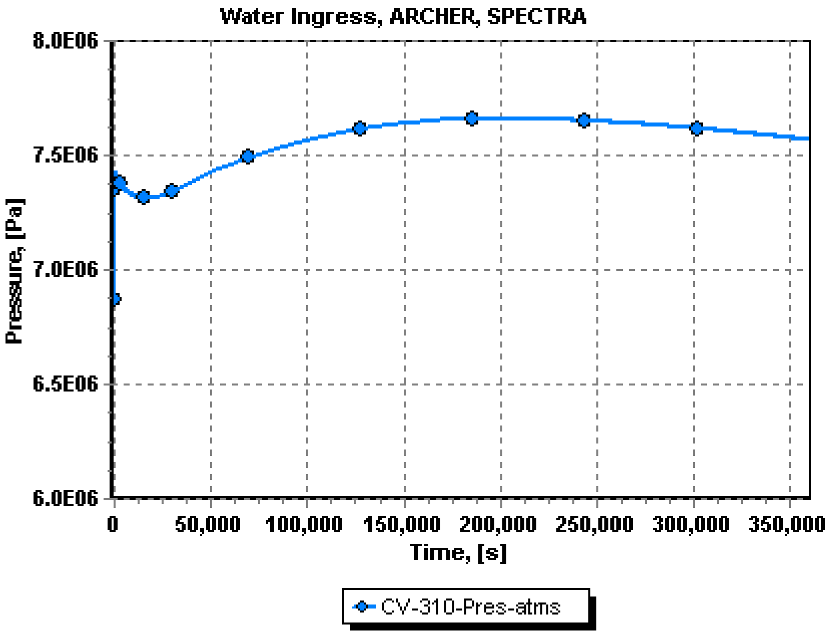

Figure 4-66 :
Primary pressure - long term (1-tube, top of SG, failure of SG drain)

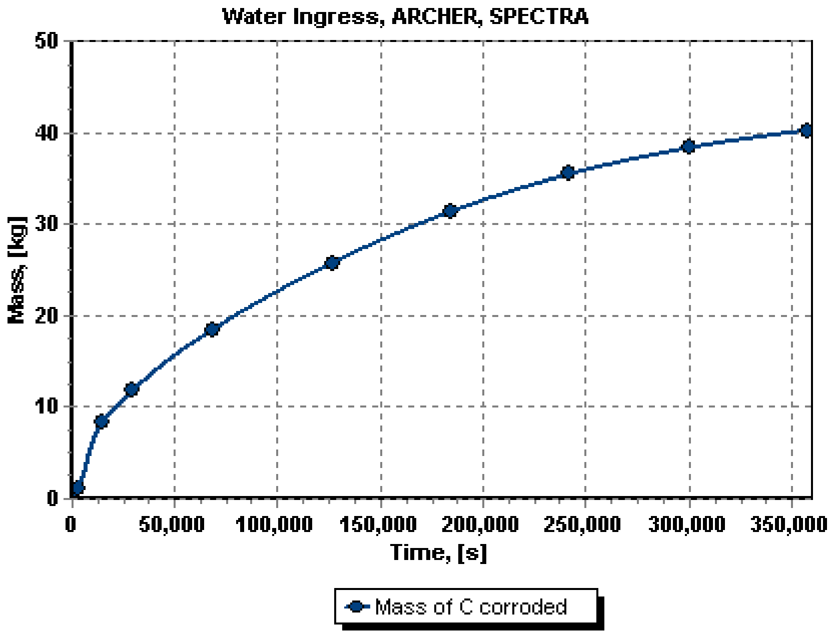

Figure 4-67 :
Graphite corrosion mass (1-tube, top of SG, failure of SG drain)

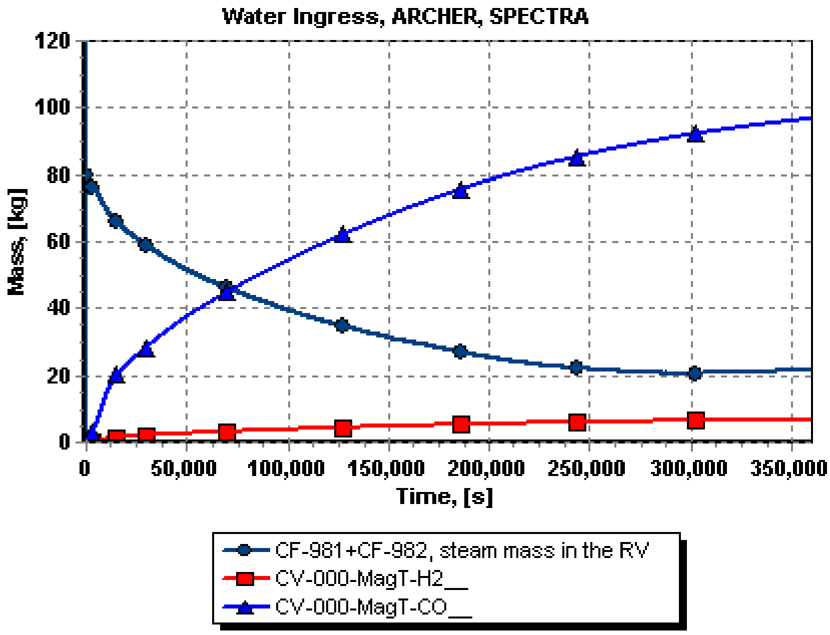

Figure 4-68 :
Mass of steam in RV and total mass of generated H_2 and CO (1-tube, top of SG, failure of SG drain)

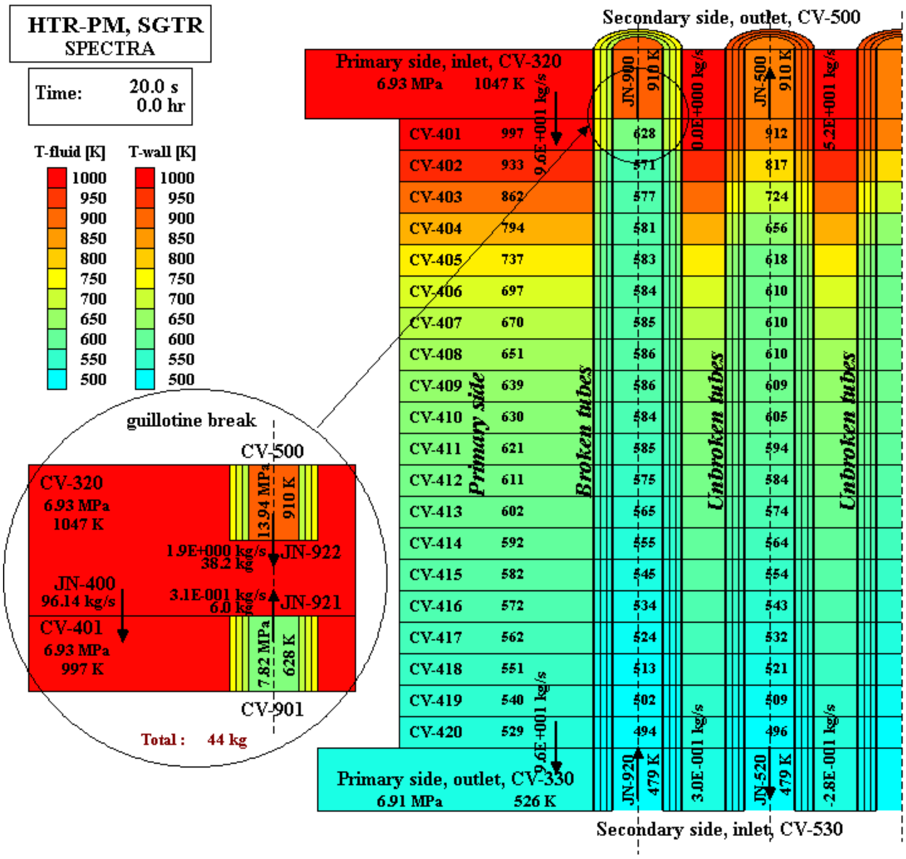

Figure 4-69 :

Break at *t*=20 s (1-tube, top of SG, failure of SG drain)

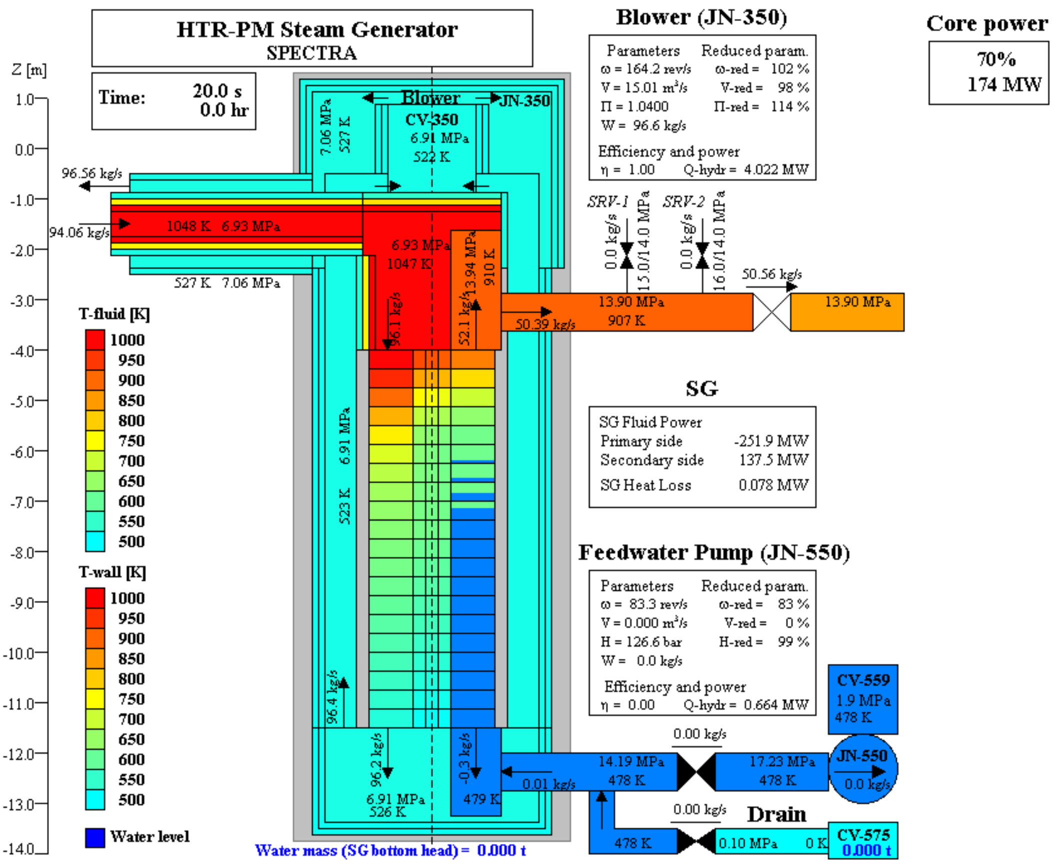

Figure 4-70 :

SG vessel at *t*=20 s (1-tube, top of SG, failure of SG drain)

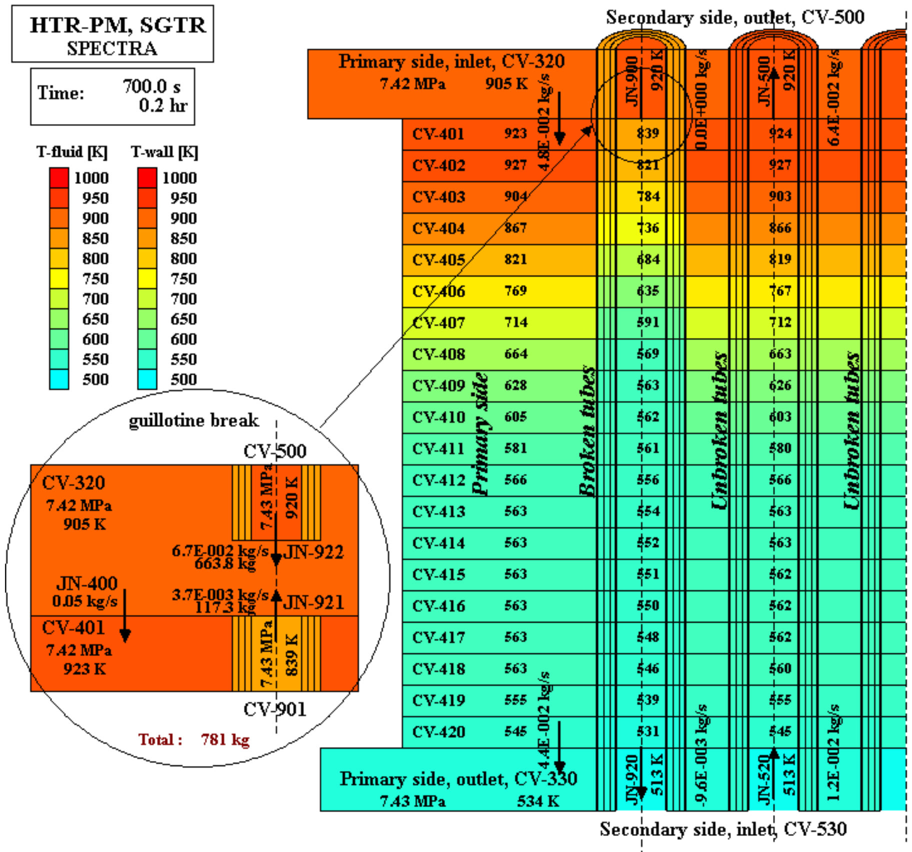

Figure 4-71 :
Break at *t*=700 s (1-tube, top of SG, failure of SG drain)

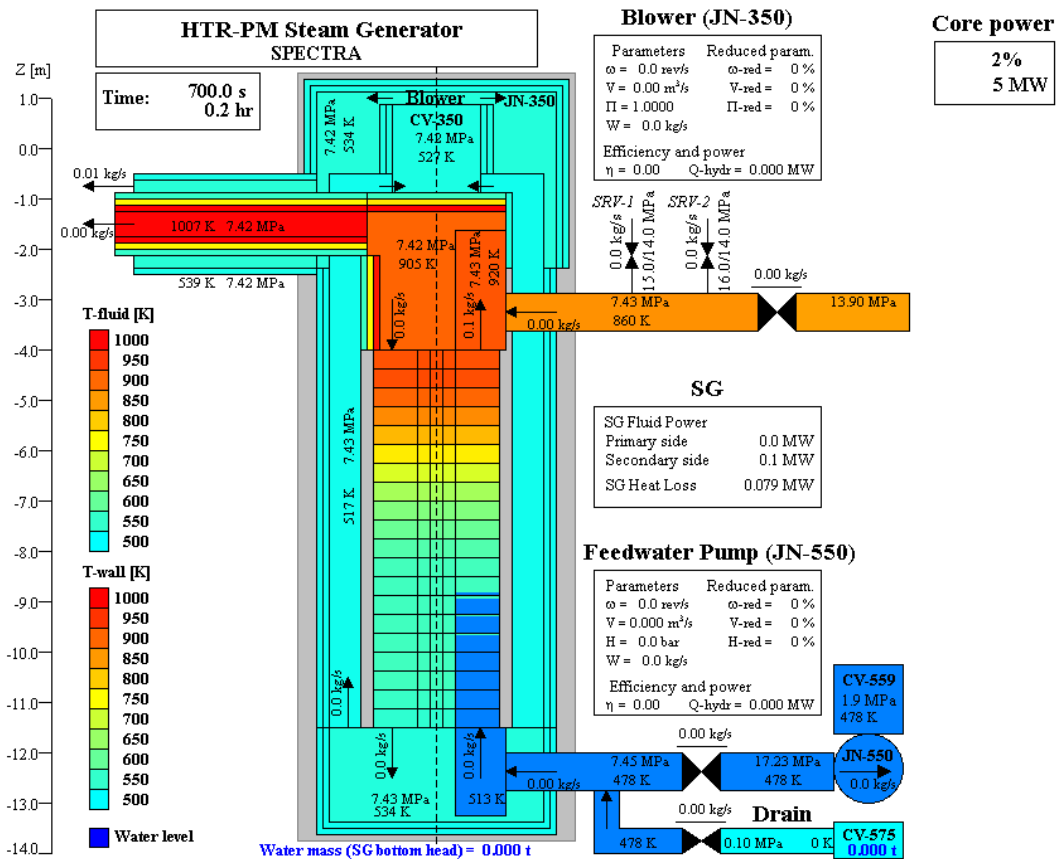

Figure 4-72 :
SG vessel at *t*=700 s (1-tube, top of SG, failure of SG drain)

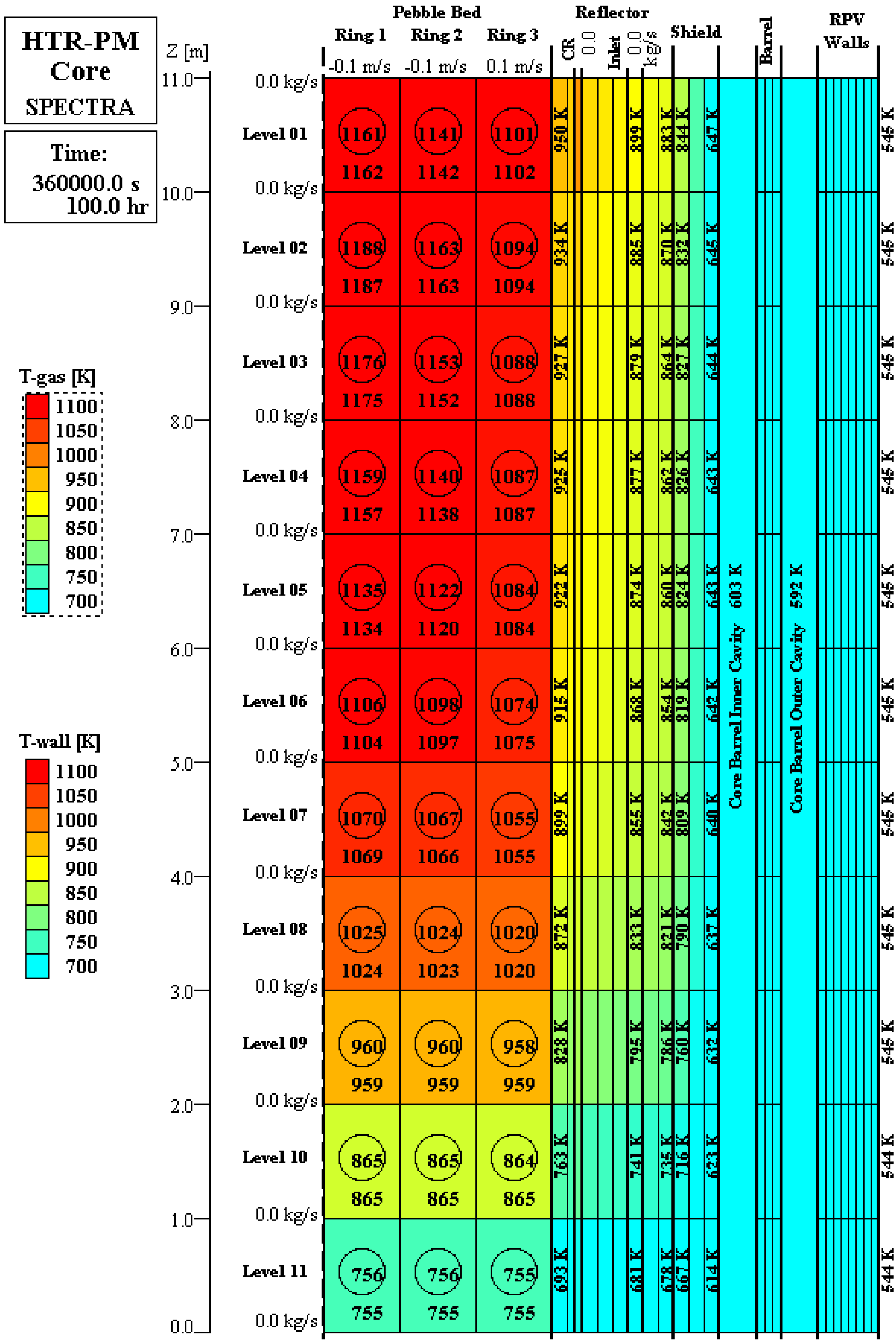

Figure 4-73 :

Temperatures at *t*=100 hr (1-tube, top of SG, failure of SG drain)

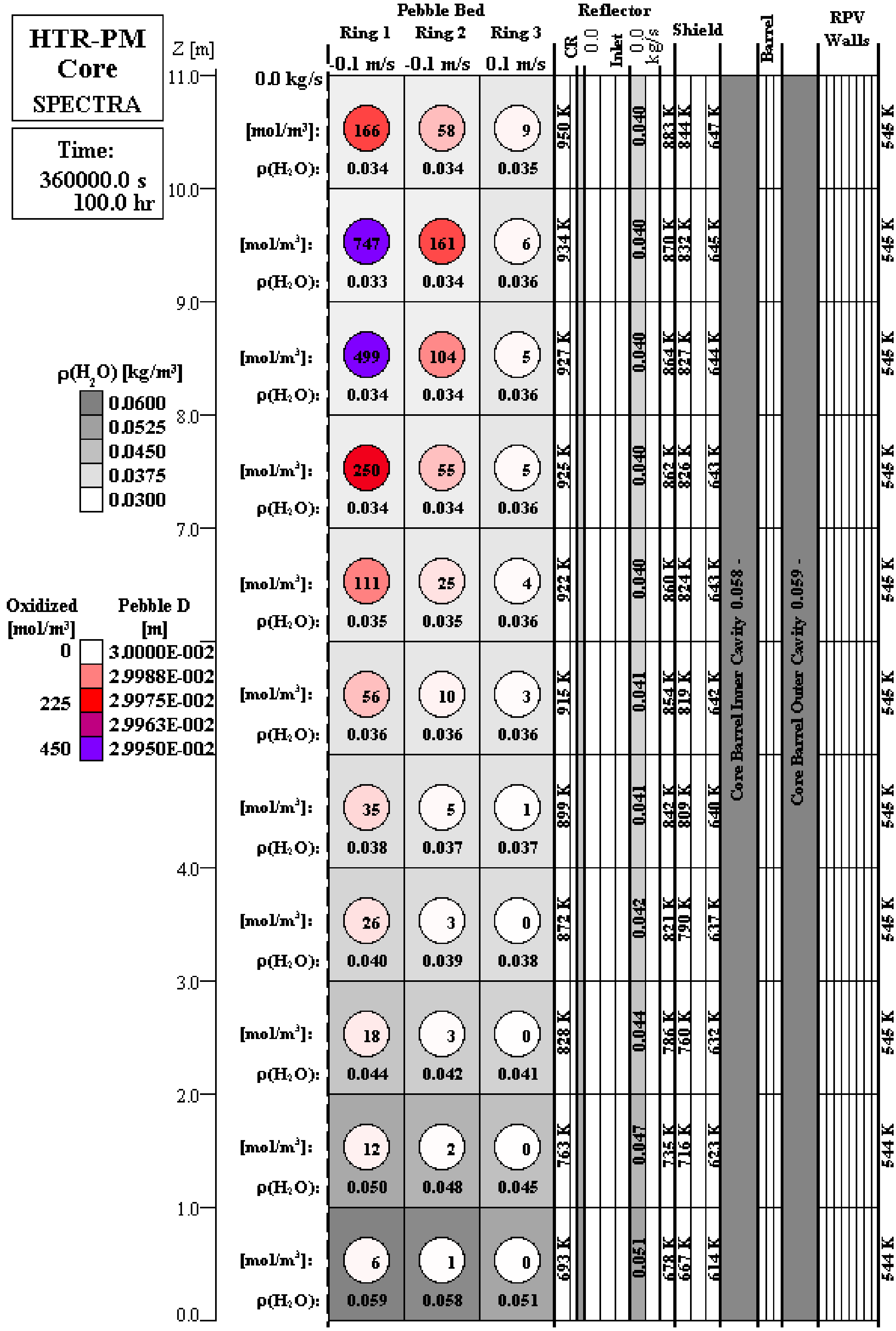

Figure 4-74 :
Oxidation at *t*=100 hr (1-tube, top of SG, failure of SG drain)

Table 4-13 : Oxidation at *t*= 100 hr (1-tube, top of SG, failure of SG drain)

HTR-PM Oxidation Summary SPECTRA							Time: 3.60E+005 s 1.00E+002 hr
Oxidation depth, [mm]				Oxidized mass, [mol/m³]			
	Ring 1	Ring 2	Ring 3		Ring 1	Ring 2	Ring 3
01	0.018	0.006	0.001	01	166.5	57.9	9.1
02	0.083	0.018	0.001	02	747.4	161.1	6.3
03	0.055	0.012	0.001	03	498.6	104.1	5.4
04	0.028	0.006	0.000	04	249.7	55.2	4.5
05	0.012	0.003	0.000	05	111.3	25.3	3.6
06	0.006	0.001	0.000	06	56.1	10.0	2.7
07	0.004	0.000	0.000	07	35.3	4.5	0.9
08	0.003	0.000	0.000	08	26.3	2.7	0.0
09	0.002	0.000	0.000	09	18.1	2.7	0.0
10	0.001	0.000	0.000	10	11.8	1.8	0.0
11	0.001	0.000	0.000	11	6.3	0.9	0.0

Table 4-14 : State at *t*= 20 s (1-tube, top of SG, failure of SG drain)

HTR-PM Water Ingress Summary SPECTRA — Time: 2.00E+001 s 5.56E-003 hr

Steam masses	abs. [kg]	rel. [%]	Water masses	abs. [kg]	rel. [%]
RV, pebble bed:	18.5	41.8%	RV, pebble bed:	0.0	0.0%
RV, other:	2.7	6.2%	RV, other:	0.0	0.0%
SG primary side:	20.9	47.1%	SG primary side:	0.0	0.0%
SG tubes, primary:	2.2	4.9%	SG tubes, primary:	0.0	0.0%
Primary system, total:	44.3	100.0%	Primary system, total:	0.0	0.0%

Total masses [kg]		Drained mass [kg]		Integrated flow through the break [kg]	
Liquid:	4177.2	CV-575:	0.0	Integrated flow, total:	44.2
Gases:		Reacted C [kg]			
He:	3045.6				
H_2:	0.0	Measur. 1:	0.0		
CO:	0.0	Measur. 2:	0.0		

Table 4-15 : State at *t*= 100 hr (1-tube, top of SG, failure of SG drain)

HTR-PM Water Ingress Summary SPECTRA — Time: 3.60E+005 s 1.00E+002 hr

Steam masses	abs. [kg]	rel. [%]	Water masses	abs. [kg]	rel. [%]
RV, pebble bed:	11.2	4.8%	RV, pebble bed:	0.0	0.0%
RV, other:	10.6	4.6%	RV, other:	0.0	0.0%
SG primary side:	177.1	75.9%	SG primary side:	587.8	100.0%
SG tubes, primary:	34.4	14.8%	SG tubes, primary:	0.0	0.0%
Primary system, total:	233.3	100.0%	Primary system, total:	587.8	100.0%

Total masses [kg]		Drained mass [kg]		Integrated flow through the break [kg]	
Liquid:	3082.3	CV-575:	0.0	Integrated flow, total:	892.2
Gases:		Reacted C [kg]			
He:	3045.6				
H_2:	6.7	Measur. 1:	40.1		
CO:	96.4	Measur. 2:	40.2		

4.2.3 1-Tube Rupture, Failure of SG Drain and Blower Flaps Closure

This section presents results of a break of single tube at the top of SG, with simultaneous failure of the SG drain system and failure to close the blower flaps. Results are shown in Figure 4-75 through Figure 4-88 and Table 4-16 through Table 4-18.

The mass flow through the break is shown in Figure 4-75. At the end of blowdown (about 400 s) - Figure 4-85 - about **556 kg** of steam has entered the primary system, most of it through the plenum side of the break (JN-922: 469 kg). In contrast to the break at the bottom of SG tubes, where a lot of water is deposited in the SG lower head (401 kg - Figure 4-43), in the present case there is practically no water in the SG head - Figure 4-86. At the end of the calculations the integrated mass through the break is 525 kg - Table 4-18. The maximum water ingress is observed at the end of blowdown, is equal to **556 kg**.

The humidity detectors are assumed to initiate safety actions at 10 seconds. The reactor SCRAM is initiated with a 2 seconds delay. The total drop time of the control rods is 50 seconds [10]. Additionally small absorber spheres are dropped to ensure long term subcriticality [10]. Maximum reactor power, about 109% or 272 MW is observed at 12 seconds. Maximum reactivity due to steam ingress is about 1.2 $, corresponding to the steam density of about 2.5 kg/m^3 - Figure 4-77. It is much higher than in previous cases because of larger amount of steam in the core. The maximum reactivity is observed at about 180 s.

The SG drain system and the blower flaps closure are assumed to fail in this scenario. As a consequence of the open blower flaps, there is a continuous natural circulation flow through steam generator. The circulation flow is shown in Figure 4-76, showing the mass flow at JN-251 (Figure 3-7) with the reverse sign. The circulation flow is in reverse direction compared to the normal flow. As a consequence of this flow, steam present in the SG will slowly be transported into the reactor vessel.

The maximum and average fuel temperatures are shown in Figure 4-78. Maximum fuel temperature is 1257 K (984°C). Natural convection in the core results in a shift of the core maximum temperatures (Figure 4-87) and consequently the maximum corrosion (Figure 4-88) to the upper part of the core.

The system pressures are shown in Figure 4-79 and Figure 4-80. The blowdown is finished within about 400 seconds. The primary pressure never reaches the setpoint of the primary pressure release system, 7.9 MPa.

Graphite corrosion is shown in Figure 4-81 and Table 4-16. After 100 hours the total mass of carbon reacted is about 87.5 kg. The maximum corrosion depth is about 0.140 mm, corresponding to the oxidation density of 1266 mol/m^3. The maximum oxidation depth of 0.140 mm corresponds to the oxidized volume of 1.39 vol.%. This means the maximum corrosion is 19.4% of ECD.

maximum corrosion = 1.39 vol.% = 19.4% of ECD

Gas masses are shown in Figure 4-82, including the mass of steam in the reactor vessel and the total amounts of the gases generated due to corrosion: H_2 and CO. It is seen that the mass of steam in the RV, equal to about 400 kg soon after the break, slowly decreases as the corrosion proceeds. At the same time the mass of reaction products increases. At 100 hours there is still about 300 kg of steam in the RV (Figure 4-82, Table 4-18).

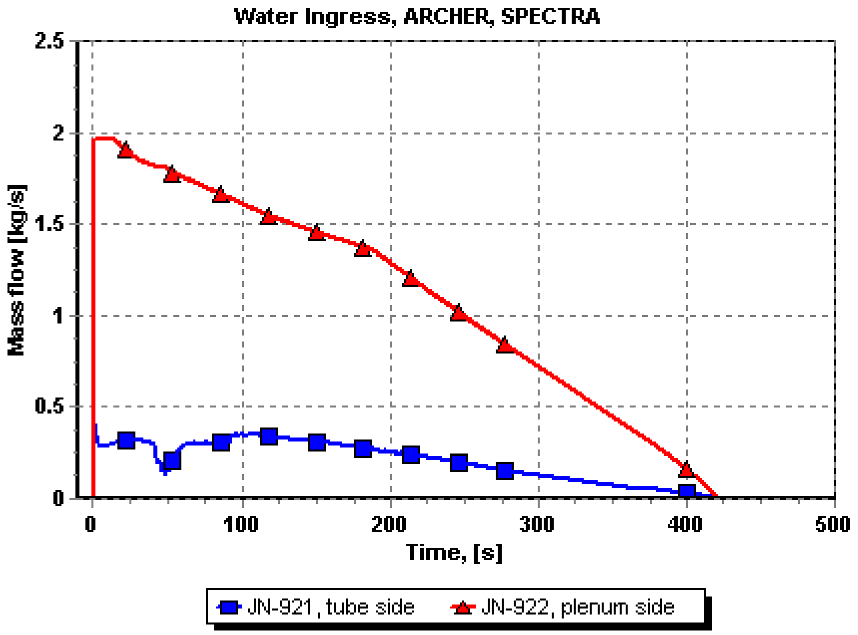

Figure 4-75 :
Break flows (1-tube, top of SG, failure of SG drain and blower flaps closure)

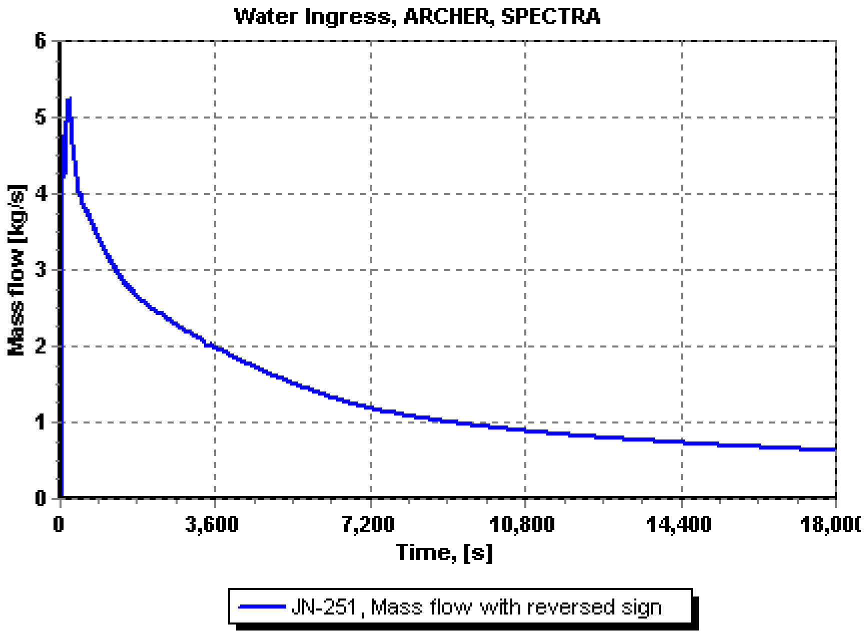

Figure 4-76 :
Natural circulation flow (1-tube, top of SG, failure of SG drain and blower flaps closure)

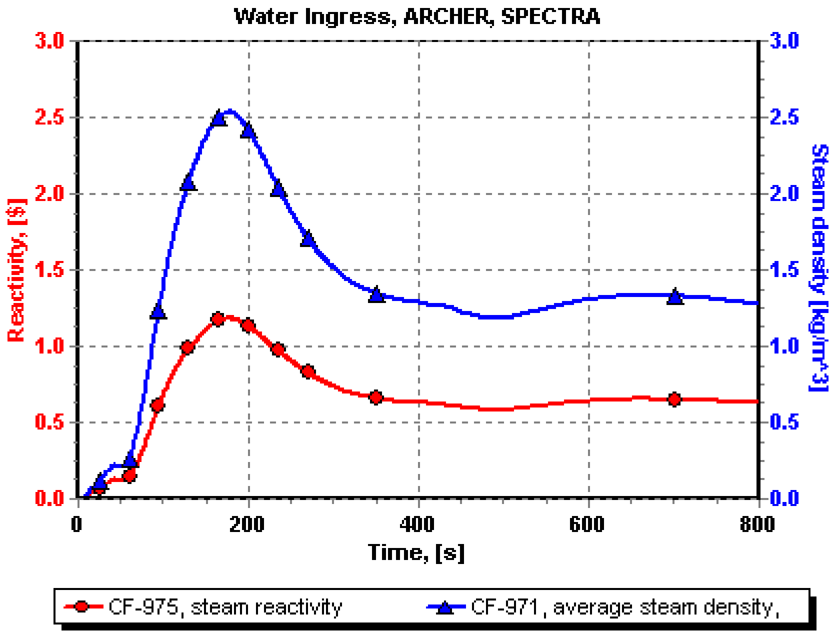

Figure 4-77 :
Steam density and reactivity (1-tube, top of SG, failure of SG drain and blower flaps closure)

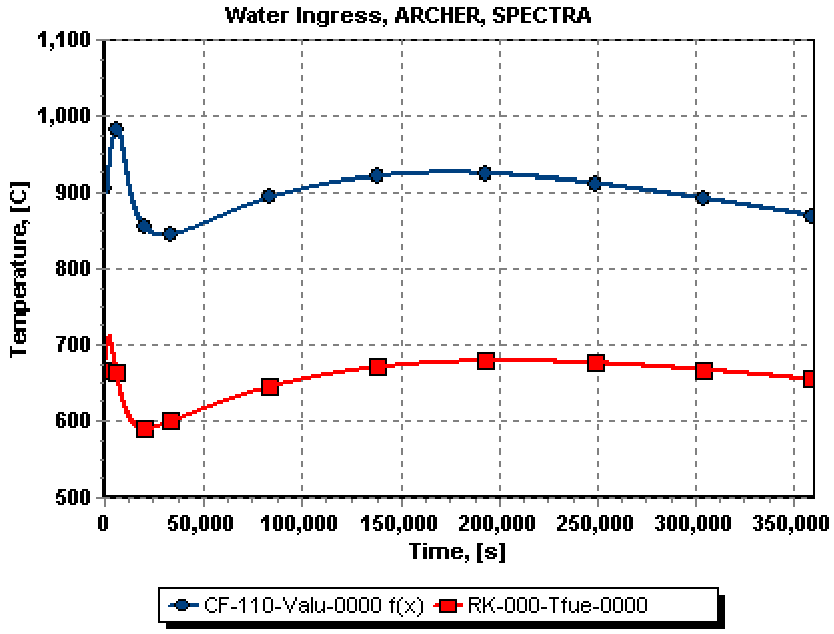

Figure 4-78 :
Fuel temperatures (1-tube, top of SG, failure of SG drain and blower flaps closure)

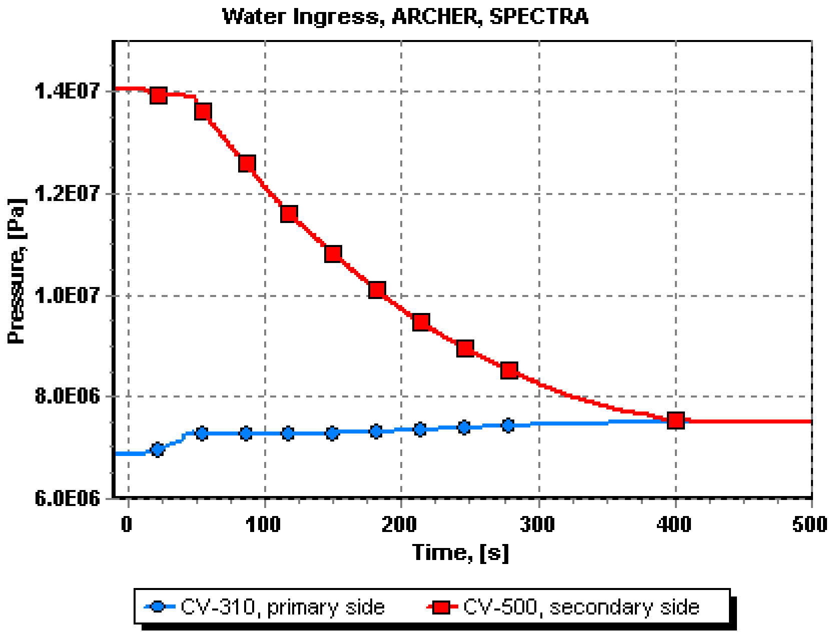

Figure 4-79 :
Pressures - short term (1-tube, top of SG, failure of SG drain and blower flaps closure)

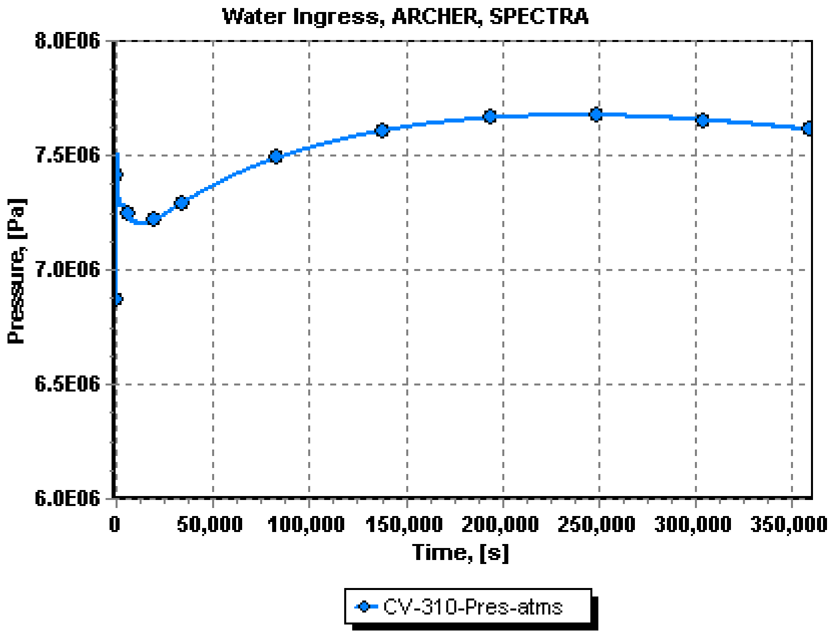

Figure 4-80 :
Primary pressure - long term (1-tube, top of SG, failure of SG drain and blower flaps closure)

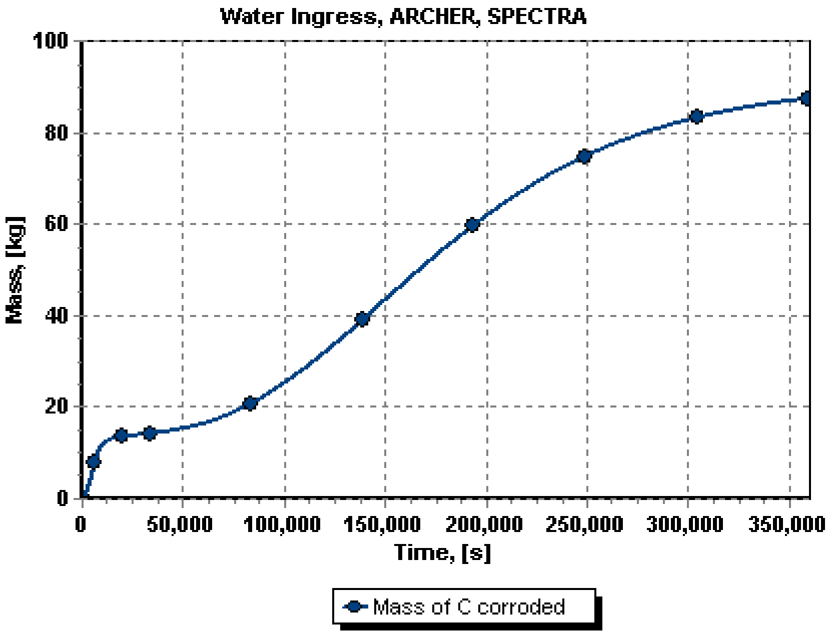

Figure 4-81 :
Graphite corrosion mass (1-tube, top of SG, failure of SG drain and blower flaps closure)

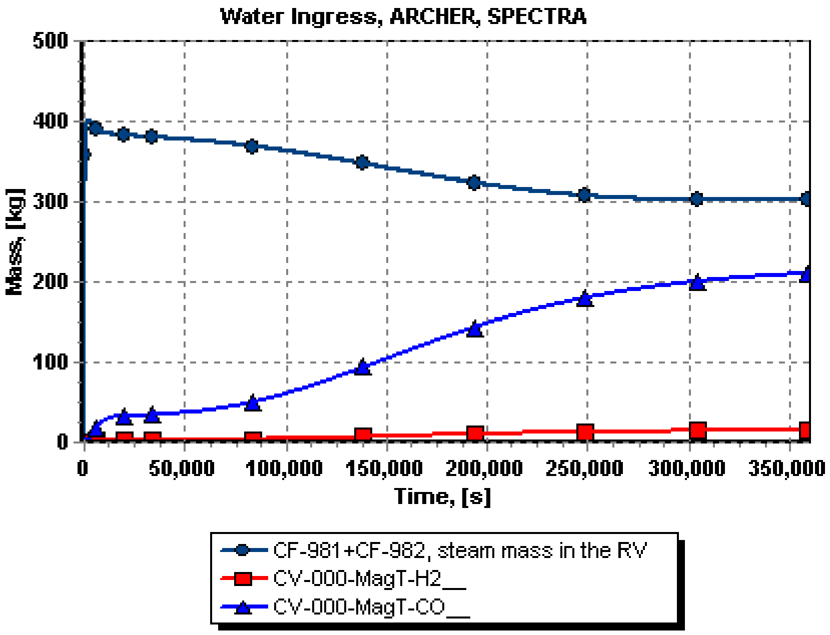

Figure 4-82 :
Mass of steam in RV and total mass of generated H_2 and CO
(1-tube, top of SG, failure of SG drain and blower flaps closure)

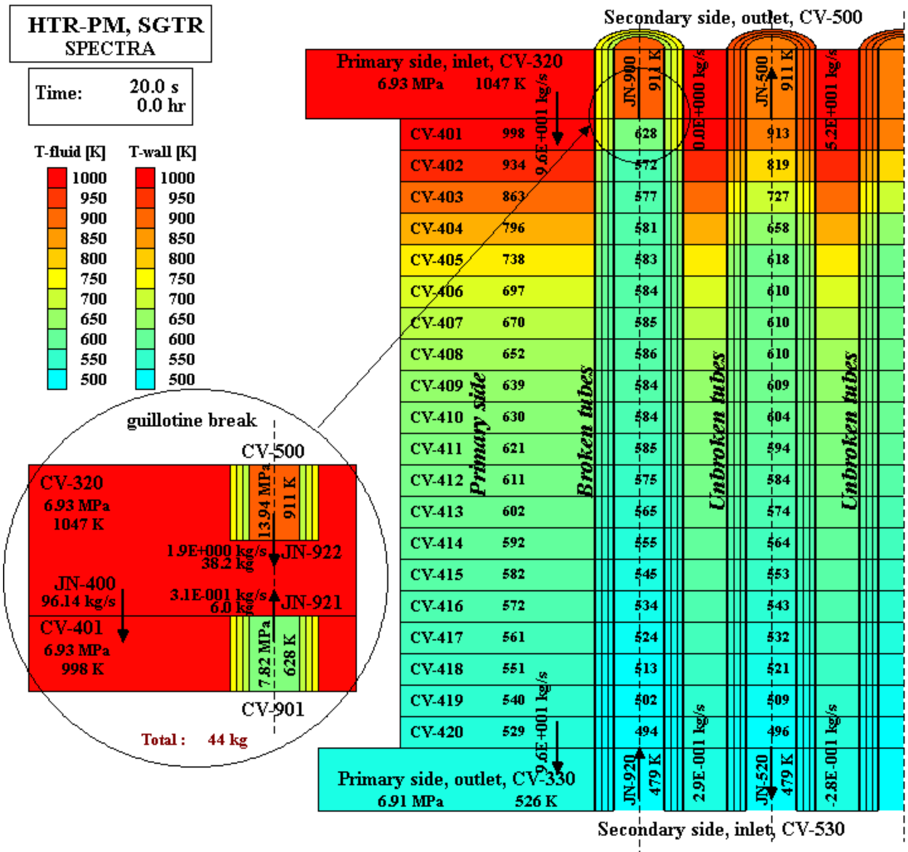

Figure 4-83 :

Break at *t*=20 s (1-tube, top of SG, failure of SG drain and blower flaps closure)

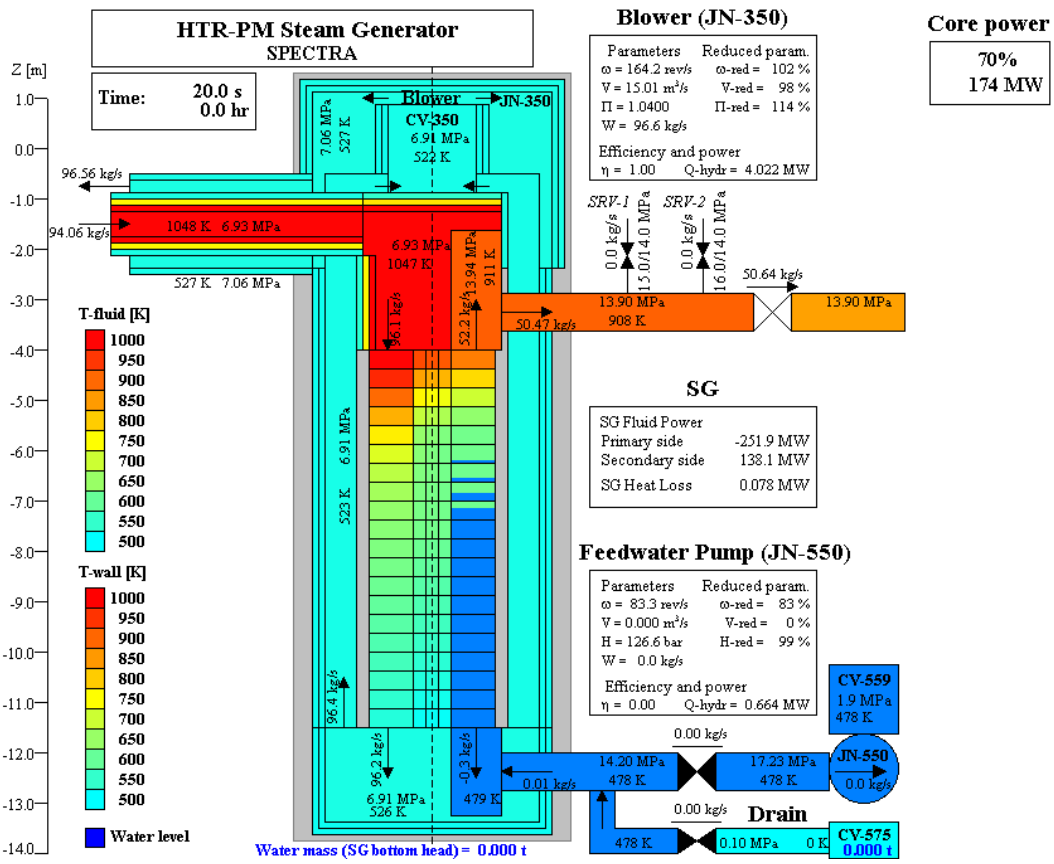

Figure 4-84 :

SG vessel at *t*=20 s (1-tube, top of SG, failure of SG drain and blower flaps closure)

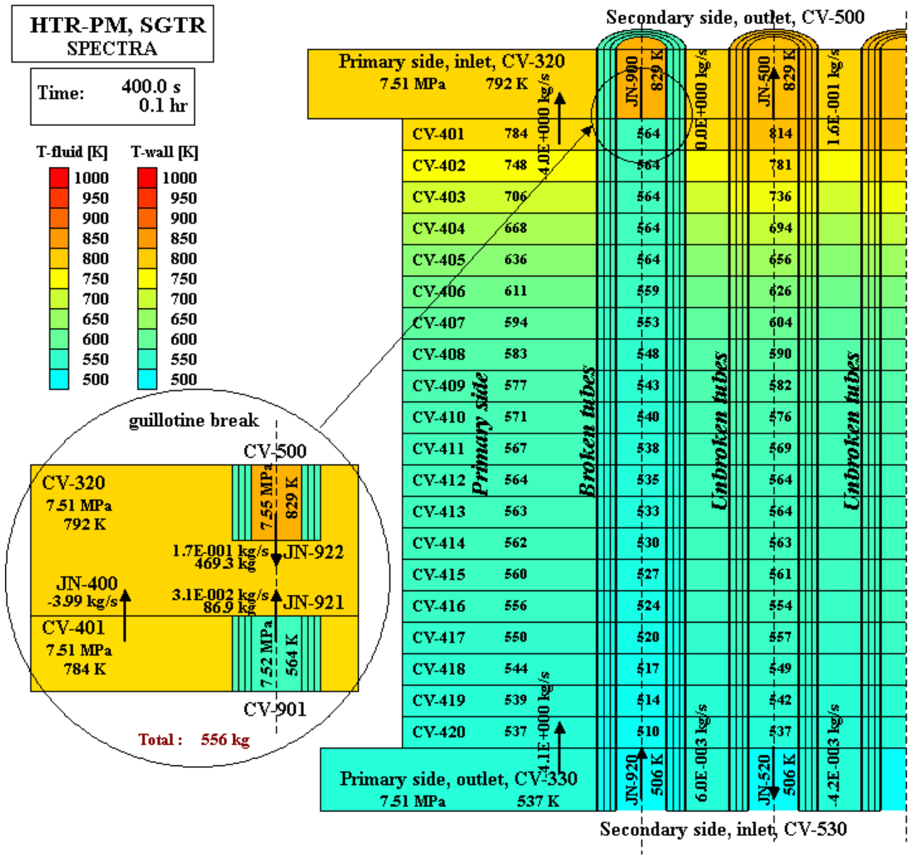

Figure 4-85 :
Break at *t*=400 s (1-tube, top of SG, failure of SG drain and blower flaps closure)

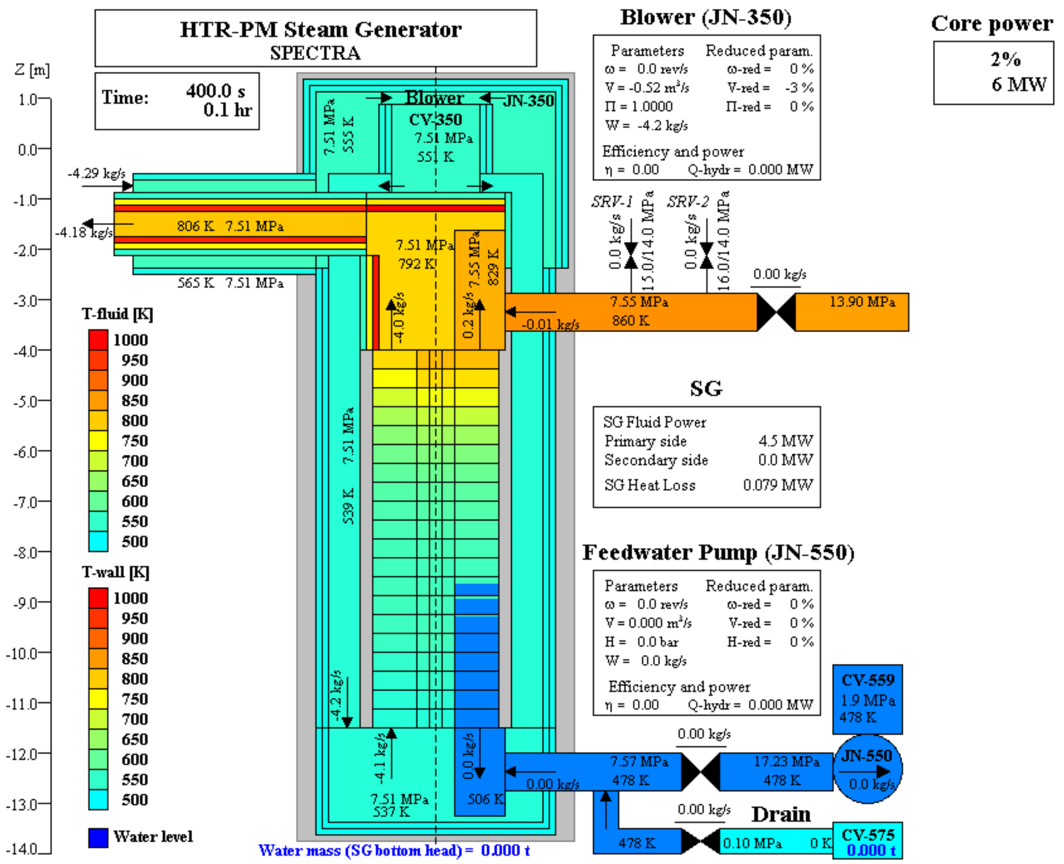

Figure 4-86 :
SG vessel at *t*=400 s (1-tube, top of SG, failure of SG drain and blower flaps closure)

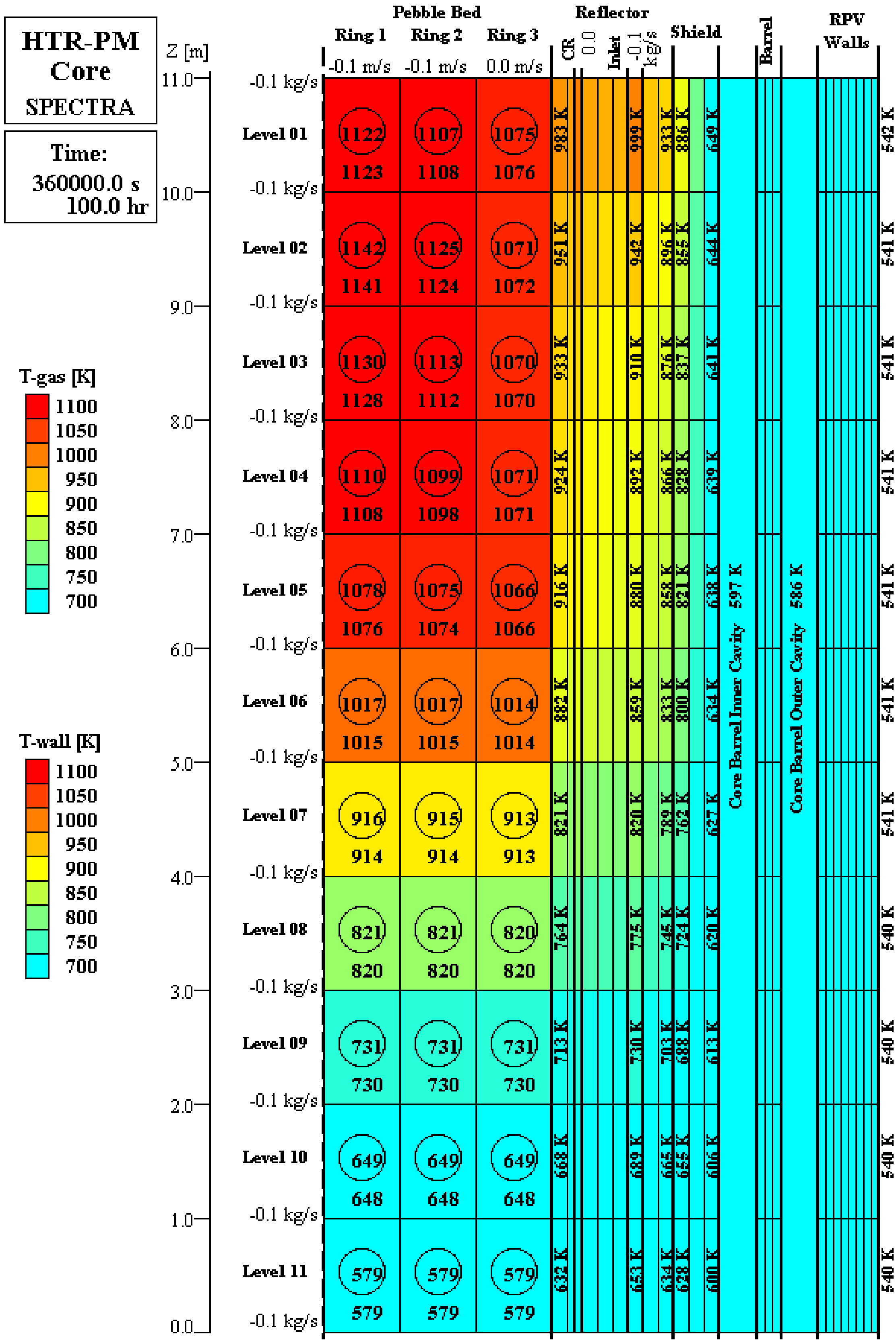

Figure 4-87 :

Temperatures at *t*=100 hr (1-tube, top of SG, failure of SG drain and blower flaps closure)

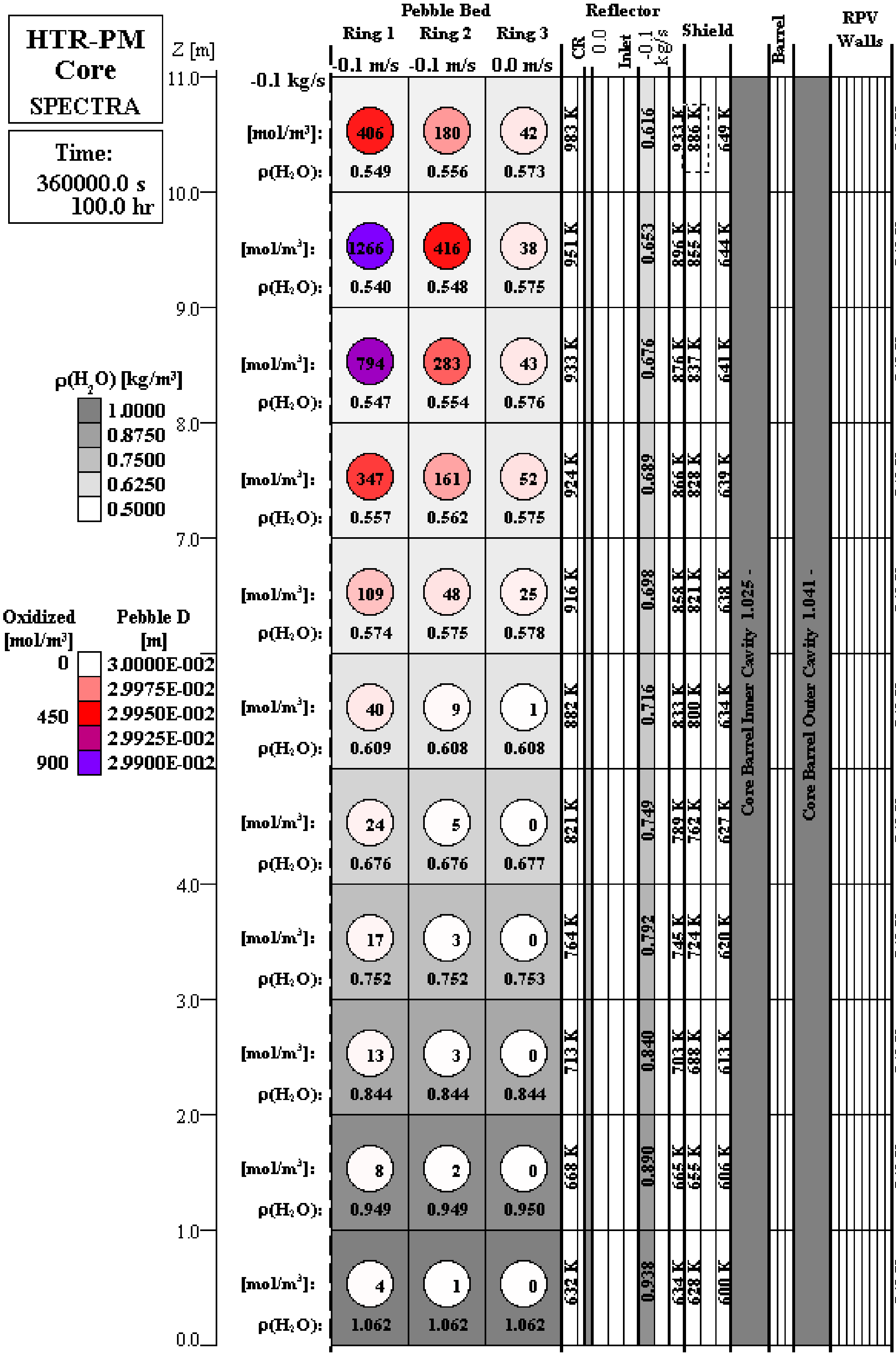

Figure 4-88 :

Oxidation at *t*=100 hr (1-tube, top of SG, failure of SG drain and blower flaps closure)

Table 4-16 : Oxidation at *t*= 100 hr (1-tube, top of SG, failure of SG drain and blower flaps closure)

HTR-PM Oxidation Summary
SPECTRA

Time: 3.60E+005 s / 1.00E+002 hr

	Oxidation depth, [mm]				Oxidized mass, [mol/m³]		
	Ring 1	Ring 2	Ring 3		Ring 1	Ring 2	Ring 3
01	0.045	0.020	0.005	01	406.3	180.1	41.6
02	0.140	0.046	0.004	02	1265.9	416.2	38.0
03	0.088	0.031	0.005	03	794.5	283.2	42.5
04	0.038	0.018	0.006	04	346.6	161.1	51.6
05	0.012	0.005	0.003	05	109.5	48.0	25.3
06	0.004	0.001	0.000	06	39.8	9.1	0.9
07	0.003	0.000	0.000	07	24.4	4.5	0.0
08	0.002	0.000	0.000	08	17.2	2.7	0.0
09	0.001	0.000	0.000	09	12.7	2.7	0.0
10	0.001	0.000	0.000	10	8.2	1.8	0.0
11	0.000	0.000	0.000	11	3.6	0.9	0.0

Table 4-17 : State at *t*= 20 s (1-tube, top of SG, failure of SG drain and blower flaps closure)

HTR-PM Water Ingress Summary
SPECTRA

Time: 2.00E+001 s / 5.56E-003 hr

Steam masses	abs. [kg]	rel. [%]	Water masses	abs. [kg]	rel. [%]
RV, pebble bed:	18.5	41.8%	RV, pebble bed:	0.0	0.0%
RV, other:	2.7	6.2%	RV, other:	0.0	0.0%
SG primary side:	20.9	47.1%	SG primary side:	0.0	0.0%
SG tubes, primary:	2.2	4.9%	SG tubes, primary:	0.0	0.0%
Primary system, total:	44.3	100.0%	Primary system, total:	0.0	0.0%

Total masses [kg]		Drained mass [kg]		Integrated flow through the break [kg]	
Liquid:	4177.2	CV-575:	0.0	Integrated flow, total:	44.2
Gases:		Reacted C [kg]			
He:	3045.6				
H_2:	0.0	Measur. 1:	0.0		
CO:	0.0	Measur. 2:	0.0		

Table 4-18 : State at *t*= 100 hr (1-tube, top of SG, failure of SG drain and blower flaps closure)

HTR-PM Water Ingress Summary
SPECTRA

Time: 3.60E+005 s / 1.00E+002 hr

Steam masses	abs. [kg]	rel. [%]	Water masses	abs. [kg]	rel. [%]
RV, pebble bed:	196.4	45.8%	RV, pebble bed:	0.0	0.0%
RV, other:	106.4	24.8%	RV, other:	0.0	0.0%
SG primary side:	113.1	26.4%	SG primary side:	0.0	0.0%
SG tubes, primary:	12.7	3.0%	SG tubes, primary:	0.0	0.0%
Primary system, total:	428.6	100.0%	Primary system, total:	0.0	0.0%

Total masses [kg]		Drained mass [kg]		Integrated flow through the break [kg]	
Liquid:	2913.7	CV-575:	0.0	Integrated flow, total:	525.0
Gases:		Reacted C [kg]			
He:	3045.6				
H_2:	14.7	Measur. 1:	87.4		
CO:	210.3	Measur. 2:	87.6		

4.3 Influence of Oxidation Model

This section shows results obtained with the conservative oxidation model. The conservative multiplier of:

$$M_C = 1.8$$

was used - section 2.2.1. The results are compared with the results obtained with the best estimate oxidation model discussed in the previous sections, in Table 4-19 through Table 4-24.

In all cases the overall oxidation is higher. In some cases (Table 4-19, Table 4-20, Table 4-22, and Table 4-23) the maximum oxidation depth is smaller. The reason is larger oxidation in the lower parts of the core. This causes depletion of steam in the upper parts of the core and smaller maximum oxidation depth. The total oxidation is not smaller, which is seen by total amount of hydrogen produced or carbon reacted (Table 5-1).

In other cases (Table 4-21, Table 4-24) the maximum oxidation depth is clearly higher if the conservative oxidation model is applied. In those cases there is a relatively large amount of steam ingress into the core and therefore there is enough steam in the upper part of the core in spite of increased oxidation in the lower part of the core.

Table 4-19 : Oxidation at *t*= 100 hr (1-tube, bottom of SG, safety systems available)

Best Estimate oxidation model

HTR-PM Oxidation Summary, SPECTRA — Time: 3.60E+005 s, 1.00E+002 hr

	Oxidation depth, [mm]			Oxidized mass, [mol/m³]		
	Ring 1	Ring 2	Ring 3	Ring 1	Ring 2	Ring 3
01	0.002	0.001	0.000	16.3	5.4	0.9
02	0.007	0.002	0.000	67.9	16.3	0.9
03	0.007	0.001	0.000	64.2	11.8	0.0
04	0.005	0.001	0.000	42.5	6.3	0.0
05	0.003	0.000	0.000	22.6	2.7	0.0
06	0.002	0.000	0.000	13.6	1.8	0.0
07	0.001	0.000	0.000	9.1	0.9	0.0
08	0.001	0.000	0.000	7.2	0.9	0.0
09	0.001	0.000	0.000	5.4	0.9	0.0
10	0.000	0.000	0.000	3.6	0.9	0.0
11	0.000	0.000	0.000	1.8	0.0	0.0

Conservative oxidation model

HTR-PM Oxidation Summary, SPECTRA — Time: 3.60E+005 s, 1.00E+002 hr

	Oxidation depth, [mm]			Oxidized mass, [mol/m³]		
	Ring 1	Ring 2	Ring 3	Ring 1	Ring 2	Ring 3
01	0.001	0.000	0.000	10.9	3.6	0.9
02	0.005	0.001	0.000	44.3	12.7	0.0
03	0.006	0.001	0.000	55.2	10.9	0.0
04	0.005	0.001	0.000	48.0	6.3	0.0
05	0.003	0.000	0.000	30.8	3.6	0.0
06	0.002	0.000	0.000	19.0	1.8	0.0
07	0.002	0.000	0.000	15.4	1.8	0.0
08	0.002	0.000	0.000	14.5	1.8	0.0
09	0.002	0.000	0.000	13.6	1.8	0.0
10	0.001	0.000	0.000	10.9	1.8	0.0
11	0.001	0.000	0.000	6.3	0.9	0.0

Table 4-20 : Oxidation at *t*= 100 hr (1-tube, bottom of SG, failure of SG drain)

Best Estimate oxidation model

HTR-PM Oxidation Summary, SPECTRA — Time: 3.60E+005 s, 1.00E+002 hr

	Oxidation depth, [mm]			Oxidized mass, [mol/m³]		
	Ring 1	Ring 2	Ring 3	Ring 1	Ring 2	Ring 3
01	0.002	0.001	0.000	20.8	6.3	0.9
02	0.010	0.002	0.000	93.2	19.0	0.9
03	0.009	0.002	0.000	84.2	13.6	0.9
04	0.006	0.001	0.000	53.4	7.2	0.9
05	0.003	0.000	0.000	29.0	3.6	0.0
06	0.002	0.000	0.000	17.2	1.8	0.0
07	0.001	0.000	0.000	11.8	0.9	0.0
08	0.001	0.000	0.000	8.2	0.9	0.0
09	0.001	0.000	0.000	5.4	0.9	0.0
10	0.000	0.000	0.000	3.6	0.9	0.0
11	0.000	0.000	0.000	1.8	0.0	0.0

Conservative oxidation model

HTR-PM Oxidation Summary, SPECTRA — Time: 3.60E+005 s, 1.00E+002 hr

	Oxidation depth, [mm]			Oxidized mass, [mol/m³]		
	Ring 1	Ring 2	Ring 3	Ring 1	Ring 2	Ring 3
01	0.001	0.000	0.000	12.7	4.5	0.9
02	0.006	0.002	0.000	52.5	13.6	0.9
03	0.007	0.001	0.000	65.2	11.8	0.0
04	0.007	0.001	0.000	60.6	7.2	0.0
05	0.005	0.000	0.000	43.4	3.6	0.0
06	0.003	0.000	0.000	29.9	1.8	0.0
07	0.003	0.000	0.000	23.5	1.8	0.0
08	0.002	0.000	0.000	19.9	1.8	0.0
09	0.002	0.000	0.000	16.3	1.8	0.0
10	0.001	0.000	0.000	11.8	1.8	0.0
11	0.001	0.000	0.000	6.3	0.9	0.0

Table 4-21 : Oxidation at *t*= 100 hr (1-tube, bottom of SG, failure of SG drain and flaps)

Best Estimate oxidation model

HTR-PM Oxidation Summary
SPECTRA

Time: 3.60E+005 s
1.00E+002 hr

	Oxidation depth, [mm]			Oxidized mass, [mol/m³]		
	Ring 1	Ring 2	Ring 3	Ring 1	Ring 2	Ring 3
01	0.143	0.057	0.012	1296.6	512.2	109.5
02	0.466	0.149	0.010	4213.8	1350.9	91.4
03	0.271	0.089	0.010	2451.2	800.8	86.0
04	0.102	0.047	0.011	923.8	426.2	95.0
05	0.027	0.016	0.008	240.7	144.8	68.8
06	0.005	0.003	0.002	49.8	22.6	13.6
07	0.002	0.000	0.000	19.0	3.6	0.0
08	0.001	0.000	0.000	11.8	2.7	0.0
09	0.001	0.000	0.000	8.2	1.8	0.0
10	0.000	0.000	0.000	4.5	0.9	0.0
11	0.000	0.000	0.000	1.8	0.0	0.0

Conservative oxidation model

HTR-PM Oxidation Summary
SPECTRA

Time: 3.60E+005 s
1.00E+002 hr

	Oxidation depth, [mm]			Oxidized mass, [mol/m³]		
	Ring 1	Ring 2	Ring 3	Ring 1	Ring 2	Ring 3
01	0.332	0.157	0.040	3003.2	1418.8	362.8
02	0.808	0.328	0.034	7310.2	2966.1	303.1
03	0.507	0.214	0.031	4587.5	1937.3	277.8
04	0.242	0.126	0.033	2190.6	1138.3	295.0
05	0.081	0.048	0.024	732.9	433.4	215.4
06	0.021	0.008	0.005	190.0	76.9	46.2
07	0.009	0.002	0.000	81.4	15.4	0.9
08	0.006	0.001	0.000	54.3	10.0	0.0
09	0.004	0.001	0.000	37.1	7.2	0.0
10	0.002	0.000	0.000	21.7	4.5	0.0
11	0.001	0.000	0.000	9.1	1.8	0.0

Table 4-22 : Oxidation at *t*= 100 hr (1-tube, top of SG, safety systems available)

Best Estimate oxidation model

HTR-PM Oxidation Summary
SPECTRA

Time: 3.60E+005 s
1.00E+002 hr

	Oxidation depth, [mm]			Oxidized mass, [mol/m³]		
	Ring 1	Ring 2	Ring 3	Ring 1	Ring 2	Ring 3
01	0.012	0.004	0.001	111.3	38.9	6.3
02	0.055	0.012	0.000	501.3	111.3	4.5
03	0.038	0.008	0.000	345.7	71.5	2.7
04	0.020	0.004	0.000	177.4	38.0	2.7
05	0.009	0.002	0.000	81.4	17.2	2.7
06	0.005	0.001	0.000	41.6	6.3	1.8
07	0.003	0.000	0.000	27.2	2.7	0.9
08	0.002	0.000	0.000	19.0	1.8	0.0
09	0.002	0.000	0.000	13.6	1.8	0.0
10	0.001	0.000	0.000	8.2	1.8	0.0
11	0.000	0.000	0.000	3.6	0.9	0.0

Conservative oxidation model

HTR-PM Oxidation Summary
SPECTRA

Time: 3.60E+005 s
1.00E+002 hr

	Oxidation depth, [mm]			Oxidized mass, [mol/m³]		
	Ring 1	Ring 2	Ring 3	Ring 1	Ring 2	Ring 3
01	0.011	0.003	0.000	103.2	30.8	4.5
02	0.047	0.011	0.000	429.8	95.0	3.6
03	0.044	0.008	0.000	399.0	68.8	2.7
04	0.029	0.004	0.000	259.7	39.8	1.8
05	0.016	0.002	0.000	143.0	19.0	1.8
06	0.010	0.001	0.000	87.8	9.1	0.9
07	0.007	0.001	0.000	67.0	5.4	0.9
08	0.006	0.001	0.000	54.3	5.4	0.0
09	0.005	0.001	0.000	42.5	5.4	0.0
10	0.003	0.000	0.000	29.0	4.5	0.0
11	0.002	0.000	0.000	14.5	2.7	0.0

Table 4-23 : Oxidation at *t*= 100 hr (1-tube, top of SG, failure of SG drain)

Best Estimate oxidation model

HTR-PM Oxidation Summary
SPECTRA

Time: 3.60E+005 s
1.00E+002 hr

	Oxidation depth, [mm]			Oxidized mass, [mol/m³]		
	Ring 1	Ring 2	Ring 3	Ring 1	Ring 2	Ring 3
01	0.018	0.006	0.001	166.5	57.9	9.1
02	0.083	0.018	0.001	747.4	161.1	6.3
03	0.055	0.012	0.001	498.6	104.1	5.4
04	0.028	0.006	0.000	249.7	55.2	4.5
05	0.012	0.003	0.000	111.3	25.3	3.6
06	0.006	0.001	0.000	56.1	10.0	2.7
07	0.004	0.000	0.000	35.3	4.5	0.9
08	0.003	0.000	0.000	26.3	2.7	0.0
09	0.002	0.000	0.000	18.1	2.7	0.0
10	0.001	0.000	0.000	11.8	1.8	0.0
11	0.001	0.000	0.000	6.3	0.9	0.0

Conservative oxidation model

HTR-PM Oxidation Summary
SPECTRA

Time: 3.60E+005 s
1.00E+002 hr

	Oxidation depth, [mm]			Oxidized mass, [mol/m³]		
	Ring 1	Ring 2	Ring 3	Ring 1	Ring 2	Ring 3
01	0.020	0.007	0.001	184.6	59.7	10.0
02	0.079	0.018	0.001	717.6	164.7	7.2
03	0.066	0.013	0.001	600.8	113.1	5.4
04	0.042	0.007	0.000	380.9	64.2	4.5
05	0.023	0.003	0.000	210.8	30.8	4.5
06	0.014	0.002	0.000	130.3	13.6	2.7
07	0.011	0.001	0.000	97.7	8.2	0.9
08	0.009	0.001	0.000	78.7	7.2	0.0
09	0.007	0.001	0.000	60.6	7.2	0.0
10	0.005	0.001	0.000	42.5	6.3	0.0
11	0.003	0.000	0.000	24.4	4.5	0.0

Table 4-24 : Oxidation at *t*= 100 hr (1-tube, top of SG, failure of SG drain and flaps)

Best Estimate oxidation model

HTR-PM Oxidation Summary SPECTRA — Time: 3.60E+005 s, 1.00E+002 hr

	Oxidation depth, [mm] Ring 1	Ring 2	Ring 3	Oxidized mass, [mol/m³] Ring 1	Ring 2	Ring 3
01	0.045	0.020	0.005	406.3	180.1	41.6
02	0.140	0.046	0.004	1265.9	416.2	38.0
03	0.088	0.031	0.005	794.5	283.2	42.5
04	0.038	0.018	0.006	346.6	161.1	51.6
05	0.012	0.005	0.003	109.5	48.0	25.3
06	0.004	0.001	0.000	39.8	9.1	0.9
07	0.003	0.000	0.000	24.4	4.5	0.0
08	0.002	0.000	0.000	17.2	2.7	0.0
09	0.001	0.000	0.000	12.7	2.7	0.0
10	0.001	0.000	0.000	8.2	1.8	0.0
11	0.000	0.000	0.000	3.6	0.9	0.0

Conservative oxidation model

HTR-PM Oxidation Summary SPECTRA — Time: 3.60E+005 s, 1.00E+002 hr

	Oxidation depth, [mm] Ring 1	Ring 2	Ring 3	Oxidized mass, [mol/m³] Ring 1	Ring 2	Ring 3
01	0.103	0.047	0.011	935.6	422.6	103.2
02	0.280	0.099	0.010	2534.4	896.7	93.2
03	0.204	0.072	0.012	1849.5	649.7	105.0
04	0.107	0.044	0.014	967.3	395.4	126.7
05	0.042	0.014	0.007	379.1	131.2	61.5
06	0.019	0.004	0.000	168.3	32.6	2.7
07	0.012	0.002	0.000	104.1	18.1	0.0
08	0.008	0.001	0.000	76.9	12.7	0.0
09	0.006	0.001	0.000	57.9	10.0	0.9
10	0.004	0.001	0.000	38.9	7.2	0.9
11	0.002	0.000	0.000	20.8	4.5	0.0

5 Summary of Calculated Results

All results are summarized in Table 5-1 through Table 5-5. Table 5-1 shows the total mass of generated hydrogen and the total mass of reacted carbon. Table 5-2 shows the total mass of steam/water entering the primary system. Table 5-3 shows the maximum mass of steam, observed at any time point in the reactor core and in the reactor vessel. The differences in maximum steam mass in RV between the conservative and the best estimate cases are explained as follows. The conservative model gives higher oxidation rates, so steam is consumed somewhat faster. Consequently the amount of steam present at every instant time in the core is somewhat smaller. The difference is visible only if the peak value of steam mass in RV occurs when intensive oxidation takes place, so not very early into the accident. This is the case in the second and third case (Figure 4-25 and Figure 4-39). In all other cases the peak value occurs very soon after the break (Figure 4-11, Figure 4-54, Figure 4-68, Figure 4-82).

Table 5-4 shows maximum oxidation depths and maximum oxidation density. Table 5-5 shows burn-off in volume % and as % of estimated critical depth.

It is seen that the largest oxidation is observed when blower flaps fail to close. Even in those cases oxidation depth is clearly smaller than the thickness of the fuel-free zone.

Table 5-1 : Total mass of hydrogen generated and carbon reacted

Break Location	Emergency Systems Available	Mass, hydrogen [kg] Best Est.	Mass, hydrogen [kg] Conserv.	Break Location	Emergency Systems Available	Mass, carbon [kg] Best Est.	Mass, carbon [kg] Conserv.
Bot	all (except He purif.)	0.8	0.8	**Bot**	all (except He purif.)	4.9	5.0
	no drain	1.0	1.0		no drain	6.0	6.1
	no drain, no flaps	43	99		no drain, no flaps	254	591
Top	all (except He purif.)	4.6	5.1	**Top**	all (except He purif.)	27.5	30.6
	no drain	6.7	8.3		no drain	40.1	49.3
	no drain, no flaps	14.7	34.7		no drain, no flaps	87.5	206

Table 5-2 : Total mass of steam/water entering the primary system

Break Location	Emergency Systems Available	Mass, primary [kg]	
		Best Est.	Conserv.
Bot	all (except He purif.)	224	228
	no drain	2659	2663
	no drain, no flaps	2648	2612
Top	all (except He purif.)	171	204
	no drain	892	858
	no drain, no flaps	556	556

Table 5-3 : Maximum mass of steam in the reactor vessel and in the core

Break Location	Emergency Systems Available	Mass, RV [kg]		Break Location	Emergency Systems Available	Mass, Core [kg]	
		Best Est.	Conserv.			Best Est.	Conserv.
Bot	all (except He purif.)	8.5	8.5	Bot	all (except He purif.)	6.8	6.7
	no drain	10.8	9.5		no drain	6.5	6.5
	no drain, no flaps	1030	920		no drain, no flaps	669	600
Top	all (except He purif.)	52	52	Top	all (except He purif.)	42	41
	no drain	80	80		no drain	52	51
	no drain, no flaps	400	400		no drain, no flaps	297	296

Table 5-4 : Maximum oxidation depth and oxidation density

Break Location	Emergency Systems Available	Depth [mm]		Break Location	Emergency Systems Available	Oxidation [mol/m3]	
		Best Est.	Conserv.			Best Est.	Conserv.
Bot	all (except He purif.)	0.007	0.006	Bot	all (except He purif.)	68	55
	no drain	0.010	0.007		no drain	93	65
	no drain, no flaps	0.466	0.808		no drain, no flaps	4214	7310
Top	all (except He purif.)	0.055	0.047	Top	all (except He purif.)	501	430
	no drain	0.083	0.079		no drain	747	718
	no drain, no flaps	0.140	0.280		no drain, no flaps	1266	2534

Table 5-5 : Maximum oxidation burn-off in vol.% and % of ECD

Break Location	Emergency Systems Available	Burn-off [vol.%]		Break Location	Emergency Systems Available	Burn-off [%]	
		Best Est.	Conserv.			Best Est.	Conserv.
Bot	all (except He purif.)	0.07	0.06	Bot	all (except He purif.)	1.0	0.8
	no drain	0.10	0.07		no drain	1.4	1.0
	no drain, no flaps	4.59	7.86		no drain, no flaps	64.7	112.2
Top	all (except He purif.)	0.55	0.47	Top	all (except He purif.)	7.6	6.5
	no drain	0.83	0.79		no drain	11.5	11.0
	no drain, no flaps	1.39	2.77		no drain, no flaps	19.4	38.9

6 Comparison with RETRAN-02 Results of INET

Current results are compared to the results obtained at INET using the computer code RETRAN-02 [11]. In the RETRAN model the primary side was replaced by a constant pressure boundary condition. Analysis of the blowdown was performed. Sensitivity study was performed varying the diameter of the SG drain valve, from 60 mm to 150 mm. The current results are compared here to the INET results for two cases:

- single tube break at the bottom (inlet) of SG
- single break at the top (outlet) of SG

In case of break at the bottom (inlet) of SG, the break flows calculated presently are in good agreement with the values presented in [11]. The mass flow through the plenum side of the break (Figure 4-2) is close to 1 kg/s slowly decreasing until the blowdown is over at about 65 s. This flow is mainly determined by the orifice at inlet to the SG tubes. This flow brings most of the steam/vapor during the blowdown phase. For this flow there is a very good agreement between current calculations and INET calculations.

For the tube side of the break there is a short peak which lasts for a few seconds only. In SPECTRA calculation this peak is about 1.7 kg/s (Figure 4-2). In RETRAN calculations it is about 5 kg/s. Consequently the water ingress reported in [11] is somewhat higher, 68 kg versus 52 kg in current analysis. This flow depends on the SG tube parameters such as wall roughness, resistance factors. In the current SPECTRA model the wall roughness was assumed as 5.0×10^{-5} m, the loss factors for a helical coil were estimated based on the *K*-factor data for flow in bends. Sensitivity calculations showed that the loss factor has minor effect on the results but the roughness has a much larger impact.

Figure 6-1 shows results obtained with roughness set to 5.0×10^{-6} m. The maximum flow was 2.1 kg/s, still smaller than that calculated in [11]. Next sensitivity calculation was performed with inertial length of the tube. A SG tube has a length of 88.9 m. When the tube breaks at the bottom of SG, the flow has to stop, reverse direction and flow back. This cannot be instantaneous because of the relatively large inertia of the fluid in the tube. In the SPECTRA model the inertial length for each node has a true value, giving a total inertial length of 88.9 m. In sensitivity calculation the length was reduced to 0.1 m per node, giving a total inertial length of 2.0 m.

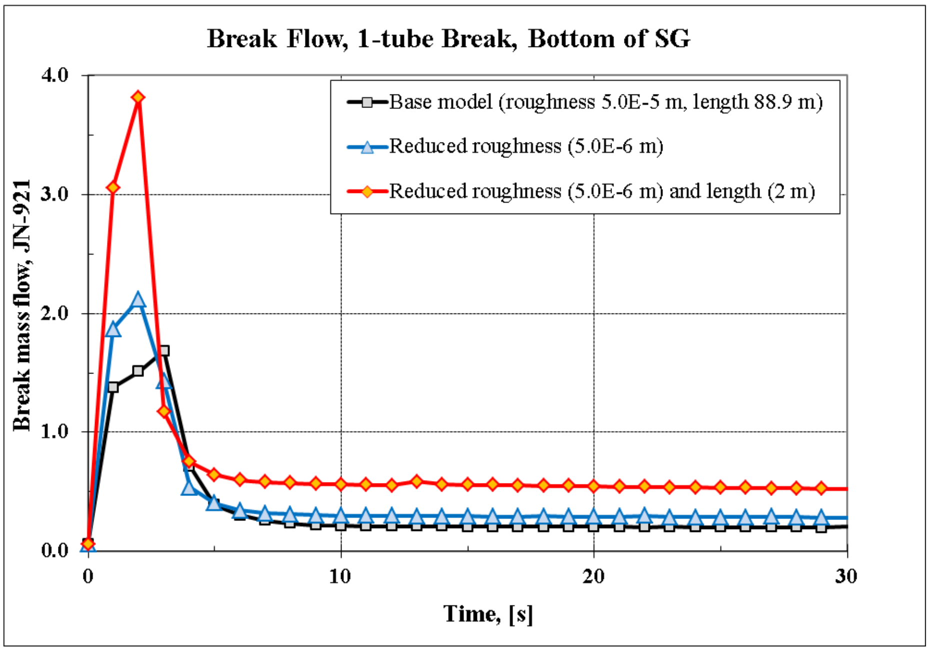

Figure 6-1 :
Break flow, tube side (1-tube, bottom of SG, safety systems available)

The results are summarized below.

- Base model (R = 5.0×10^{-5} m, L = 88.9 m) Peak flow: **1.7 kg/s** ingress at 65 s: **52 kg**
- R = 5.0×10^{-6} m, L = 88.9 m Peak flow: **2.1 kg/s** ingress at 65 s: **57 kg**
- R = 5.0×10^{-6} m, L = 2.0 m Peak flow: **3.8 kg/s** ingress at 65 s: **73 kg**
- RETRAN-02 results from [11] Peak flow: **4-5 kg/s** ingress at 65 s: **68 kg**

For better understanding of difference one would need to have a better understanding of modeling assumptions taken in [11], such as wall roughness, loss factors, inertial lengths, etc. While this may be done in the future to gain more insight in the modeling details, for the purpose of the present analysis it is concluded that for the blowdown period the agreement is sufficiently good.

For the long term water ingress no calculations were presented in [11]. Instead, it was conservatively estimated that the long term water ingress will be equal to the mass of steam and water remaining in SG after the drain valve is closed. Therefore the value from [11], 263 kg, is an upper bound estimation of the possible ingress. Current SPECTRA result, 172 to 176 kg, is about 2/3 of that value and is therefore reasonable. Therefore it is concluded that current results confirm the previous INET results. The results are summarized in Table 6-1.

Table 6-1 : Total water ingress into primary system - break at the bottom (inlet) of SG

Parameter	Best Estimate	Conservative	INET result [11]
Blowdown phase	52 kg	54 kg	68 kg (RETRAN calculations)
Long term	172 kg	174 kg	263 kg (upper bound estimation)
Total	224 kg	228 kg	331 kg

For the case of break at the top (outlet) of SG, the results are summarized in Table 6-2. Again, for the blowdown phase the SPECTRA value is somewhat smaller than the RETRAN value. This may possibly be a consequence of a larger roughness, or other parameters mentioned above. For the long term ingress, the current SPECTRA result, 36 to 66 kg is only 10% to 20% of the upper bound value from [11].

Table 6-2 : Total water ingress into primary system - break at the top (outlet) of SG

Parameter	Best Estimate	Conservative	INET result [11]
Blowdown phase	135 kg	138 kg	163 kg (RETRAN calculations)
Long term	36 kg	66 kg	362 kg (upper bound estimation)
Total	171 kg	204 kg	525 kg

Summarizing, the current results confirm the previous INET results and furthermore the present analysis reduces the conservatism taken in [11] by performing integrated (primary + secondary system) long term analysis. While the conclusion from [11] was that the water mass ingress does exceed 600 kg, the current calculations show that in fact it does not exceed 230 kg.

Concerning the behavior on the primary side, INET performed calculations of the primary side using TINTE code [10] with water ingress taken as boundary condition based on values from [11]. Those results are based on conservative water ingress of 600 kg and therefore not directly comparable to the present results.

7 Conclusions

Due to the steam cycle turbine adopted in the HTR-PM, the large amount of water ingress into the primary circuit is generally recognized as the most severe hazard potential for the reactor plant. A series of very special features are deliberately considered during the design to minimize the water-ingress amount and mitigate the accident consequences.

Within the work presented in this report a double-ended guillotine break of a heating tube of the steam generator has been analyzed. The obtained results lead to the following conclusions:

- If the break is located at the bottom of SG, the total mass entering the primary system is larger but it consists mostly of liquid which remains in the SG head and does not enter the core. If the break is located at the top of SG, the total mass entering the primary system is smaller but it consists mostly of steam which enters the core and causes corrosion of pebbles.
- If the blower flaps fail to close, a reverse natural circulation flow will be established after the blower is stopped. This will gradually bring a large amount of steam into the core and cause relatively large oxidation. Therefore the largest oxidation depth is observed when blower flaps fail to close.
- Even in the worst case, the largest oxidation depth was less than 0.5 mm. This is about 5 vol.% or 65% of Estimated Critical Depth.
- The largest increase of power due to positive reactivity feedback was only 4%.

Some interesting observations were made:

- When the break is at the bottom of the SG tubes, the amount of steam entering the core is not larger when the SG drain system fails. Failure of the SG drain keeps the break under a “protective” layer of water.
- When the break is at the bottom of the SG tubes, failure to close blower flaps causes significant corrosion due to evaporation of water in the SG lower head and transport of the steam into the reactor vessel.

Current results are in good agreement with the results obtained by INET with RETRAN-02. Because the present analyses were performed with an integrated (primary + secondary system) model, it was possible to eliminate some conservatism in the earlier INET analyses, where primary and secondary systems were studied separately, with different codes. While the conservative estimation from INET led to the conclusion that water ingress does exceed 600 kg, the current calculations showed that it does not exceed 230 kg.

Current results were obtained without taking into account the helium purification system. With the helium purification system, steam can be removed from the core within several hours [10].

From the calculated results it is concluded that HTR-PM shows the inherent safety features, expected of the modular high temperature gas-cooled reactors, and has a relatively good natural plant response even under water-ingress accidents with simultaneous failure of several safety systems.

Current results were obtained using an integrated model of the HTR plant, including primary system, secondary system as well as residual heat removal system. This model allows a complete simulation of a water ingress accident. Possible future improvements of the current model include:

- **Local power increase - 3-D kinetics model**. Current calculations were performed with point kinetics. The reactivity increase, resulting from steam ingress into the core, is calculated using average density of steam in the whole core. The steam density increases first in the upper part of the cores and there the reactivity effect will be larger and consequently local power increase will be higher. This effect cannot be calculated by a point kinetics. In order to model this local power increase a 3-D kinetics model is needed. Current SPECTRA version does not have a model for 3-D kinetics, so it was not possible to perform such calculations. However, the power increase from the positive steam feedback is rather small - only a few percent before the reactor shutdown. Therefore it is expected that even with 3-D effect the power increase will not have an important effect on the results.
- **Liquid ingress into the core - droplet formation and transport model.** During a water ingress accident water and steam enter the primary system. Part of the liquid water evaporates upon entering

the relatively low pressure region. The remaining water will be in a form of droplets. The droplets will partly deposit on the SG lower head or be entrained and transported in gas and may reach the core. Current calculations were performed using the option that the water remaining after flashing is deposited in the pool of a Control Volume. Droplet transport was not taken into account. SPECTRA does have models for droplet generation and transport. Therefore such analysis is possible but was not done in the current scope. The correlations for diameter of generated droplets are appropriate for typical Light Water Reactors and it should be checked if they are appropriate for High Temperature Reactors.

- **Secondary chemical reactions.** The secondary reactions: the Boudouard reaction and the water-shift reaction, were not taken into account in the current calculations. The water-shift reaction can effectively reduce graphite corrosion. Therefore the obtained amounts of graphite corrosion are conservative. Appropriate models exist and they can be activated in the future.

8 References

[1] M.M. Stempniewicz, “SPECTRA Sophisticated Plant Evaluation Code for Thermal-Hydraulic Response Assessment, Version 3.60, April 2010, Volume 1 – Program Description, Volume 2 – User’s Guide, Volume 3 – Subroutine Description, Volume 4 - Verification and Validation”, NRG report K5024/10.101640, Arnhem April 21, 2010.

[2] H.C. Hottel, “Radiant Heat Transmission”, Chapter 4 in W.H. McAdams, “Heat Transmission”, Robert E. Krieger Publishing Company, Third Edition, Malabar, Florida, 1985.

[3] J.J. Duderstad, L.J. Hamilton, "Nuclear Reactor Analysis", ISBN 0-471-22363-8, John Wiley & Sons, Inc., New York, 1976.

[4] A.F. Henry, "Nuclear Reactor Analysis", ISBN 0-262-08081-8, Massachusetts Institute of Technology, Cambridge, 1975.

[5] W. Breitung, et al., "Flame Acceleration and Deflagration-to-Detonation Transition in Nuclear Safety", OECD report, NEA/CSNI/R(2000)7, August 2000.

[6] M.M. Stempniewicz, "D22.21: Implementation of models and data for graphite-water interaction in SPECTRA", ARCHER project, contract number 269892, Deliverable D22.21, July 1, 2013.

[7] P.E. McDonald, “NGNP Point Design - Results of the Initial Neutronics and Thermal-Hydraulics Assessment during FY-03”, INEEL/EXT-03-00870, September 2003.

[8] R. van Bremen, “Water ingress scenario analyses of a thorium fuelled HTR”, NERA-131-2013-006, Thesis at Technical University Delft, July 2013.

[9] J. Lapins, M. Buck, “D22.24: Report on results for water ingress with TORT-TD/ATTICA3D”, ARCHER – D22.24 – revision 0 – Issued by USTUTT-IKE on 27/07/13.

[10] Y. Zheng, L. Shi, Y. Wang, “Water-ingress analysis for the 200 MWe pebble-bed modular high temperature gas-cooled reactor”, *Nuclear Engineering and Design*, Vol. **240**, pp. 3095-3107, 2010.

[11] Y. Wang, Y. Zheng, F. Li, L. Shi, Z. Zhou, “The water-ingress mass analysis on steam generator heat-exchange tube rupture accident of high temperature gas-cooled reactor”, *Proceedings of the 17-th International Conference on Nuclear Engineering, ICONE17*, ICONE17-76034, pp. 821-827, Brussels, Belgium, July 12-16, 2009.

[12] Turner, 2008, “NGNP and Hydrogen Production Preconceptual Design Study, Contamination Control”, NGNP-NHS-50-CC, Revision A, April 2008.

[13] H. Reutler, “Plant Design and Safety Concept of the HTR-Module”, *Nuclear Engineering and Design*, Vol. **109**, pp. 335-340, 1988.

[14] C. Stoker, “PBMR Nuclear Design and Safety Analysis: An Overview”, PSYHOR-2006, ANS Topical Meeting on Reactor Physics, Vancouver, Canada, September 10-14, 2006.

[15] Y. Zheng, L. Shi, Y. Dong, “Thermo-hydraulic transient studies of the Chinese 200 MWe HTR-PM for loss of forced cooling accidents”, Annals of Nuclear Energy 36 (2009) 742–751.

[16] R. Moormann, "Effect of Delays in Afterheat Removal on Consequences of Massive Air Ingress Accidents in High Temperature Gas Cooled Reactors", *Journal of Nuclear Science and Technology*, **21** (11), pp. 824-835, November 1984.

[17] W. Graven, J. Long, "Kinetics and Mechanisms of the Two Opposing Reactions of the Equilibrium $CO + H_2O = CO_2 + H_2$", *Journal of the American Chemical Society*, **76**, 1954.

[18] I.E. Idelchik, "Handbook of Hydraulic Resistance", Second Edition, Hemisphere Publishing Corp., 1986.

[19] Kubaschewski, P., Heinrich B (1981). "Graphitkorrosion durch Wasserdampf, Hochtemperaturreaktorbau GmbH", pp. 30-42 in Nieder R. et al. "Chemie des Hochtemperaturreaktors", Jülich, November 1981, Jül-Conf-43, ISSN 0344-5798

[20] M.M. Stempniewicz. "Correlation for steam-graphite reaction", in press, *Nuclear Engineering and Design* (2014), http://dx.doi.org/10.1016/j.nucengdes.2014.09.027.